



Departament d'Enginyeria Química

Escola Tècnica Superior d'Enginyeria Química

Universitat Rovira i Virgili

**Development of displacement
electrochemical immunosensors:
The case of 2, 4, 6-trichloroanisole**

**María Viviana Duarte
Tarragona, 2007**

UNIVERSITAT ROVIRA I VIRGLI

DEVENLOPMENT OF DISPLACEMENT ELECTROCHEMICAL INMUNOSENSORS: THE CASE OF 2,4,6-TRICHLOROANISOLE

Maria Viviana Duarte

ISBN:978-84-691-2700-1/DL:T-385-2008

Dr. Ioanis Katakis, professor titular del Departament d'Enginyeria Química de la Universitat Rovira i Virgili i **Dr. Pablo Lozano-Sanchez** personal investigador de la Universitat Rovira i Virgili:

FAN CONSTAR

que el present treball que porta el títol:

**DEVELOPMENT OF DISPLACEMENT ELECTROCHEMICAL IMMUNOSENSORS:
THE CASE OF 2, 4, 6-TRICHLOROANISOLE**

que presenta en/na **María Viviana Duarte** per optar al grau de Doctor per la Universitat Rovira i Virgili, ha estat realitzat sota la seva direcció en els laboratoris del Departament d'Enginyeria Química de la Universitat Rovira i Virgili, i que tots els resultats presentats i la seva anàlisi són fruit de la investigació realitzada per l'esmentat/da doctorant.

I per a que se'n prengui coneixement i tingui els efectes que correspongui, signo aquesta certificació.

Tarragona, Diciembre 2007

Dr. Ioanis Katakis
Profesor titular

Dr. Pablo Lozano Sanchez

UNIVERSITAT ROVIRA I VIRGLI

DEVENLOPMENT OF DISPLACEMENT ELECTROCHEMICAL INMUNOSENSORS: THE CASE OF 2,4,6-TRICHLOROANISOLE

Maria Viviana Duarte

ISBN:978-84-691-2700-1/DL:T-385-2008

Table of contents

CONTENTS

List of abbreviations.....	v
Abstract	viii
CHAPTER 1	1
Introduction	1
1.1 Introduction	1
1.2 Biosensors.....	2
1.2.1 Biosensors. Brief description.....	2
1.2.2 Sensors and Biosensors in history	3
1.3 Immunosensors	4
1.3.1 Immunosensors. Brief description.....	4
1.3.2 Biological Recognition Element: The antibody.....	5
1.3.2.1 The immunosystem.....	5
1.3.2.2 Ab structure and function	6
1.3.2.3 Ab-Ag interaction	9
1.3.2.4 Factors affecting the immunoassay performance.....	10
1.3.3 Transducers.....	11
1.3.3.1 Amperometric transduction	12
1.3.3.2 Potentiometric transduction	13
1.3.3.3 Conductimetric transduction.....	14
1.3.3.4 Impedimetric transduction	14
1.3.4 Immobilization methods	15
1.3.4.1 Immunosensor surface modification.....	15
1.3.4.2 Biomolecule immobilization.....	17
1.3.5 Immunoassay formats.....	18
1.4 Overcoming Non Specific Adsorption.....	21
1.5 Commercialization.....	21
1.6 The real-time, reagentless and fast responding paradigm	22
1.7 The TCA problem. An overview	24
1.8 Economic sectors affected by TCA.....	25
1.9 Cork as wine stopper	25
1.9.1 <i>Quercus suber</i> for cork production.....	25
1.9.2 Chemical composition of Cork.....	26
1.9.3 Cork stoppers production.....	27
1.9.4 Cork taint components	29
1.9.5 How does TCA reach wine?.....	31
1.9.6 Removal of TCA	31
1.10 TCA detection	32
1.10.1 Sensory detection.....	32
1.10.2 Detection in wine.....	33
1.10.3 Detection in cork	35
1.10.4 Detection in water.....	35
1.11 Description of the industrial problem	35
1.12 Objectives	37
1.13 Bibliography.....	38
CHAPTER 2	43
Indirect competitive ELISA for 2,4,6-trichloroanisole (TCA) detection.....	43
2.1 Introduction and aims	43
2.2 Materials.....	45
2.2.1 Chemicals	45
2.2.2 Instrumentation and apparatus	47
2.2.3 Haptens production.....	48

Table of contents

2.2.4 Hapten carrier (KHL-Hapten A) and coating haptens (BSA-Hapten) preparation	48
2.2.5 TCA detection by Gas Chromatography.....	49
2.2.5 ELISA procedures	50
2.2.5.1 Procedure 1: Indirect non-competitive ELISA (INCE)	50
2.2.5.2 Procedure 2: Indirect non-competitive ELISA (INCE) for cross-reactivity study.....	50
2.2.5.3 Procedure 3: Indirect non-competitive ELISA (INCE) for ethanol effects study.....	51
2.2.5.4 Procedure 4: Indirect competitive ELISA (ICE) for pre-incubation time study	53
2.2.5.5 Procedure 5: Optimized Indirect competitive ELISA (OICE)	55
2.2.6 Accelerated Aging test.....	56
2.3 Results.....	58
2.3.1 Selection of monoclonal Antibody. Cross-reactivity study	58
2.3.2 Effect of ethanol content in TCA samples.....	59
2.3.3 Affinity Constant (K_{aff}) estimation	60
2.3.3.1 MAb-coating hapten affinity estimation. Indirect non-competitive ELISA	60
2.3.3.2 MAb- compounds in solution affinity. Indirect competitive ELISA	62
2.3.4 Selection of coating hapten towards indirect competitive ELISA for TCA determination.....	62
2.3.5 Pre-incubation time effect.....	63
2.3.6 Optimized indirect competitive ELISA for TCA detection	66
2.3.7 Spiked water samples	67
2.3.8 Matrix Effects	69
2.3.9 Post-aging testing	70
2.4 Discussion	72
2.4.1 Immunogenic hapten selection	72
2.4.2 Coating hapten selection towards indirect competitive ELISA	73
2.4.3 Affinity Constant (K_{aff}) estimation	73
2.4.3.1 Estimation of MAb- immobilized coating hapten affinity.....	74
2.4.3.2 Estimation of MAb- compounds-in- solution affinity	75
2.4.3.3 Equilibrium and kinetic constants.....	76
2.4.4 Accelerated Aging (AA) Study.....	78
2.4.5 Achievements of the developed ICE.....	80
2.5 Conclusions	82
2.6 Bibliography.....	84
CHAPTER 3	86
Mathematical Modelling of the Displacement Immunosensor	86
3.1 Introduction and aims	86
3.2 Materials and methods.....	91
3.2.1 Mathematical Model for displacement immunosensor.....	91
3.2.1.1 System description.....	91
3.2.1.2 Equations for equilibrium Mathematical Model (MM)	94
3.2.2 Expression of the predicted DEI response.....	96
3.2.3 Parameters and equation solving	97
3.3 Results.....	97
3.3.1 Mathematical Model solution	97
3.3.2 Predictions of the DEI behaviour.....	97
3.3.2.1 Effects of S/V changes in the DEI response	98
3.3.2.2 Effects of K^* and S/V changes in the DEI response.....	99
3.3.2.3 Effects of higher and lower affinities (K and K^*) in the MM predictions	101
3.3.2.4 Predicted DEI response.....	104
3.3.2.5 Effects of K , K^* and K/K^* ratio in the DEI response.....	104
3.3.2.6 Prediction of K needed to detect ppt of TCA.....	106
3.4 Discussion	108
3.4.1 Predicted DEI response.....	108
3.4.2 Predicted DEI range of detection.....	109
3.4.3 Validity of the developed MM.....	109
3.5 Conclusions	110

Table of contents

3.6 Bibliography.....	112
3.7 Annex. Example of Matlab routine.....	113
CHAPTER 4	114
Strategy for Displacement Electrochemical Immunosensors Development:.....	114
4.1 Introduction and aims	114
4.1.1 Introduction	114
4.1.2 Non-Specific Adsorption (NSA) and strategies to control it.....	115
4.1.2.1 Adsorption of proteins.....	115
4.1.2.2 Adsorption of proteins on metal	118
4.1.2.3 Effects of protein adsorption on electron transfer.....	119
4.1.2.4 Construction of protein resistant surfaces.....	119
4.1.2.5 Self-assembled monolayer (SAM)s formation	120
4.1.2.6 SAM on Cu.....	121
4.1.2.7 SAM on Cu UPD.....	123
4.1.3 Displacement phenomenon.....	125
4.1.4 TCA detection.....	127
4.2 Materials.....	128
4.2.1 Chemicals	128
4.2.2 Instrumentation and Apparatus.....	129
4.2.3 Conjugation of HRP to Hapten 3 (H3HRP).....	130
4.2.4 Immunolectrodes	130
4.2.4.1 Analyte and sub-optimum antigen.....	130
4.2.4.2 Preparation of Immunolectrodes.....	131
4.2.5 Electrochemical measurements.....	134
4.2.6 Displacement studies procedures.....	135
4.2.6.1 Displacement Electrochemical Immunosensor (DEI) for TCA detection. On-line experiments.....	136
4.2.6.2 Displacement Electrochemical Immunosensor (DEI) for TCA detection. Batch experiments.....	139
4.3 Results.....	141
4.3.1 Optimization of the electrode modification procedure	141
4.3.1.1 Thiol selection for self-assembled monolayer (SAM) formation	141
4.3.1.2 Preliminary study of NSA control by Cu.....	144
4.3.1.3 Effects of Cu UPD on modified electrode	146
4.3.1.4 Effect of Cu UPD on displacement experiments	149
4.3.2 Displacement on optimized immunolectrodes	151
4.3.2.1 Displacement Electrochemical Immunosensor (DEI). On-line Experiments	151
4.3.2.2 DEI Limit of Detection.....	153
4.3.2.3 DEI range of operation	153
4.3.3 Loss of current due to buffer effects- "Washing effect".....	154
4.3.4 TCA - TCP Cross-reactivity	156
4.4 Discussion	157
4.4.1 Controlling the Non-Specific Adsorption (NSA) phenomenon.....	157
4.4.2 Detection of displacement phenomenon.....	159
4.4.3 Fitting of predicted and experimental results.....	160
4.4.4 DEI range of operation	161
4.5 Conclusions	162
4.6 Bibliography.....	164
CHAPTER 5	168
Overall conclusions	168

List of abbreviations

List of abbreviations

List of abbreviations

$\%NDC_{TCA}$	net displaced current due to tca displacing effect
(DFT)	density functional theory
AA	accelerated aging
AAF	accelerated aging factor
AAT	accelerated aging time
Ab	antibody
Ab _{free}	total free antibody
Ab ₀	total initial concentrations of antibody
AbAg	antibody-antigen immunocomplex
AbAg*	antibody- sub-optimum labeled antigen immunocomplex
AbAg* ₀	antibody- sub-optimum labeled antigen immunocomplex before displacement (mathematical model)
Ab _{s controls}	control's absorbance
Ab _{s i}	corrected absorbance
Ab _{s NCi}	non corrected absorbance
AED	atomic emission detector
AES	auger electron spectroscopy
Ag	analyte or antigen of interest
Ag* ₀	initial labeled sub-optimum antigen (mathematical model)
Ag ₀	total initial concentrations of antigen
ASTM	american society for testing and materials international
BRE	bio-recognition element
BSA	bovine serum albumin
DDC	n,n-dicyclo-hexylcarbodiimide
DEI	displacement electrochemical immunosensor
DGE	disk gold electrode
DMSO	dimethyl sulfoxide
ECD	electron capture detector
EDC	1-ethyl-3-[3-(dimethylamino)propyl carbodiimide hydrochloride
ELISA	enzyme-linked immunosorbent assay
EtOH	ethanol
Fc	constant fraction of IgG
GC	gas chromatography
H1	hapten 1 [2,4,6-trichlorophenoxyacetic acid]
H3	hapten 3 [3-chloro-2-methylphenoxyacetic acid]
H3HRP	hapten 3 conjugated to horseradish peroxidase

List of abbreviations

HA	hapten A [3-(2,4,6-trichloro-3-methoxy phenyl) propionic acid]
HB	hapten B [5-(2,4,6-trichlorophenoxy) pentanoic acid]
HPh	hapten Ph [3-(3-hydroxy-2,4,6-trichlorophenyl)-propanoic acid]
HPLC	high pressure layer chromatography
HRP	horseradish peroxidase
HSPME	headspace solid-phase extraction
Hx	generic hapten.
HZ	hapten Z [3-(4-methoxyphenyl) propionic acid]
ICE	indirect competitive elisa
IgG	immunoglobuline G
INCE	indirect non-competitive elisa
K_{aff}	affinity constant
K_{D}	dissociation constant
KLH	keyhole limpet hemocyanin
k_{off}	dissociation rate constant
k_{on}	association rate constant
LOD	the limit of detection
mAb	tca specific monoclonal antibody
mAb ₀	total initial concentrations of tca specific monoclonal antibody
MALDI-TOF-MS spectrometry	matrix assisted laser desorption ionization-time-of-flight mass spectrometry
MeOH	methanol
MPA	3-mercaptopropionic acid
MS	mediator solution
MSD	mass spectrometer detector
MUA	11-mercaptoundecanoic acid
MW	molecular weight
NHS	n-hydroxi-succinimide
NSA	non specific adsorption
OICE	optimized indirect competitive elisa
PBS	phosphate-buffered saline
ppb	parts per billion
ppm	parts per million
ppt	parts per trillion
Q10	aging factor
RT	desired simulated real time
S/V	surface of electrode to volume ratio
SAM	self assembled monolayer
SGE	sputtered gold electrode
SPE	solid-phase extraction
SPME	solid-phase microextraction

List of abbreviations

PDMS	polydimethylsiloxane
T1	treatment 1, coated plates subjected to accelerated aging test
T2	treatment 2, coated and blocked plates subjected to accelerated
aging test	
TA	thioctic acid
TAA	selected accelerated aging temperature (°c)
TCA	2,4,6-trichloroanisole
TCP	2,4,6-trichlorophenol
TMB	3,3',5,5'-tetramethylbenzidine
TRT	ambient temperature (°c)
UPD	underpotential deposition

Abstract

Abstract

The purpose of this work is to explore and exploit the principles of Displacement Electrochemical Immunosensing (DEI) and Indirect Competitive ELISA (ICE) to detect 2,4,6-trichloroanisole (TCA).

The rational design of indirect competitive ELISA for TCA detection is attempted. The developed assay detects TCA at concentrations from 1ppt to 1 ppm, with a limit of detection of 4.2 ppt. The assay can be commercially useful in situations where less than 80 minutes total assay time is required.

A mathematical model (MM) is developed for the rational design of an electrochemical displacement immunosensor (DEI). Despite the low affinity constants of the antibodies obtained for this work a functional DEI is developed with the predicted by the MM high limit of detection for TCA (0.2 ppm). The non-specific adsorption (NSA) of proteins is identified as a critical problem inhibiting further optimization of the DEI. The use non-insulating Cu UPD as NSA controller or electrochemically compatible blocking, together with amperometric displacement detection are proposed as a platform that could permit further development of reagentless and labelless immunosensors.

Abstract

CHAPTER 1

Introduction

1.1 Introduction

Biosensors play an important role in the improvement of productive processes and living conditions. Biosensors are powerful tools for diagnostics, and have little competition when fast, portable, selective and specific analytical tools are required [1]. They have relatively low cost of manufacture and storage, potential for miniaturization, and they can be easily used in automated analysis [2, 3].

Biosensors are integrated devices in which a Biological Recognition Element (BRE) and a transducer are in intimate contact. The BRE selectively interacts with a target analyte, and the transducer translates the biological interaction into a discernable signal. Using antibodies as BRE configures an immunosensor.

Immunosensors have widely contributed to advancements in environmental monitoring, detection of biological warfare agents, public health, clinical chemistry and food quality [4-15].

The main components of an immunosensor are: (i) the antibody, (ii) the transduction element, which will also decide the transduction technique, and (iii) the immobilization chemistry. The following briefly defines and reviews these components and processes.

1.2 Biosensors

1.2.1 Biosensors. Brief description

Sensor families can be divided into chemical and biochemical. Chemical sensors transform chemical information into an analytically useful signal. They are composed of a chemical recognition system and a physicochemical transducer. One of the first great achievements in the history of chemical sensors, was the creation of the glass pH electrode in 1922 [16].

When the recognition system of a sensor consists of a biochemical mechanism, a chemical sensor is called Biosensor [17]. Examples of biological recognition elements are enzymes, antibodies, fragments of antibodies, organs, tissues, cells, aptamers, peptides and oligonucleotides [18-20].

Biosensor function consists of two main steps: recognition and transduction. The recognition step is facilitated by the Bio-Recognition Element (BRE) that can recognize analytes specifically and with high sensitivity conferred to it by evolution. The BRE is in close contact with a transducing element, which transduces the BRE-analyte biorecognition event into a signal. The signal has to be transduced rapidly and sensitively by thermal, electrical, optical or electronic elements. A more precise definition of an electrochemical biosensor by IUPAC [17] is:

“(...) an electrochemical biosensor is a self-contained integrated device, which is capable of providing specific quantitative or semi-quantitative analytical information using a biological recognition element (biochemical receptor) which is retained in direct spatial contact with an electrochemical transduction element (...)”

1.2.2 Sensors and Biosensors in history

The earliest sensors developed were physical sensors that measured time, temperature and other physical parameters, and the technologies developed for these sensors provided the transduction basis for chemical and biological sensors. First demonstrations of sensing devices were associated with chemical sensors. As pointed out in the previous section, glass pH electrodes were introduced in the 1920's. Next, oxidation-reduction reactions were utilized in sensor technology to give rise to devices detecting metallic ions and organic compounds. The introduction of ion selective electrodes gave rise to the first transducers for chemical sensors and biosensors.

Interposing a membrane between the solution and the electrode, gave rise to one of the first biosensor created, for glucose detection, by Clark and Lyons in 1962 [2, 21] . The greatest progress in biosensors took place in the 1970s – 1980s with the incorporation of enzyme electrodes and newer transduction and immobilization techniques [16]. In 1976, the lactate analyzer was introduced (LA 640, La Roche, Switzerland) in which the soluble mediator, hexacyanoferrate was utilized. This gave rise to the generation of mediated biosensors. Later, use of ferrocene and its derivatives as immobilized mediators, with oxidoreductases became common for the fabrication of enzyme electrodes [21]. Discoveries related to new BREs, transduction and immobilization techniques keep biosensor technologies in continuous advance.

1.3 Immunosensors

1.3.1 Immunosensors. Brief description

An immunosensor is an affinity biosensor designed to detect the direct binding of an antibody or an antigen, forming an immunocomplex, on the sensor surface. The recognition of the analyte (antibody or antigen) by the immobilized receptor (antigen or antibody) induces variation in optical properties, electric charge, mass or heat, which can be detected directly or indirectly by a variety of transducers. These include electrochemical (potentiometric, amperometric, conductimetric, impedance), optical (surface plasmon resonance (SPR), reflectometric interference spectroscopy (RIfS)), mass sensitive (piezoelectric, acoustic surface waves SAW) or thermoelectric (thermosistors) transducers [22-24].

Electrochemical immunosensors that depend upon voltammetric, conductimetric or amperometric detection are considered to have an important place in modern analytical methods. The full potential of electrochemical immunosensors is considered not to be totally developed, reasons being the difficulty and high initial cost of assembling a new, widely accepted electrochemical immunoassay [25]. Once developed, electrochemical immunosensors permit simultaneous, fast and cost-effective analysis. The advantages of immunosensors such as high specificity, small sample volumes, ability for simultaneous analysis of multiple samples, simple sample preparation, minimization of use of chemicals and waste production, and easy automation, easily offset the limitations in their development process [26].

1.3.2 Biological Recognition Element: The antibody

The merits of immunosensors are related to the selectivity and affinity of the antibody-analyte binding reaction. Thus, the production and selection of antibodies are crucial for the optimal functioning of immunosensors. In what follows in this section, antibody structure, production and interaction with antigens are visited.

1.3.2.1 The immunosystem

Mammals possess a system of surveillance called the immune-system, which protects them from disease-causing invasions. The protection afforded by the immune-system can be divided in two: the innate immune-system and the adaptive immune-system.

Innate immunity (*e.g.*, phagocytes) corresponds to the first line of defence responding to infectious agents. If this defence is overcome, the adaptive immune system is activated. The adaptive immune-system generates a specific molecule that can attach at one end to the infectious agent and at the other end to the phagocytic cell. These specific molecules are called antibodies (Ab) [27].

Antibodies are host proteins produced in response to the presence of foreign agents, called antigens (Ag), in the body. Antibodies are synthesized predominantly by plasma cells (mature B-lymphocytes). Antibodies circulate throughout the blood and lymph, where they bind to the antigens forming the antibody-antigen immunocomplexes. These immunocomplexes are removed from circulation mostly through phagocytosis by macrophages. Host organisms use this mechanism to protect themselves from foreign agents [28].

1.3.2.2 Ab structure and function

Antibodies, also known as immunoglobulins are divided into five classes: G, A, M, D and E differing in the constant regions of the heavy chains. Immunoglobulin G (IgG) or γ -globulin (Fig. 1. 1) is the principal antibody in serum corresponding to a 75 % participation in serum [29].

The IgG (MW 150 kDa) antibody has two heavy and two light chains (50 kDa and 23-25 kDa respectively), each containing several domains held together by disulfide bonds.

The heavy (H) chain is divided into four sub-domains and the light (L) chain is divided into two sub-domains. At the same time, the sub-domains are divided according to the variability of their amino acid sequence into constant (C) and variable (V) regions. The H chain has three constant regions (C_{H1} to C_{H3}) and one variable region (V_H). The light chain has one constant (C_L) and one variable (V_L) region. The base of the Y shape is called the Fc fragment and is formed by the association of the two C_{H2} and the two C_{H3} domains. Each arm of the Y shape is the Fab fragment that contains the binding sites, and is formed by C_{H1}- C_L and V_H and V_L associations.

The antigen specificity is conferred by the variable regions of both the light and heavy chains, which contain the complementary-determining regions (CDRs).

Antibodies can be produced through the immunization of mammals (usually rats, mice or sheep) by introducing an Ag into their blood stream. As low molecular weight organic molecules/analytes are not alone able to elicit an immune response in an animal (these are metabolized), it is necessary to transform the analyte into an immunogenic molecule, consisting of a “hapten” covalently coupled to a protein. An ideal or optimum hapten is one that preserves most of the steric and electronic characteristics of the analyte when conjugated to a large molecular weight protein, thus exposing it to the immune system.

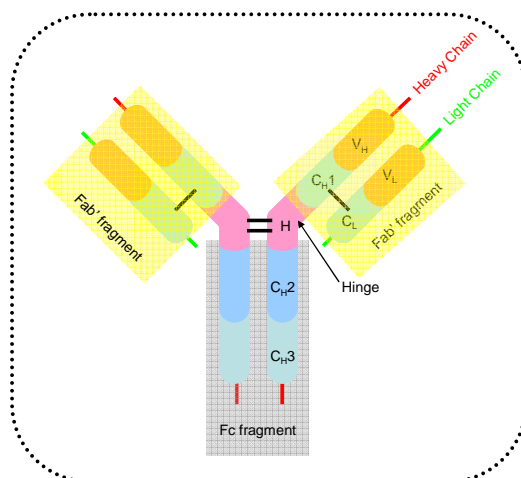


Fig. 1. 1: Immunoglobulin G (IgG) structure

Most often, an animal will produce large groups of antibodies that recognize independent epitopes (the antibody-binding site of an antigen) on the antigen. Different clones of plasma cells can secrete antibodies which bind only to one epitope. The collection of antibodies in serum results to the production of many different antibodies. These *polyclonal* antibodies are obtained from purified animal antiserum.

If antibodies are produced via hybridoma techniques they are called *monoclonal* antibodies (MAbs). All these antibodies are identical, with specific and easily studied properties of antigen recognition. Alternatively, *recombinant* antibodies are obtained through genetic engineering. Recombinant antibody technology makes it possible to modify the antibody molecule with high precision [30]. The future of immunosensors is considered to be linked to the generation of recombinant antibody libraries, which would provide a repertoire of new antibody types, generated at the DNA level [23].

Polyclonal antibodies are broadly used for immunochemical techniques. They are used normally as crude serum samples and in this form suffice for many purposes. Nevertheless, *monoclonal* antibodies (MAbs) have the advantage of a defined affinity constant with the antigen, and of the reproducibility of their production from the isolated hybridomas.

1.3.2.3 Ab-Ag interaction

The interaction of the antibody with the antigen is the basis for all immunochemical techniques. The strength of such interaction is described by its affinity, while the stability of the immunocomplex is described by its avidity.

The variable regions of the heavy and light chains of the antibody make up the antigen-binding site of the antibody. The antibody-antigen complex is held together by multiple, non-covalent bonds including hydrogen bonds, van der Waals forces, and coulombic and hydrophobic interactions. The immunocomplex is stabilized by the combination of weak interactions that depend on the precise alignment of the antigen and the antibody. The overall interaction is a balance of many attractive and repulsive interactions at the interface. Small changes in antigen structure can greatly affect the strength of the interaction [28, 31].

The antibody-antigen binding is reversible and can be interpreted in terms of an equilibrium reaction between the antibody (Ab) and the antigen (Ag) to form the immunocomplex (AbAg) with an affinity constant (K_{aff}) (Eq. 1. 1):

$$K_{aff} = \frac{[AbAg]}{[Ab][Ag]} \quad \text{Eq. 1. 1}$$

Unlike the affinity polyclonal antibodies, that of monoclonal antibodies can be determined exactly. Affinity constants have been reported to range from below 10^5 M^{-1} to 10^{13} M^{-1} [32].

In some immunoassays, the antibody that demonstrates the highest binding constant does not necessarily give an assay with the greatest sensitivity. For example, in displacement assays (section 1.3.5), an antibody with a high binding constant would make the displacement process much more difficult and would therefore require much higher concentrations of the antigen or a longer antibody–antigen contact time.

1.3.2.4 Factors affecting the immunoassay performance

Finding the antibody with the highest affinity for the antigen is not a guarantee of success for an immunoassay. Different factors may affect its performance, for example:

- *The specificity of the antibody for the antigen:* Antibodies could cross-react with molecules distinct to the target analyte or the selected hapten. To counteract this, cross-reactions of antibodies should be studied and controlled by selection of appropriate experimental conditions.

-
- *The alterations that binding sites may suffer during the assay:* Denaturation and chemical modifications of binding sites and epitopes should be avoided or controlled as these strongly affect the affinity of the immunoreaction.
 - *Steric impediment for the antibody and the antigen to meet:* The presence of other molecules or problems in the orientation of the antibody can negatively affect the immunoreaction.

Since antibody affinity and specificity determine the analytical capability of the immunosensor, the properties of the antibodies represent an important factor in developing the immunological method. However, what determines that certain antibodies recognize a particular antigen or group of antigens can not be quantified. This limits the possibilities for designing antibodies with desired specificity and affinity [33].

1.3.3 Transducers

Transduction elements convert the antibody-antigen interaction to a detectable signal. The immunointeraction can give rise to changes in fluorescence, optical density, mass or electrical properties which need to be suitably transduced. Immunosensors can take advantage of a variety of transduction elements, such as optical, piezoelectric, thermal and electrochemical transducers.

Electrochemical transducers – the type explored in this thesis- are basically electrodes where various electrical/electrochemical properties changes, such as conductivity, surface potential or steady state currents are measured.

According to the nature of the electrical signal, electrochemical sensors can be divided into four categories:

- 1 Amperometric
- 2 Potentiometric
- 3 Conductimetric
- 4 Impedimetric

1.3.3.1 Amperometric transduction

Amperometric transduction is accomplished by maintaining the potential of the working electrode at a fixed value relative to the reference electrode and monitoring the current produced as a function of time. The interaction of electroactive species involved in the recognition process is detected.

The driving force for the electron transfer reaction of the electroactive species is the applied potential that forces the species to gain or lose electrons. The obtained current is a direct measure of the rate of the electron transfer reaction, which at the same time is representative of the recognition process and thus, proportional to the analyte concentration.

The working electrode is where the electrochemical reactions of the studied species occur. Consequently, the selection of working electrode is critical for the design of the amperometric immunosensor. An appropriate working electrode should yield high sensitivity, selectivity and stability by providing a highly electroactive surface. The

factors considered in the selection of the working electrode material are the potential limits, background processes of coexisting electroactive species and amenable properties for biocompound immobilization. Solid electrodes such as platinum, gold, glassy carbon and carbon paste have been broadly used [34].

Together with the working electrode an amperometric immunosensor contains a reference electrode that should have a stable potential to which the potential of the working electrode is compared. Silver/silver chloride electrodes are commonly used as reference electrodes. A third auxiliary electrode is included for compensating the currents occurring at the working electrode. Finally, the three electrode system is connected to a potentiostat to control the potential of the working electrode and monitor the obtained current.

It is obvious that an amperometric immunosensor needs an electrochemical reaction to function. It is also obvious that the Ab-Ag interaction does not involve an electrochemical reaction. It is therefore necessary for amperometric immunosensors to use a labelling system to translate the affinity interaction into an electrochemical reaction.

1.3.3.2 Potentiometric transduction

In potentiometric immunosensors the recognition process is converted into a potential signal proportional to the concentration of species generated or consumed in the recognition process. The liberation of ions or gases leads to the development of a potential across the sample/transducer interface. The analytical signal of the process is generated under conditions of zero current.

Potentiometric transduction is simple and of low cost. Nevertheless, amperometric transduction still has advantages since it is more sensitive and faster than the potentiometric one.

The interaction of Ab-Ag on the electrode surface produces effective charge redistribution that under some conditions could be measured as potential signal. However, such changes are small and usually some labelling is needed for immunosensors.

1.3.3.3 Conductimetric transduction

Conductimetric transduction relies on the biological or chemical modulation of the surface conductivity. Conductimetric transduction is fast, inexpensive, does not require a reference electrode and is suitable for miniaturization. Strong dependence of the response upon the buffer capacity and upon the number of ions represents disadvantages of the conductimetric transduction.

1.3.3.4 Impedimetric transduction

Impedance spectroscopy (including Faradaic impedance in the presence of a redox probe and non-Faradaic-capacitance methods) is considered as a rapid technique for the characterization of the structure and functional operation of biomaterial-functionalized electrodes [3, 35]. The immobilization of biomaterials on electrodes produces changes in the capacitance and interfacial electron transfer resistance of electrodes causing changes

in the impedance. Hence interfacial changes generated by biorecognition processes can be detected by this electrochemical technique.

Faradaic impedance spectroscopy has been considered as a time-consuming method since typical duration time for an impedance spectrum experiment is 15 -20 minutes, due to the need of recording the impedance features within a broad region of frequencies [24]. This limitation could be overcome by the use of a single frequency value; however less accurate results may be obtained from this limited-frequency-range method.

Although the need for mobile electrolytes and the fact that electrodes can be easily fouled have been pointed out as disadvantages of electrochemical transduction [36], the use of conducting polymer coatings and the rational design of the immunosensor can help to overcome or minimize such possible drawbacks.

1.3.4 Immobilization methods

Methods for immobilization of the biological components include covalent binding, entrapment, cross-linking and adsorption. The appropriate immobilization of the immunoassay components is necessary for the retention of native conformation and binding characteristics of antibodies [37].

1.3.4.1 Immunosensor surface modification

Chemical modification of sensor surfaces has two main purposes: a) to attach selective groups that will later recognize the analyte and b) to increase the selectivity of the sensor by reducing interferences from non specific interactions.

Several chemical groups can be attached to surfaces, including small molecules or macromolecules. The formation of self assembled monolayers (SAMs) is widely used as a method of functionalization of the surface to immobilize biological compounds. This occurs through the formation of strong metal-S bonds of thiols that expose free carboxylate or amine groups that can be linked easily to biological compounds [38].

The major advantages of organized SAM immobilization compared to random immobilization such as hydrogel entrapment, are that SAMs allow ordered immobilizations and that the functionalized surface can be easily tailored by only changing the head groups of thiols. Also mass transport limitations are not as significant in monolayers as in hydrogels, a fact that is important in the case of high-molecular-weight molecule diffusion. Finally, in the case of SAM based immobilizations the bioactive molecules are positioned at a uniform distance from the surface/electrode layer rather than being distributed throughout a thick layer hydrogel [39]. Novel strategies for protein immobilization on metal surfaces using supramolecular chemistry have also been reported [40, 41].

1.3.4.2 Biomolecule immobilization

Of great importance in immunosensor development is the formation of an active surface with functional molecules. The immobilized molecules will decide the major part of the performance of the electrodes and they should be specifically orientated in order to enhance the immunosensor performance. Immobilization can be achieved through [42, 43] :

1. *Covalent binding* of the biomelecule or Ag to activated surface groups
2. *Entrapment* into a film or coating.
3. *Cross-linking* which is similar to entrapment, with the addition of a polymerization agent (*e.g.* glutaraldehyde) used to provide additional chemical linkages between the active and entrapped component and the film.
4. *Adsorption* via hydrophobic, hydrophilic or ionic interaction with a film or coating.
5. *Biological binding* by strong affinity interactions.

Reproducible immobilization of functional biomolecules is the challenge nowadays in biosensor development. Many immobilization methods are too complex or need too many

steps to be successfully transferred to large scale production. Entrapment and cross-linking methods are the simplest procedures for immobilization but they do not guarantee an orientated immobilization of the active molecule. The literature defines as ideal, the immobilization procedure which can be carried out in no more than three easy-to-do steps, can guarantee the adequate orientation of the functional molecule and is stable for at least 1 year with retention of more than 90 % of its specificity and sensitivity [16].

1.3.5 Immunoassay formats

Immunoassays can be divided into four main formats: direct binding, competition, displacement and sandwich formats. Fig. 1. 2 illustrates the basic configuration of the four formats. Introduction of a secondary labelled antibody, coating of surface with antigens covalently attached to macromolecules and pre-incubation of competing species are also widely used according to the analytical problem to be solved, the nature of the analyte, cost and availability of the immunoreactants and stability of the conjugates.

Direct binding (Fig. 1. 2 (a)): The analyte/antibody in solution binds directly to the receptor (antibody/analyte) on the surface. If the species in solution are labelled, then the procedure is called “direct”, oppositely if a second labelled compound (like a second labelled antibody) is needed, then the procedure is called indirect ELISA.

Competition assay (Fig. 1. 2 (b)): This assay involves competition between two reactants for a third one. One of the reactants is immobilized on the surfaces and the other two are

added simultaneously. A modification of this assay consists of a pre-incubation step for the two non-immobilized species before putting them in contact with the third one.

Displacement assay (Fig. 1. 2 (c)): In this assay, an analogue of the analyte of interest (sub-optimum antigen) is added to react with the immunoreactant on the surface. In direct assays the sub-optimum antigen is labelled while for indirect assays the labelled species are introduced in a later step.

In the case of labelled sub-optimum antigen, the addition of the analyte of interest displaces the sub-optimum labelled antigen and binds to the labelled antibody or simply displaces the labelled antigen from the immobilized immunoreactant. Higher analyte concentrations cause lower signals.

Displacement assay have the advantage of being short-time-requiring assays. The time needed is essentially the time required for the analytes to displace sufficient amount of the displaced compound. The time needed to displace a sufficient amount of detectable labelled antigen can be as short as a few seconds [44].

Competition and displacement assays are applied for the detection of small molecules in particular. [45].

Sandwich assay (Fig. 1. 2 (d)): This assay requires large antigens, as two antibodies are meant to bind to it. Therefore, small analytes cannot be detected by this format. Increasing analyte concentration generates an increase in signal. The use of a labelled antibody in the third step or the need for another labelled antibody (meaning a total of three antibody layers) give rise to direct or indirect sandwich assay respectively.

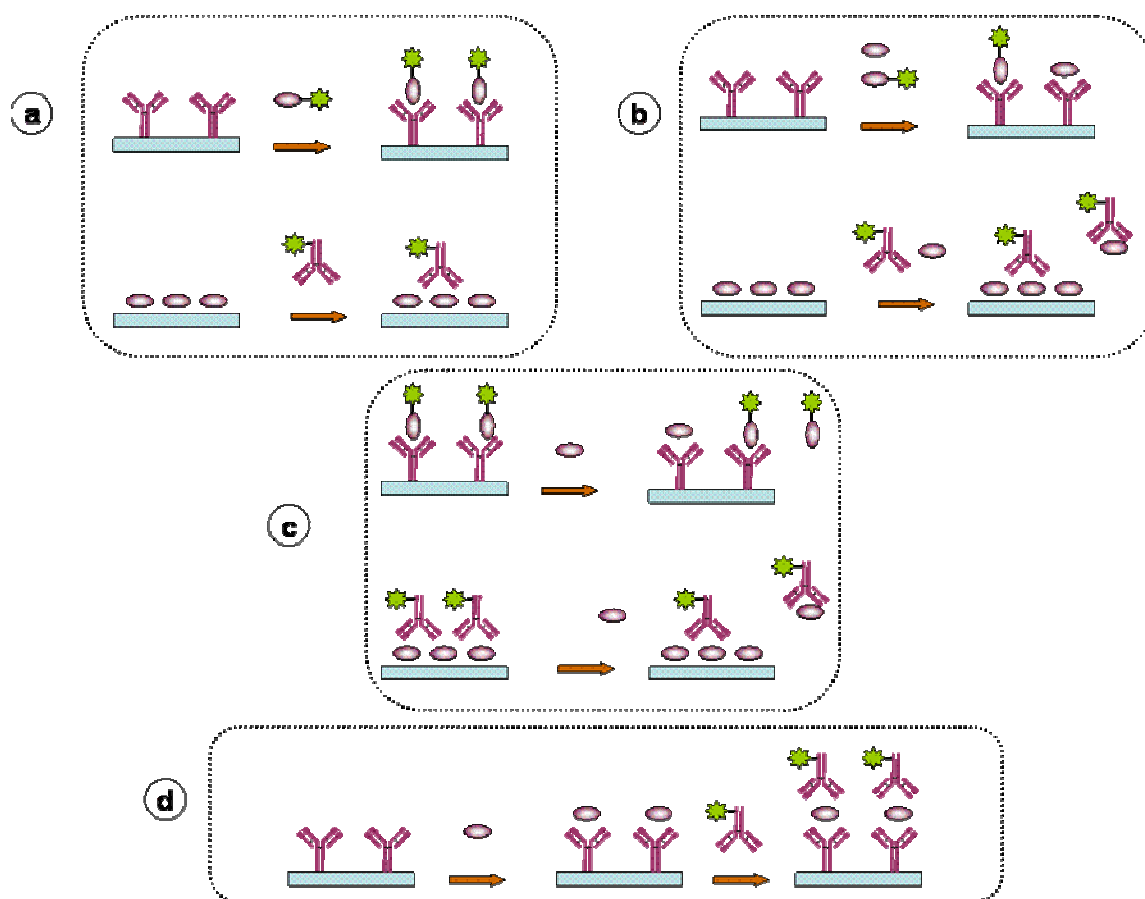


Fig. 1. 2:Immunoassay formats. (a) Direct binding; (b) Competition; (c) Displacement and (d) Sandwich assay

1.4 Overcoming Non Specific Adsorption

The developed immunosensor should be highly sensitive to the analyte of interest and at the same time should have high resistance to interactions with irrelevant components of the sample matrix, so as to avoid false sensor signal.

Several strategies have been reported to combat the NSA phenomenon; the use of proteins like bovine serum albumin (BSA) is an example of a protein broadly used to block the sensor surface [19]. Blocking agents include proteins (gelatin, casein), surfactants (Tween 20), Langmuir-Blodgett (LB) films and chemically designed surfaces [46-49]. The use of merely Fab portions has been found to minimize NSA, as this avoids using the entire immunoglobulin molecule which contains Fc sections to which molecules may attach [50]. The NSA phenomenon plays an especially critical role for low concentrations of analyte and has been reported as one of the main factors affecting the sensitivity of an immunoassay [51]. The lowest limit of detection of an immunoassay has been reported to be determined not only by the binding constant of the antibody but also by the NSA of the assay [44].

1.5 Commercialization

Biosensor technologies have a broad potential for commercialization in food, drink and chemical industries where real-time methods for monitoring, quantification and differential analysis of chemical processes and products are required [3, 4, 21].

However, despite the great number of immunosensor publications, only a few systems are commercially available. Limited lifetime of the biological components, difficulties in mass production and a “not-easy-to-do” analysis are considered as drawbacks for their commercialization [3]. Future improvements in the immunosensor field are anticipated to arise with the construction of immunosensor arrays and the expansion of antibody production by recombinant technologies [23].

1.6 The real-time, reagentless and fast responding paradigm

Of great interest is the development of biosensors that allow rapid and easy-to-do detection of the analyte of interest. The ability to use unmodified sample without the addition of any other reagents to obtain real time data is also desirable. The idea of simply applying a drop of untreated sample on a biosensor in order to obtain the required information is what motivates the exploration and advancement of these devices, *i.e.*, reagentless and real time immunosensors are called for.

To reach this objective immunosensors operating by displacement could result in reagentless, labelless and fast responding devices. Displacement immunosensors are based on the use of a labelled sub-optimum antigen that binds to the antibody and forms an immunocomplex to produce a detectable signal. These labelled sub-optimum antigens are displaced by the analyte generating a change in the generated signal. If the signal of the label is produced in the absence of other reactants, then displacement is the key point to reagentless and labelless immunosensors. Electrochemical devices have been described as simple and inexpensive. Additionally amperometric devices offer the simplest

operational mode [52]. Still, only a small percentage of the literature is dedicated to the development and study of displacement electrochemical immunosensors.

As far real time detection, optical signal transduction of surface plasmon resonance (SPR) has been widely used [9, 45, 53, 54]. Real time detection of small molecules like 2,4,6-trinitrotoluene (TNT) has been carried out by SPR under direct and indirect competitive immunoassays [55, 56]. Competitive real time detection of TNT has also been reported with the use of a flow system using fluorescence [57, 58]. An example of electrochemical, real time detection is the analysis of the pesticide atrazine using a competition format [7].

Regarding the application of a displacement format; electrochemical detection of polycyclic aromatic hydrocarbons (PAHs) has been reported using an indirect displacement immunoassay. The electrochemical detection was carried out via the addition of reagents it was not performed in real time [59]. Another example is the displacement electrochemical immunosensor for the herbicide 2,4-dichlorophenoxyacetic acid (2,4-D) [60] where, again, detection was not achieved in real time. The authors reported that the displacement efficiency can also be modulated by the antibody valency [61]. Displacement was used in an affinity column with electrochemical detection of the effluent [62, 63].

DNA sensors (another type of affinity sensors) are easier to be adapted to displacement [18]. Single-step electronic detection of femtomolar DNA by target-induced strand

displacement has been reported in a real time and label-free electronic DNA sensor. The authors achieved a subpicomolar detection limit [64].

Examples of reagentless detection include the immobilization of compounds covalently modified with the mediator [65, 66], or the use of redox polymers which also function as a network where other immunosensor components can be immobilized [65, 67, 68].

According to the previously mentioned published works, not many displacement electrochemical immunosensors (DEI) have been reported. In this work, the development of DEI is explored and implemented for the detection of 2,4,6-trichloroanisole.

1.7 The TCA problem. An overview

Cork taint is a musty, mouldy, earthy [69], corky [70], fungal-must [71] off-flavour in wine which has been mainly attributed to the presence of 2,4,6-trichloroanisole (TCA, Table 1. 1) in cork stoppers [69, 72-75]. The presence of this off-flavour costs the wine industry about 1 billion euro annually and a negative effect on the reputation of wineries [72, 76-78]. Different wine types can be distinctly affected by cork taint; higher incidence in white wines compared to red wines have been reported [79]. TCA sensory threshold in wine have been situated in the ppt range depending of the wine type; 3 ppt to 10 ppt for white wines [80-83] and 40 ppt to 50 ppt for red wines [81, 84]. Still, the wine industry widely uses cork stoppers because some enologists believe that they have a positive contribution to wine ageing and excellent sealing properties [85], and because of the positive image they create for the consumer.

Table 1. 1: TCA physical properties

TCA physical properties	
Synonym	2,4,6-trichloro-1-methoxybenzene
Molecular formula	$\text{Cl}_3\text{C}_6\text{H}_2\text{OCH}_3$
Molecular Weight	211.47
Boiling Point	132 °C 280 °mm Hg
Melting Point	60 – 62 °C
Water solubility	10 ppm [86] and 5.4 ppm [87]

1.8 Economic sectors affected by TCA

The most visible sectors affected by TCA are the wine and cork industries. Nevertheless, musty odours have also been reported in surface water [88, 89], potatoes (Nova Scotia potatoes) [90], sake [91] and Mexican coffee [92].

In most of the cases, the presence of TCA has been attributed to fungal and bacterial transformation of precursors that exist naturally in wood, although the problem is compounded by the use of pesticides and herbicides that provide the chlorine atoms [93].

1.9 Cork as wine stopper

1.9.1 *Quercus suber* for cork production

Cork is obtained from a species of oak tree (*Quercus suber*) that grows in several Mediterranean countries. It is fabricated from the outer bark (*suberose parenchyma*) of the oak tree.

Harvesting the first commercially acceptable cork can take over 43 years of tree growth (Fig. 1. 3). After the first 25 years, the virgin cork (first bark) is removed. At this stage the tree should have reached more than 0.6 m in diameter and 1.2 m in height. The second cork bark stripping occurs 10 years later. At this stage cork bark is not structurally homogeneous enough to produce natural (one-piece) cork stoppers. After another nine years approximately, the third generation of cork bark is ready to be commercialized. Each tree can be harvested every nine years which represents about 10 to 15 times in their lifetime as oak trees can live 150 to 250 years.

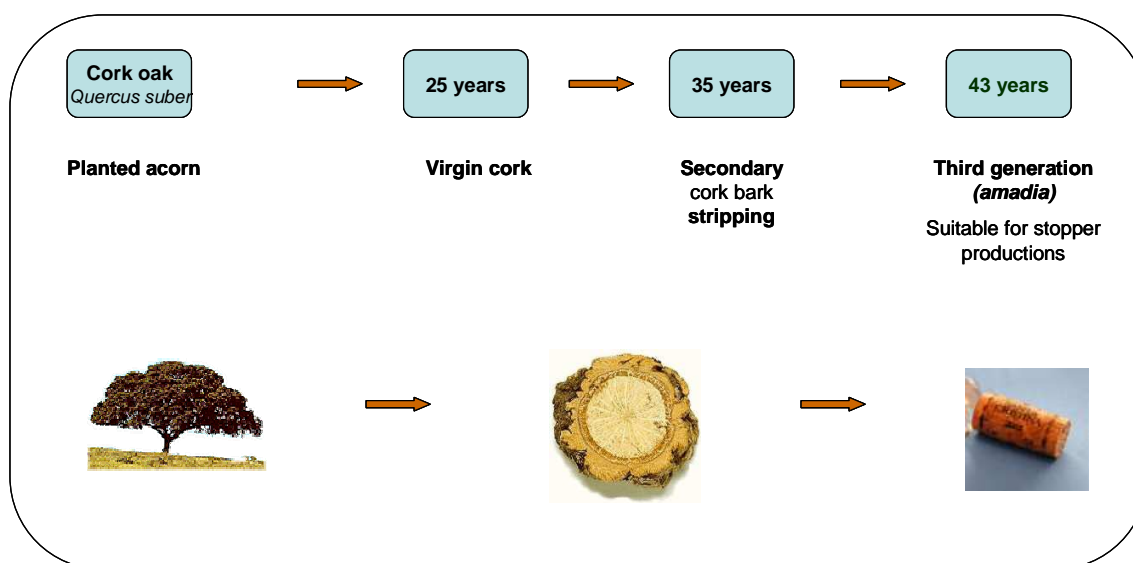


Fig. 1. 3: Cork harvesting (www.canadaportugalchamber.ca/cork.htm)

1.9.2 Chemical composition of Cork

The chemical composition of cork is approximately 43 % *suberin* (a polyester with mainly fatty acids side chains), 28 % lignin, 13 % cellulose, 6 % tannins, 5 % waxes and 5 % ash. About 90 % of the cork stopper is gas, resulting in a density of 0.12 to 0.20 kg

L⁻¹. Its excellent resilience after insertion into a bottle gives cork a unique capability as a bottle seal. This capability is conferred from its structure consisting of polygonal cells (30 to 42 million cm⁻³) separated by spaces filled with gas which slows oxygen diffusion without completely eliminating it [69].

1.9.3 Cork stoppers production

Once harvested, different washing, drying and cutting steps are required to finally obtain the bottle stopper (Fig. 1. 4).

Bark is harvested during spring and summer when new cells are growing making it more easily removable from the inner bark (*phloem*). After stripping, cork bark boards are stored in the forest or on factory yards as raw material for cork stopper production.

The next step is the boiling of the bark boards in large brick tubs for about one hour. The aim of this boiling step is to straighten out the boards and wash out some of the bitter and astringent tannins which are undesirable for its future use in wine bottling. Cork boards are then air-dried, boiled and dried a second time.

It is during the drying process when mould growth occurs, covering the boards with a white blanket of mycelia. This undesirable growth of mycelia could be avoided if washing and drying steps were carried out under controlled conditions in the cork industry. Autoclaving the cork boards are recommended, as during traditional boiling, the temperature within the boards does not exceed 87 °C. Therefore mould spores are not destroyed.

Afterwards, cork boards are sliced into sections, and sanded and graded into the desired cork size. Several washing and bleaching steps are applied to sanitize and to lighten the colour of the cork stoppers. Corks are dipped into a calcium hypochlorite bath for less than five minutes, and then kept at room temperature for at least two hours before rinsing and neutralizing the oxidant with oxalic acid solution.

Hypochlorite has been blamed as another possible source of chlorine atoms and therefore alternatives such as hydrogen peroxide are today widely used together with citric acid as a neutralizing agent. Other alternatives are potassium metabisulfide and sulfamic acid. In the case of sparkling wine corks, which are prepared from bark cork disks that are glued to an agglomerated section, ethanol and citric acid at elevated temperature are used. Ozone is now examined as an economically viable alternative.

The final steps consist of rinsing with clean water and adjusting moisture levels (5.5 % to 8 %) in continuous tunnel dryers to avoid the growth of microorganisms on the washed corks. Accurately adjusting the moisture levels helps to avoid conditions for mould growth, and at the same time maintains the expected flexibility necessary for sealing bottles.

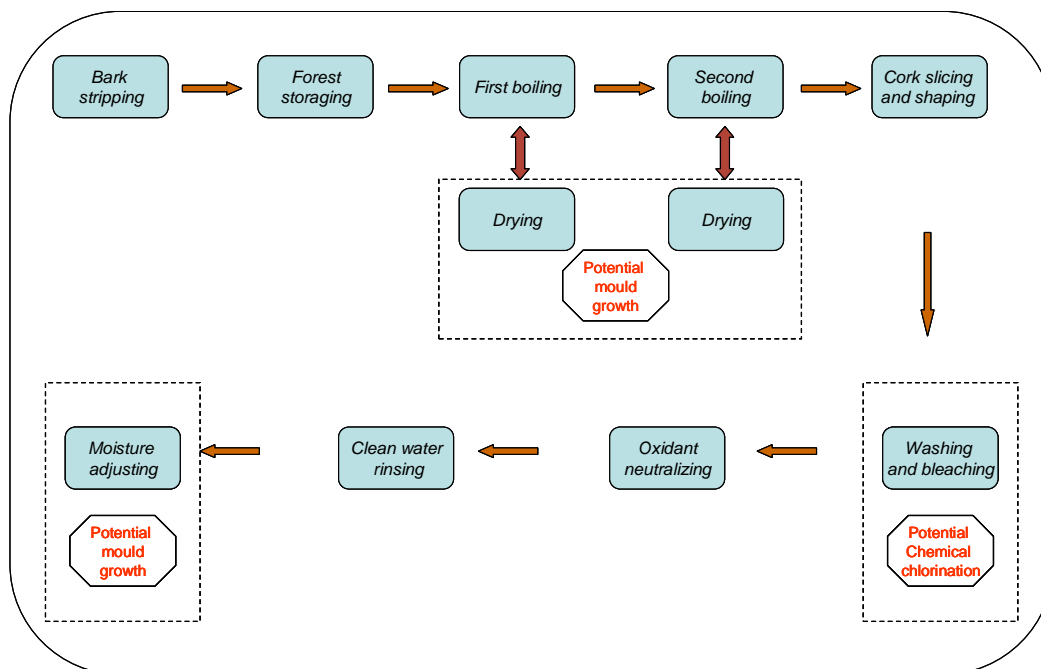


Fig. 1. 4: Schematic of cork stopper production

1.9.4 Cork taint components

Although the presence of TCA has been pointed out as the major reason for cork taint; over one-hundred volatiles have been reported in finished corks [69]. There are different chemical/biochemical pathways through which TCA can be formed during cork production (Fig. 1. 5) which essentially involve phenols as the basic structure, a chemical chlorination step and a microbial methylation [94]. Other mechanisms begin with the microbial methylation of phenolic components from the cork lignin. Mould genera that have been isolated from cork are *Penecillium*, *Aspergillus*, *Alternaria* (“yellow stain”), *Mucor*, *Monilia*, *Trichoderma*, *Cladosporium*, *Paecilomyces*, and *Phizoctonia* [95].

The chlorination of anisole in cork occurs during the hypochlorite wash step in cork processing, which forms TCA. Another important source of TCA is the original presence of chlorophenols in the cork bark. Their presence have been attributed to environmental pollution, the use of certain pesticides and herbicides in the cork forest, and absorption from wood preservatives during storage [70, 73, 78]. Trichlorophenol (TCP) can be methylated at any stage of cork processing or storage if moisture levels allow for mould activity.

Other compounds having sensory characteristics similar to TCA are tetra and pentachloroanisoles (2,3,4,6-tetrachloroanisole and pentachloroanisole) and bromoanisoles [96] (2,4,6-tribromoanisole TBA). Microbial dechlorination of tetra/pentachloroanisoles introduces these compounds for TCA formation [97, 98].

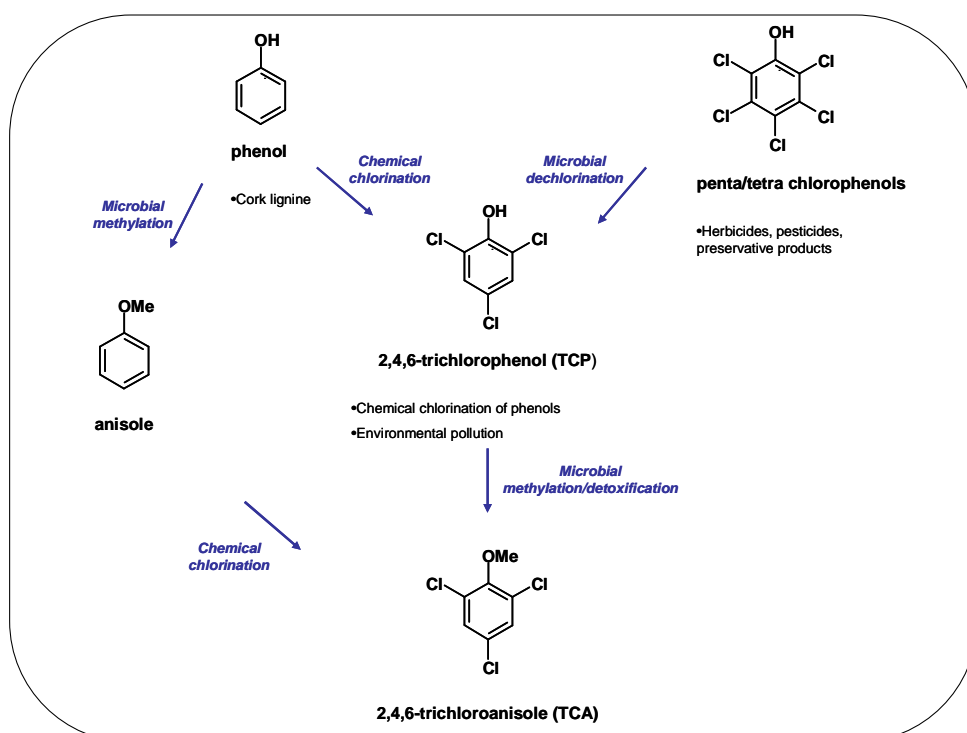


Fig. 1. 5: TCA formation chemical-biochemical pathways

1.9.5 How does TCA reach wine?

The transfer of TCA from cork to wine occurs mainly due to extraction in wine. TCA migration depends on factors such as [77]:

- TCA affinity for the surface and the interior part of the cork
- TCA location (surface of within the closure)
- the rates at which TCA can migrate through the cork matrix
- the contact area of the closure with wine

Contact surface, temperature and time were indicated as factors affecting TCA migration [99].

In an investigation of TCA migration utilizing corks spiked with 1 μ g TCA, it was revealed that after 4 and 8 months, detected migration was 4 % and 8 % respectively [100].

1.9.6 Removal of TCA

Methods which do not affect cork's mechanical and bottling properties like oxidation, irradiation, ultrafiltration and fungi have been employed with the aim of eliminating TCA.

Ozone and other sterilizing gases such as steam have been reported to efficiently remove bacteria and moulds from cork stoppers [72]. The use of ozone as a TCA removal agent in water was demonstrated to be capable of oxidizing most of the taste and odour compounds more efficiently than typical drinking water treatments [101].

The use of irradiation transforms TCA into molecular residues which do not confer negative organoleptic characteristics on cork. Electron beam irradiation of contaminated cork transformed TCA molecules into non-hazardous radiolytic products, with 2,4-dichloroanisole and 4-chloroanisole as the main components [102, 103].

Ultrafiltration with hydrophobic membranes has also been successfully utilized in the removal of TCA from surface water [82].

The use of fungi (*Chrysonilia sitophila*) has been recommended for industrial cork stopper production since it inhibits the development of other moulds and they do not produce the compounds responsible for cork taint, even in the presence of chlorophenols [104].

1.10 TCA detection

Because of its volatility, cork and wine matrix complexity and the low human taste threshold, TCA detection is especially challenging and beyond the sensitivity of most analytical systems [105].

1.10.1 Sensory detection

Sensory analyses have been widely used for the detection of TCA in corks and wine samples. Nevertheless, the type of evaluated wine can affect the ability of panelists, especially at low TCA concentrations [106]. For example, in a sample of red wines sensorially qualified as TCA-spoiled, only 75 % of the samples were actually contaminated with 2 to 25 ppt of TCA [107].

High correlation coefficient between sensory and instrumental (Gas Chromatography with Electron Capture Detection after Headspace Solid Phase Microextraction- HSPME GC ECD) analyses of TCA in white wine has been reported [108].

1.10.2 Detection in wine

The foremost techniques reported for TCA detection in wine are chromatography methods, where preparation and preconcentration steps are required.

Reviewing the literature (ISI Web of knowledge), the reported work on TCA detection in wine can be roughly divided so: 80 % detection with gas chromatography (GC), 15 % with immunoassays and 4 % with the application of electrochemical bioanalytical devices.

Gas chromatography (GC) works focus on the optimization of extraction, preconcentration and pretreatment for the detection with GC analysis. Extraction and preconcentration of TCA using headspace microextraction (HS SPME) followed by GC and electron-capture detection (GC-EDC) have been widely reported [87, 105, 109-114]. These methodologies achieved limits of detection at ppt level [84, 87, 114]. Limits of detection below the sensorial threshold level (0.2 to 2.4 ppt) have also been reported [115, 116].

Two-dimensional detection by coupling an electron capture detector (ECD) to an inductively coupled plasma mass spectrometer (ICP-MS) [117], purge-and-trap pre-

concentration coupled to capillary GC with atomic emission detection (PT-GC-AED) [118], and pervaporation of the analytes with a final determination by GC have also been reported [119, 120].

Magnetic stir bars with coating compounds specific for TCA adsorption prior to GC detection also demonstrated their suitability for TCA quantification [121, 122].

With regard to detection using immunoassays, indirect competitive enzyme-linked immunosorbent assay (ELISA), achieving limits of detection in the range of tens of ppt have been reported [83, 86]. Monoclonal and polyclonal antibodies were utilized in these works; amplification of the signal was also presented as an alternative. The use of selective antibody-antigen solid-phase extraction (SPE) of TCA prior to ELISA detection allowed limits of detection of 200-400 ppt [99].

Electrochemical immunosensing of TCA using polyclonal antibodies has been reported. The developed methodology achieved limits of detection in the ppt range. The reported limits of detection depend on the presence of ethanol in the samples [76].

Among the reported strategies for the detection of TCA in wine, electrochemical immunosensing is the strategy that requires the least experimental time since chromatography and ELISA methods, depending on the extraction, preconcentration and preparation steps required longer experimental time.

1.10.3 Detection in cork

Reported works of TCA detection in cork are mainly aimed at optimizing the extraction step prior to detection by GC [123]. Microwave-assisted extraction (MAE) [124], solid-phase microextraction (SPME) [125], liquid-solid extraction followed by stir bar sorptive extraction [126], pressurized liquid extraction [127] and supercritical fluid extraction [128] have been reported as steps in pre-concentration/preparation of cork samples for later quantification of TCA content by GC.

1.10.4 Detection in water

Reported detection techniques for TCA in water mainly consist of extraction, pre-concentration and GC detection [129-135].

1.11 Description of the industrial problem

It is now accepted that to guarantee the quality of cork for its use as a wine closure, a combination of innovations have to be implemented from the forest to the bottler. An important part in this process is the cork manufacturing factory. In this step, a combination of prevention, elimination, and detection innovations can reach acceptable levels of quality and standardization guarantee. A unit operation in this step that is very important is the initial boiling of cork bark. This is a batch or semi-batch process with a residence time of approximately 120 minutes. If it were possible to detect on line in the boiling water the presence of TCA, measures could be taken to either reject the raw material, extend the boiling period or replace the boiling water. The task of this on-line

control is therefore reduced to detecting TCA in water within a time appropriate to take these decisions at the levels that guarantee the quality of the product. It is established [136] that an acceptable product is guaranteed when a TCA concentration up to 10 ppt is found in the boiling water. If boiling is performed in appropriate equipment that permit the condensation of vapours from the boiling water a 15-fold enrichment in TCA concentration occurs. Any method of detection that could lead to an alarm at levels between 10 to 150 ppt would therefore be appropriate for implementation as an on-line device for cork stopper quality control and assurance. As discussed, SPME on PDMS fiber for 30 minutes with a thermal desorption of 3 minutes and GC/ECD or GC/MS detection allows quantification of TCA at ppt levels with total analysis time of about 45 minutes with robotic automation of sample preparation. This thesis examines the possibility of providing an easier to use method with the same or better performance characteristics base on immunodetection.

1.12 Objectives

The overall objective of this thesis has been to demonstrate the rational design of a Displacement Electrochemical Immunosensor (DEI) through its application to the detection of 2,4,6-trichloroanisole (TCA).

The following specific objectives have been established in order to achieve the overall objective:

1. Production and characterization of anti-TCA antibodies and development of an Indirect Competitive ELISA for the detection of TCA at human threshold concentration levels.
2. Description of the displacement phenomenon through a Mathematical Model that could aid the rational design of the Displacement Electrochemical Immunosensor.
3. Development of a Displacement Electrochemical Immunosensor for TCA detection.

1.13 Bibliography

- [1] Kissinger, P. *Biosens. Bioelectron.*, 2005, **20**, p. 2512-2516.
- [2] Sadana, A. *Engineering Biosensors. Kinetics and Design applications*. 2002, San Diego, California. USA, Academic Press.
- [3] Dornelles Mello, L., Tatsuo Kubota, L. *Food Chem.*, 2002, **77**, p. 237-256.
- [4] Weetall, H. H. *Biosens. Bioelectron.*, 1999, **14**, p. 237-242.
- [5] Rodriguez-Mozaz, S., Marco, M.P., Lopez de Alda, M.J., Barcelo, D. *Pure Appl. Chem.*, 2004, **76**(4), p. 723-752.
- [6] Rodriguez-Mozaz, S., Lopez de Alda, M.J., Marco, M.P., Barcelo, D. *Talanta*, 2005, **65**, p. 291-297.
- [7] Killard, A. J., Micheli, L., Grennan, K., Franek, M., Kolar, V., Moscone, D., Palchetti, I., Smyth, M. *Anal. Chim. Acta*, 2001, **427**, p. 173-180.
- [8] May, M. *The Scientist*, 2004, **18**(10), p. 36-41.
- [9] Campagnolo, C., Meyers, K., Ryan, T., Atkinson, R., Chen, Y., Scanlan, M., Ritter, G., Old, L., Batt, C. *J. Biochem. Biophys. Methods*, 2004, **61**, p. 283-298.
- [10] Sapsford, K., Charles, P., Patterson, C., Ligler, F. *Anal. Chem.*, 2002, **74**, p. 1061-1068.
- [11] Singh, S. *J. Hazardous Mat.*, 2007, **144**, p. 15-28.
- [12] Castiglione, F., Liso, A. *Immunopharmacol. Immunotoxicol.*, 2005, **27**(3), p. 417-432.
- [13] Campas, M., Prieto-Simon, B., Marty, J.L. *Talanta*, 2007, **72**(3), p. 884-895.
- [14] Campas, M., Marty, J.L. *Biosens. Bioelectron.*, 2007, **22**(6), p. 1034-1040.
- [15] Bermudo, M. C., Griffin, P.B., Garzon Ransanz, M., Ellis, J., Ciclitira, P., O'Sullivan, C.K. *Anal. Chim. Acta*, 2005, **551**, p. 105-114.
- [16] Taylor, R. F., Schultz, J.S. *Handbook of Chemical and Biological Sensors*. First Ed. ed. 1996, Bristol, U.K., Institute of Physics Publishing Ltd.
- [17] Thèvenot, D. R., Toth, K., Durts, R.A., Wilson, G.S. *Inter. Union Pure Appl. Chem.*, 1999, **71**(12), p. 2333-2348.
- [18] Mir, M., Katakis, I. *Anal. Bioanal. Chem.*, 2005, **381**, p. 1033-1035.
- [19] Shankaran, D. R., Gobi, K. v., Miura, N. *Sens. Actuators B*, 2007, **121**, p. 158-177.
- [20] Mairal, T., Oezalp, C., Lozano-Sanchez, P., Mir, M., Katakis, I., O'Sullivan, C. *Anal. Bioanal. Chem.*, 2007.
- [21] Chaubey, A., Malhotra, B. D. *Biosens. Bioelectron.*, 2002, **17**, p. 441-456.
- [22] Katz, E., Willner, I. *J. Electroanal. Chem.*, 1996, **418**, p. 67-72.
- [23] Hock, B. *Anal. Chim. Acta*, 1997, **347**, p. 177-186.
- [24] Katz, E., Willner, I. *Electroanalysis*, 2003, **15**(11), p. 913-947.
- [25] Van Emon, J. *Immunoassay and other Bioanalytical Techniques*. 2007, London, Taylor and Francis Group, LLC.
- [26] Ronkainen-Matsuno, N. J., Halsall, H.B., Heineman, W., *Electrochemical Immunoassays and Immunosensors*, in *Immunoassay and other Bioanalytical Techniques*, Van Emon, J., Editor. 2007, Taylor and Francis Group, LLC: London.
- [27] Crowther, J. R., *ELISA. Theory and Practice*. 1995, Humana Press: Totowa, New Jersey.
- [28] Harlow, E., Lane, D. *Using Antibodies. A Laboratory Manual*. 1999, Cold Spring Harbor, NY, Cold Spring Harbor Laboratory Press.
- [29] Murray, R., Granner, D., Mayes, P., Rodwell, V. *Harper's Biochemistry*. 25 th ed. 2000, USA, Mc Graw-Hill.
- [30] Warsinke, A., Benkert, A., Scheller, F.W. *Fresenius J. Anal. Chem.*, 2000, **366**, p. 622-634.
- [31] Goldbaum, F. A., Cauerhff, A., Velikovskiy, C.A., Llera, A., Riottot, M.M., Poljak, R.J. *J. Immunol.*, 1999, **162**, p. 6040-6045.
- [32] Roitt, I., Brostoff, J., Male, D. *Immunology*. Fifth ed. 1998, London, UK., Mosby International Ltd.
- [33] Almagro, J. C. *J. Mol. Recognit.*, 2004, **17**, p. 132-143.

- [34] Wang, J., *Electrochemical transduction*, in *Handbook of Chemical and Biological Sensors*, Taylor, R.F., Schultz, J.S., Editor. 1996, Institute of Physics Publishing: Bristol, UK.
- [35] Radi, A., Acero Sanchez, J.L., Baldrich, E., O'Sullivan, C. *Anal. Chem.*, 2005, **77**, p. 6320-6323.
- [36] Singh, K., Kaur, J., Varshney, G., Raje, M., Suri, R. *Bioconjugate Chem.*, 2004, **15**, p. 168-173.
- [37] Corry, B., Uilk, J., Crawley, C. *Anal. Chim. Acta*, 2003, **496**, p. 103-116.
- [38] Fung, Y. S., Wong, Y.Y. *Anal. Chem.*, 2001, **73**, p. 5302-5309.
- [39] Lahiri, J., Isaacs, L., Tien, J., Whitesides, G.M. *Anal. Chem.*, 1999, **71**, p. 777-790.
- [40] Fragoso, A., Caballero, J., Amirall, E., Villalonga, R., Cao, R. *Langmuir*, 2002, **18**, p. 5051-5054.
- [41] Fragoso, A., Amirall, E., Cao, R., Echegoyen, L., Gonzalez-Jonte, R. *Chem. Commun.*, 2004, p. 2230-2231.
- [42] Shah, J., Wilkins, E. *Electroanalysis*, 2003, **15**(3), p. 157-167.
- [43] Cosnier, S. *Biosens. Bioelectron.*, 1999, **14**, p. 443-456.
- [44] Ngo, T. *Anal. Letters*, 2005, **38**, p. 1057-1069.
- [45] Soelberg, S., Chinowsky, G., Spinelli, C., Stevens, R., Near, S., Kauffman, P., Yee, S., Furlong, C. *J. Ind. Microbiol. Biotechnol.*, 2005, **32**, p. 669-674.
- [46] Liu, V. A., Jastromb, W. E., Bhatia, S. N. *J. Biomed. Mater. Res.*, 2002, **60**, p. 126-134.
- [47] Harder, P., Grunze, M., Dahint, R., Whitesides, G. M., Laibinis, P. E. *J. Phys. Chem. B*, 1998, **102**, p. 426-436.
- [48] Chapman, R. G., Ostuni, E., Takayama, R., Homlim E., Yan L., Whitesides, G.M. *J. Am. Chem. Soc.*, 2000, **122**, p. 8303-8304.
- [49] Limbut, W., Kanatharana, P., Mattiasson, B., Asawatreratanakul, P., Thavarungkul, P. *Biosens. Bioelectron.*, 2006, **22**, p. 233-240.
- [50] Byfield, M. P., Abuknesha, R.A. *Biosens. Bioelectron.*, 1994, **9**, p. 373-400.
- [51] Okano, K., Takahashi, S., Yasuda, K., Tokinaga, D., Imai, K., Koga, M. *Anal. Biochem.*, 1992, **202**, p. 120-125.
- [52] Wang, J. *Biosens. Bioelectron.*, 2006, **21**, p. 1887-1892.
- [53] Karlsson, R. *Anal. Biochem.*, 1994, **221**, p. 142-151.
- [54] Stevens, R. C., Soelberg, S.D., Eberhart, B.T., Spencer, S., Wekell, J.C., Chinowsky, T.M., Trainer, V.L., Furlong, C.E. *Harmful Algae*, 2007, **6**(2), p. 166-174.
- [55] Miura, N., Shankaran, D.R., Kawaguchi, T., Matsumoto, K., Toko, K. *Electrochem.*, 2007, **75**(1), p. 13-22.
- [56] Larsson, A., Angbrant, J., Ekeroth, J., Mansson, P., Liedberg, B. *Sens. Actuators B*, 2006, **113**, p. 730-748.
- [57] Bromage, E. S., Lackie, T., Unger, M.A., Kaattari, S.L. *Biosens. Bioelectron.*, 2007, **22**(11), p. 2532-2538.
- [58] Van der Voort, D., Pelsers, M.M.A.L., Korf, J., Hermens, W.T., Glatz, J.F.C. *Biosens. Bioelectron.*, 2003, **19**, p. 465-471.
- [59] Fahnrich, K. A., Pravda, M., Guillbault, G.G. *Biosens. Bioelectron.*, 2003, **18**, p. 73-82.
- [60] Gerdes, M., Spener, F., Meusel, M. *Quim. Anal.*, 2000, **19**, p. 8-14.
- [61] Gerdes, M., Meusel, M., Spener, F. *J. Immunol. Methods*, 1999, **223**, p. 217-226.
- [62] Kaptein, W., Zwaagstra, J.J., Venema, K., Ruiters, M. H. J., Korf, J. *Sens. Actuators B*, 1997, **45**, p. 63-69.
- [63] Valat, C., Limoges, B., Huet, D., Romette, J.L. *Anal. Chim. Acta*, 2000, **404**, p. 187-194.
- [64] Xiao, Y., Lubin, A.A., Baker, B.R., Plaxco, K.W., Heeger, A.J. *Proceedings of the national academy of sciences of the united states of america*, 2006, **103**(45), p. 16677-16680.
- [65] Radi, A., Acero Sanchez, J.L., Baldrich, E., O'Sullivan, C. *J. Am. Chem. Soc.*, 2006, **128**, p. 117-124.
- [66] Campuzano, S., Galvez, R., Pedrero, M., de Villena, F., Pingarrón, M. *J. Electroanal. Chem.*, 2002, **526**, p. 92-100.
- [67] Calvo, E. J., Danilowicz, C.B., Wolosiuk, A. *Phys. Chem. Chem. Phys.*, 2005, **7**(8), p. 1800-1806.
- [68] Reiter, S., Habermuller, K., Schuhmann, W. *Sens. Actuators B*, 2001, **79**, p. 150-156.
- [69] Butzke, C., Evans, T.J., Ebeler, S., *Detection of Cork Taint in Wine Using Automated Solid-Phase MicroExtraction in Combination with GC/MS-SIM*, in *Chemistry of Wine Flavor*, Waterhouse, A., Ebeler, S., Editor. 1998, American Chemical Society: Washington, DC.
- [70] Chatonnet, P., Labadie, D., Boutou, S. *J. Int. sci. vigne et du vin*, 2003, **37**(3), p. 181-193.

- [71] Simpson, R. F., Capone, D.L., Sefton, M.A. *J. Agric. Food Chem.*, 2004, **52**(17), p. 5425-5430.
- [72] Vlachos, P., Kampioti, A., Kornaros, M., Lyberatos, G. *Eur. Food Res. Technol.*, 2007, **225**(5-6), p. 653-663.
- [73] Simpson, R. F., Sefton, M.A. *Australian J. Grape Wine Research*, 2007, **13**(2), p. 106-116.
- [74] Boutou, S., Chatonnet, P. *J. Chromatogr. A*, 2007, **1141**(1), p. 1-9.
- [75] Pena-Neira, A., Fernandez de Simon, B., Garcia-Vallejo, M.C., Hernandez, T., Cadahia, E., Suarez, J.A. *Eur. Food Res. Technol.*, 2000, **211**(4), p. 257-261.
- [76] Moore, E., Pravda M., Guilbault, G.G. *Anal. Chim. Acta*, 2003, **484**(1), p. 15-24.
- [77] Sefton, M. A., Simpson, R.F. *Australian J. Grape Wine Research*, 2005, **11**(2), p. 226-240.
- [78] Coque, J., Alvarez-Rodriguez, M., Larriba, G. *Applied Env. Microb.*, 2003, **69**(9), p. 5089-5095.
- [79] Soleas, G. J., Yan, J., Seaver, T., Goldberg, D.M. *J. Agric. Food Chem.*, 2002, **50**(5), p. 1032-1039.
- [80] Prescott, J., Norris, L., Kunst, M., Kim, S. *Food Qual. Pref.*, 2005, **16**, p. 345-349.
- [81] Sanvicens, N., Sanchez-Baeza, F., Marco M.P. *J. Agric. Food Chem.*, 2003, **51**, p. 3924-3931.
- [82] Park, N., Lee, Y., Lee, S., Cho, J. *DESALINATION*, 2007, **212**(1-3), p. 28-36.
- [83] Lauster, R., Sanvicens, N., Marco, M.P., Hock, B. *Anal. Letters*, 2003, **36**(4), p. 713-729.
- [84] Riu, M., Mestres, A., Busto, O., Guasch, J. *J. Chromatogr. A*, 2002, **977**(1), p. 1-8.
- [85] Vasserot, Y., Pitois, C., Jeandet, P. *Am. J. Enol. Viticult.*, 2001, **52**(3), p. 280-281.
- [86] Sanvicens, N., Varela, B., Marco M.P. *J. Agric. Food Chem.*, 2003, **51**, p. 3932-3939.
- [87] Alzaga, R., Ortiz, L., Sanchez-Baeza, F., Marco, M.P., Bayona, J.M. *J. Agric. Food Ind.*, 2003, **51**, p. 3509-3514.
- [88] Salemi, A., Lacorte, S., Bagheri, H., Barcelo, D. *J. Chromatogr. A*, 2006, **1136**(2), p. 170-175.
- [89] Zhang, L. F., Hu, R.K., Yang, Z.G. *J. Chromatogr. A*, 2005, **1098**(1-2), p. 7-13.
- [90] Daniels-Lake, B. J., Prange, R.K., Gaul, S.O., McRae, K.B., de Antueno, R. *J. Am. Soc. Horticul. Sci.*, 2007, **132**(1), p. 112-119.
- [91] Miki, A., Isogai, A., Utsunomiya, H., Iwata, H. *J. Biosci. Bioeng.*, 2005, **100**(2), p. 178-183.
- [92] Cantergiani, E., Brevard, H., Krebs, Y., Feria-Morales, A., Amado, R., Yeretian, C. *Eur. Food Res. Technol.*, 2001, **212**(6), p. 648-657.
- [93] Gunschera, J., Fuhrmann, F., Salthammer, T., Schulze, A., Uhde, E. *Environ. Sci. Pollut. Res.*, 2004, **11**(3), p. 147-151.
- [94] Alvarez-Rodriguez, M. L., Lopez-Ocana, L., Lopez-Coronado, J.M., Rodriguez, E., Martinez, M.J., Larriba, G., Coque, J.J.R. *Applied Env. Microb.*, 2002, **68**(12), p. 5860-5869.
- [95] Prak, S., Gunata, Z., Guiraud, J., Schorr-Galindo, S. *Food Microbiol.*, 2007, **24**(3), p. 271-280.
- [96] Chatonnet, P., Bonnet, S., Boutou, S., Labadie, M.D. *J. Agric. Food Chem.*, 2004, **52**(5), p. 1255-1262.
- [97] Zoecklein, B., Fugelsang, K., Gump, B., Nury, F. *Análisis y Producción de Vino*, ed. Acribia, S.A. 2001, Huesca. España, Aspen Publishers, Inc.
- [98] Insa, S., Besalu, E., Iglesias, C., Salvado, V., Antico, E. *J. Agric. Food Chem.*, 2006, **54**(3), p. 627-632.
- [99] Sanvicens, N., Moore, E., Guilbault, G., Marco, M.P. *J. Agric. Food Chem.*, 2006, **42**, p. 9176-9183.
- [100] Juanola, R., Subirà, D., Salvadó, V., García, J.A., Anticó, E. *Eur. Food Res. Technol.*, 2005, **220**, p. 347-351.
- [101] Peter, A., Von Gunten, U. *Environ. Sci. Technol.*, 2007, **41**(2), p. 626-631.
- [102] Careri, M., Mazzoleni, V., Musci, M., Molteni, R. *Chromatographia*, 2001, **53**(9-10), p. 553-557.
- [103] Pereira, C., Gil, L., Carrico, L. *Rad. Phys. Chem.*, 2007, **76**(4), p. 729-732.
- [104] Pereira, C. S., Pires, A., Valle, M.J., Boas, L.V., Marques, J., San Romao, M.V. *J. Ind. Microbiol. Biotechnol.*, 2000, **24**(4), p. 256-261.
- [105] Gomez-Ariza, J. G.-B., T; Lorenzo, F; Beltran, R. *J. Chromatogr. A*, 2006, **1112**(1-2), p. 133-140.
- [106] Mazzoleni, V., Maggi, L. *Food Res. Int.*, 2007, **40**(6), p. 694-699.
- [107] Jonsson, S., Uusitalo, I., van Bavel, B., Gustafsson, I.B., Lindstrom, G. *J. Chromatogr. A*, 2006, **1111**(1), p. 71-75.
- [108] Juanola, R., Guerrero, L., Subira, D., Salvado, V., Insa, S., Regueiro, J.A.G., Antico, E. *Anal. Chim. Acta*, 2004, **513**(1), p. 291-297.
- [109] Insa, S., Besalu, E., Salvado, V., Antico, E. *J. Separation Sci.*, 2007, **30**(5), p. 722-730.

-
- [110] Carrillo, J. D., Tena, M.T. *Anal. Bioanal. Chem.*, 2006, **385**(5), p. 937-943.
- [111] Martinez-Urunuela, A., Gonzalez-Saiz, J.M., Pizarro, C. *J. Chromatogr. A*, 2005, **1089**(1-2), p. 31-38.
- [112] Lizarraga, E., Irigoyen, A., Belsue, V., Gonzalez-Penas, E. *J. Chromatogr. A*, 2004, **2004**(1-2), p. 145-149.
- [113] Martinez-Urunuela, A., Gonzalez-Saiz, J.M., Pizarro, C. *J. Chromatogr. A*, 2004, **1056**(1-2), p. 49-56.
- [114] Martendal, E., Budziak, D., Carasek, E. *J. Chromatogr. A*, 2007, **1148**(2), p. 131-136.
- [115] Martinez-Urunuela, A., Rodriguez, I., Cela, R., Gonzalez-Saiz, J.M., Pizarro, C. *Anal. Chim. Acta*, 2005, **549**(1-2), p. 117-123.
- [116] Insa, S., Antico, E., Ferreira, V. *J. Chromatogr. A*, 2005, **1089**(1-2), p. 235-242.
- [117] Gomez-Ariza, J. L., Garcia-Barrera, T., Lorenzo, F., Beltran, R. *J. Anal. Atomic Spectr.*, 2005, **20**(9), p. 883-888.
- [118] Campillo, N., Aguinaga, N., Vinas, P., Lopez-Garcia, I., Hernandez-Cordoba, M. *J. Chromatogr. A*, 2004, **1061**(1), p. 85-91.
- [119] Gomez-Ariza, J. L., Garcia-Barrera, T., Lorenzo, F., Beltran, R. *J. Chromatogr. A*, 2004, **1049**(1-2), p. 147-153.
- [120] Gomez-Ariza, J. L., Garcia-Barrera, I., Lorenzo, E. *Anal. Chim. Acta*, 2004, **516**(1-2), p. 165-170.
- [121] Zalacain, A., Alonso, G.L., Lorenzo, C., Iniguez, M., Salinas, M.R. *J. Chromatogr. A*, 2004, **1033**(1), p. 173-178.
- [122] Hayasaka, Y., MacNamara, K., Baldock, G.A., Taylor, R.L., Pollnitz, A.P. *Anal. Bioanal. Chem.*, 2003, **375**(7), p. 948-955.
- [123] Juanola, R., Subira, D., Salvado, V., Regueiro, J.A.G., Antico, E. *J. Chromatogr. A*, 2002, **953**, p. 207-214.
- [124] Pizarro, C., Perez-del-Notario, N., Gonzalez-Saiz, J.M. *J. Chromatogr. A*, 2007, **1149**(2), p. 138-144.
- [125] Carasek, E., Cudjoe, E., Pawliszyn, J. *J. Chromatogr. A*, 2007, **1138**(1-2), p. 10-17.
- [126] Callejon, R. M., Troncoso, A.M., Morales, M.L. *Talanta*, 2007, **71**(5), p. 2092-2097.
- [127] Gomez-Ariza, J. L., Garcia-Barrera, T., Lorenzo, F., Gonzalez, A.G. *Anal. Chim. Acta*, 2005, **540**(11), p. 17-24.
- [128] Taylor, M. K., Young, T.M., Butzke, C.E., Ebeler, S.E. *J. Agric. Food Chem.*, 2000, **48**(6), p. 2208-2211.
- [129] Zhang, L. F., Hu, R.K., Yang, Z.G. *Water Res.*, 2006, **40**(4), p. 699-709.
- [130] Diaz, A., Ventura, F., Galceran, T. *J. Chromatogr. A*, 2005, **1064**(1), p. 97-106.
- [131] Sung, Y. H., Li, T.Y., Huang, S.D. *Talanta*, 2005, **65**(2), p. 518-524.
- [132] Shin, H. S., Ahn, H.S. *Chromatogr.*, 2004, **59**, p. 107-113.
- [133] Benanou, D., Acobas, F., de Roubin, M.R. *Water Sci. Technol.*, 2004, **49**(9), p. 161-170.
- [134] Benanou, D., Acobas, F., de Roubin, M.R., Sandra, F. *Anal. Bioanal. Chem.*, 2003, **376**(1), p. 69-77.
- [135] Palmentier, J., Taguchi, V. *Analyst*, 2001, **126**(6), p. 840-845.
- [136] Katakis, I. p. c.-o. *INNOvation in the process of Cork prodUction for the elimination of odours responsible for cork taint. A demonstration project funded by the Fifth Framework Programme of the European Commission*. INNOCUOUS; QLK1-CT-2002-01678.

CHAPTER 2

Indirect competitive ELISA for 2,4,6-trichloroanisole (TCA) detection

2.1 Introduction and aims

Research work concerning 2,4,6-trichloroanisole (TCA) detection includes two main groups of techniques: gas chromatography usually coupled to either mass spectrometer, electron capture or atomic emission detectors [1-5] and the immunoassay alternative. Enzyme-linked immunosorbent assay (ELISA) emerged during the 1980's as a sensitive and inexpensive analytical method for both clinical and environmental applications. ELISA offers advantages such as low cost per analysis, parallel processing, high sensitivity and high selectivity [6].

The key step in immunoassay development is the production of a specific antibody against the analyte of interest. Studies for the understanding of the generation of antibodies for small molecules started back in the 1930's, when Karl Lansteiner stated

that small molecules ($MW < 2$ KDa) were not capable of inducing an immune response themselves. He proposed the use of covalently attached carrier proteins to induce an immune response [7]. Therefore, it is necessary to modify the small molecule (hapten) for coupling with macromolecules (carrier) so as to make a stable carrier-hapten complex [8]. In this sense, the most critical step in the production of selective antibodies against small molecules as target analyte, is the appropriate selection and preparation of the analyte derivative [9-11]. The right selection of haptenized antigen have demonstrated to be the crucial point for the ELISA development [9, 12, 13].

The development of ELISA for TCA detection has been reported: using polyclonal antibodies, direct competitive ELISA with limits of detection of 1 ppb ($\mu\text{g L}^{-1}$) have been developed [14]; also indirect competitive assays with or without previous solid-phase extraction (SPE), allowed limits of detection of 200-400 ppt and 44 ppt respectively [15, 16]. The detection of TCA using monoclonal antibodies in indirect competitive ELISA was also reported; in this case the limits of detection were 20 ppt and 10 ppt using two different monoclonal antibodies with and without amplification of the signal respectively, demanding a total assay time of about 3 hours [17].

It is the aim of this work to develop an ELISA with a detection limit closely matching the human TCA sensory threshold in a relatively short experimental time suitable for industrial application.

Consequently, the rational design of an indirect competitive ELISA for the detection of TCA (the antigen of interest or analyte, Ag) at parts-per-trillion (ppt) levels, using a

Chapter 2

Indirect competitive ELISA for 2,4,6-Trichloroanisole (TCA) detection

specifically developed monoclonal antibody (MAb), is described in this chapter. The design was carried out according to: *i*) Characterization and selection of specific monoclonal antibody (MAb); *ii*) Generation of suboptimum haptens; *iii*) Estimation of MAb-coating hapten (non-competitive ELISA) and MAb-Ag (indirect competitive ELISA) affinity constants (K_{aff}); *iv*) Selection of the appropriate coating hapten towards indirect competitive ELISA design; *v*) Optimization of indirect competitive ELISA and TCA determination; *iv*) Improvement of the total assay time.

In this way, an indirect competitive ELISA procedure for the detection of TCA with detection limit in the order of ppt, and an assay time of less than 80 minutes, was developed.

2.2 Materials

2.2.1 Chemicals

2,4,6-Trichloroanisole (TCA, 99 %), 2,4,6-Trichlorophenol (TCP 98 %), Keyhole Limpet Hemocyanin (KHL), Bovine Serum Albumin (BSA), 3,3',5,5'-tetramethylbenzidine (TMB, Liquid Substrate for ELISA) as well as solvents and salts for buffer preparations and chemicals reagents were purchased from Sigma-Aldrich Chemical Co. (Spain).

Anti-TCA monoclonal antibody clones were developed in collaboration with Antibodyshop (Denmark). Hybridomas were obtained from mice immunized with Keyhole Limpet Hemocyanin conjugated with 3-(2,4,6-trichloro-3-methoxy phenyl) propionic acid (KLH-Hapten A). The MAbs in 89.9 % RPMI 1640, 10.0 % Fetal Calf Serum and 0.1 % sodium azide, were selected according to cross-reactivity with TCP-

Chapter 2

Indirect competitive ELISA for 2,4,6-Trichloroanisole (TCA) detection

haptens. The selected MAb was purified (0.01 M phosphate buffer, pH 7.4 with 0.5 M NaCl and 15 mM sodium azide; Antibodyshop) and kept at 4 °C. Horseradish peroxidase (HRP)-conjugated goat anti-Mouse (antiIgG-HRP) and anti-Mouse IgG (Fc specific, antiFcIgG) antibody produced in goat were purchased from Sigma-Aldrich Chemical Co. (Spain).

All reagents were of analytical grade, unless stated otherwise.

TCA solutions containing 4 % EtOH were prepared starting with mother solutions of 1000 ppm TCA in EtOH. These mother solutions were first diluted 1000-fold in phosphate-buffered saline (PBS) containing 4 % EtOH and next dilutions from ppb to ppt level were carried out in order to keep EtOH content constant (4 %). TCA handling was carried out in glass in order to avoid TCA adsorption on the containers.

TCA solutions containing 4 % EtOH and enzyme solutions were prepared daily. Deionized water purified in a Milli-Q system (Millipore, Bedford, MA, USA) was used to prepare solutions unless otherwise indicated.

All blocking, washing and coating steps of the ELISA procedures described next were carried out using:

- Phosphate-buffered saline (PBS): 0.01 M phosphate buffer with pH 7.4
- *Washing buffer*: PBS with 0.05 % Tween 20
- *Blocking buffer*: PBS with 2 % milk powder
- *Coating buffer*: 0.05 M carbonate-bicarbonate buffer, pH 9.6

2.2.2 Instrumentation and apparatus

ELISA plates were read using a Microplate Spectrophotometer SpectraMax 340 PC from Molecular Devices (bioNOVA Científica, Spain). Absorbance measurements for activity assays were collected using Hewlett Packard UV-Vis Spectrophotometer 8453/G1103A with Deuterium discharge lamp and diode array detector, interfaced with a PC (Hewlett Packard Española. Agilent Technologies, Spain). Measurements of pH and conductivity were obtained with a CyberScan 2000 pH meter (Eutech Instruments, Netherlands) and a Crison Micro CM 2202 conductimeter (Instrumentos Científicos, Spain) respectively. Incubations were performed in an orbital incubator (SI50, Stuart Scientific, USA). Accelerated Aging experiments were carried out in a JPSelecta 2000208 oven (J.P Selecta, Spain).

Microspin G25 centrifugal device, and NAP-10 G25 columns were obtained from Amersham Biosciences (Sweden). Immunopure (Protein A) IgG Purification Kit was obtained from Pierce Biotechnology (Cultek, Spain). Polystyrene microtiter plates were purchased from Nunc (Maxisorp, Denmark).

The characterization of bioconjugates was carried out using matrix assisted laser desorption ionization-time-of-flight mass spectrometry (MALDI TOF) on a stainless steel plate with a software Voyager DE-STR High Performance from MALDI-TOF Mass Spectrometer from Applied Biosystems.

TCA detection by Gas Chromatography was carried out using a Gas Chromatograph equipped with a ⁶³Ni electron capture detector also from Varian.

2.2.3 Haptens production

Derivatives of the analyte (Haptens, Fig. 2. 1) were prepared according to published work: 3-(2,4,6-Trichloro-3-methoxyphenyl) propanoic Acid (Hapten A, HA) and 5-(2,4,6-Trichlorophenoxy) pentanoic Acid (Hapten B, HB) [18], 2,4,6-Trichlorophenoxyacetic acid (Hapten 1, H1) [10], 3-Chloro-2-methylphenoxyacetic Acid (Hapten 3, H3) [19] and 3-(3-Hydroxy-2,4,6-trichlorophenyl)-propanoic Acid (Hapten Ph, HPh) [11]. 3-(4-Methoxyphenyl) propionic acid (Hapten Z, HZ) was purchased from Sigma-Aldrich Chemical Co. (Spain).

2.2.4 Hapten carrier (KHL-Hapten A) and coating haptens (BSA-Hapten) preparation

Preparations of immunogen (KHL-Hapten A) and coating haptens (Bovine Serum Albumin BSA- Hapten; BSA-HA, BSA-HPh, BSA-HB, BSA-H1, BSA-H3, BSA-HZ) were carried out by the active ester method [17, 18]. The conjugation was characterized by MALDI-TOF-MS by mixing 5 μL of the matrix (3,5-Dimethoxy-4-hydroxycinnamic acid 10 mg mL^{-1} (Sinapic acid) in $\text{CH}_3\text{CN}/\text{H}_2\text{O}$ 1:1, 0.1 % TFA) with 5 μL of the investigated solution (10 mg mL^{-1} in $\text{CH}_3\text{CN}/\text{H}_2\text{O}$ 1:1, 0.1 % TFA) . The conjugates were lyophilized and stored freeze-dried at $-25\text{ }^\circ\text{C}$ until use.

Chapter 2

Indirect competitive ELISA for 2,4,6-Trichloroanisole (TCA) detection

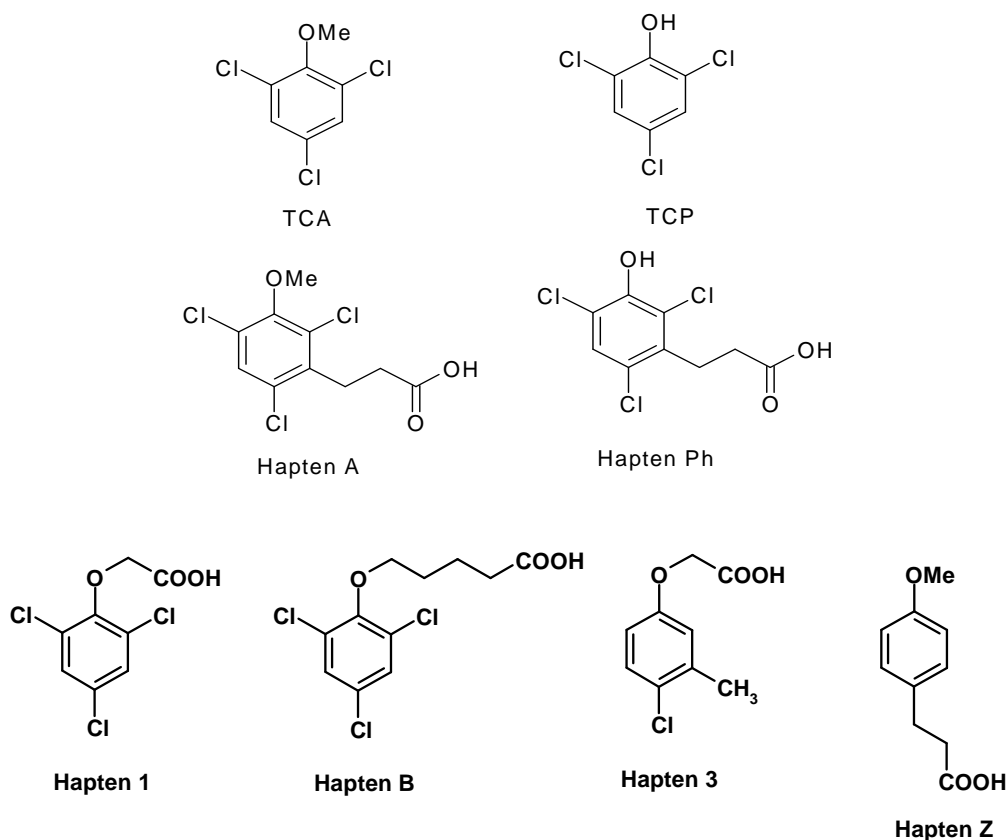


Fig. 2. 1: Chemical structures of TCA, TCP and derivates of the analyte (haptens) investigated for the design of the indirect competitive ELISA.

2.2.5 TCA detection by Gas Chromatography

The simplified SPME/GC-ECD method was as follows: Measurement of 2,4,6-TCA was carried out using GC/ECD. The Solid Phase MicroExtraction (SPME) was performed using PDMS fibers (100µm) obtained from Supelco. Chromatographic analyses were performed in a Varian 3600 Gas Chromatograph equipped with a ⁶³Ni electron capture detector also from Varian. Injection at 250°C was carried out in the splitless mode (2 min). Separation was achieved using a CP-Sil5 CB 50 m x 32 mm x 0.20 µm, Chrompack capillary column, from Varian. Carrier gas was high-purity helium flowing through the column at 2 ml/min. The oven temperature was held at 70°C for 1 min, and it was raised to 150°C with 25°C/min (2 min), and then to 200°C at 5°C/min (2 min) and finally to 250°C at 5°C/min. (5 min.). The ECD temperature was set at 300°C. TCA samples

prepared to be analysed through ELISA or electrochemical measurements were contrasted with GC results.

2.2.5 ELISA procedures

In other to evaluate the effects of several factors as well as study the improvement of the indirect competitive ELISA for TCA detection, different procedures were established.

2.2.5.1 Procedure 1: Indirect non-competitive ELISA (INCE)

Fig. 2. 2 depicts the general procedure followed for INCE. The evaluation of the interaction of the MAb with the different coating haptens (BSA-Hx, where x represents any of the investigated haptens) was carried out following Procedure 1 (Fig. 2. 2).

Controls description corresponds to the step at which the control was implemented (step 1: absence of coating hapten or absence of hapten in the coating; step 2: no addition of MAb (only PBS) and steps 1 and 2: absence of hapten in the coating together with no addition of MAb). The absorbance values used in this work always correspond to corrected absorbance values (Abs_i), where the non corrected absorbance (Abs_{NCi}) was corrected by subtracting the average absorbance of the controls ($Abs_{controls}$).

2.2.5.2 Procedure 2: Indirect non-competitive ELISA (INCE) for cross-reactivity study

In order to evaluate the cross-reactivity of the clones, procedure 1 (Fig. 2. 2) using BSA-HA or BSA-HPh as coating haptens ($1\mu\text{g mL}^{-1}$) was carried out. The cross-reactivity was calculated as follows:

Chapter 2

Indirect competitive ELISA for 2,4,6-Trichloroanisole (TCA) detection

$$\% \text{ Cross - reactivity} = \frac{\text{IC}_{50 \text{ BSA-HPh}}}{\text{IC}_{50 \text{ BSA-HA}}} * 100 \quad \text{Eq.2. 1}$$

where $\text{IC}_{50 \text{ BSA-HA}}$ is the corrected absorbance obtained when the microtiter plate was coated with BSA-HA and $\text{IC}_{50 \text{ BSA-HPh}}$ corresponds to corrected absorbance when the microtiter plate was coated with BSA-HPh.

2.2.5.3 Procedure 3: Indirect non-competitive ELISA (INCE) for ethanol effects study

Since TCA has low water solubility, organic solvents are required to produce the mother solutions. Dimethyl sulfoxide (DMSO), methanol (MeOH) and ethanol (EtOH) were investigated in preliminary experiments. In contrast to EtOH, non-reproducible data was observed for DMSO and MeOH (data not shown). EtOH was therefore used and its effects on the immunoassay were investigated.

Chapter 2

Indirect competitive ELISA for 2,4,6-Trichloroanisole (TCA) detection

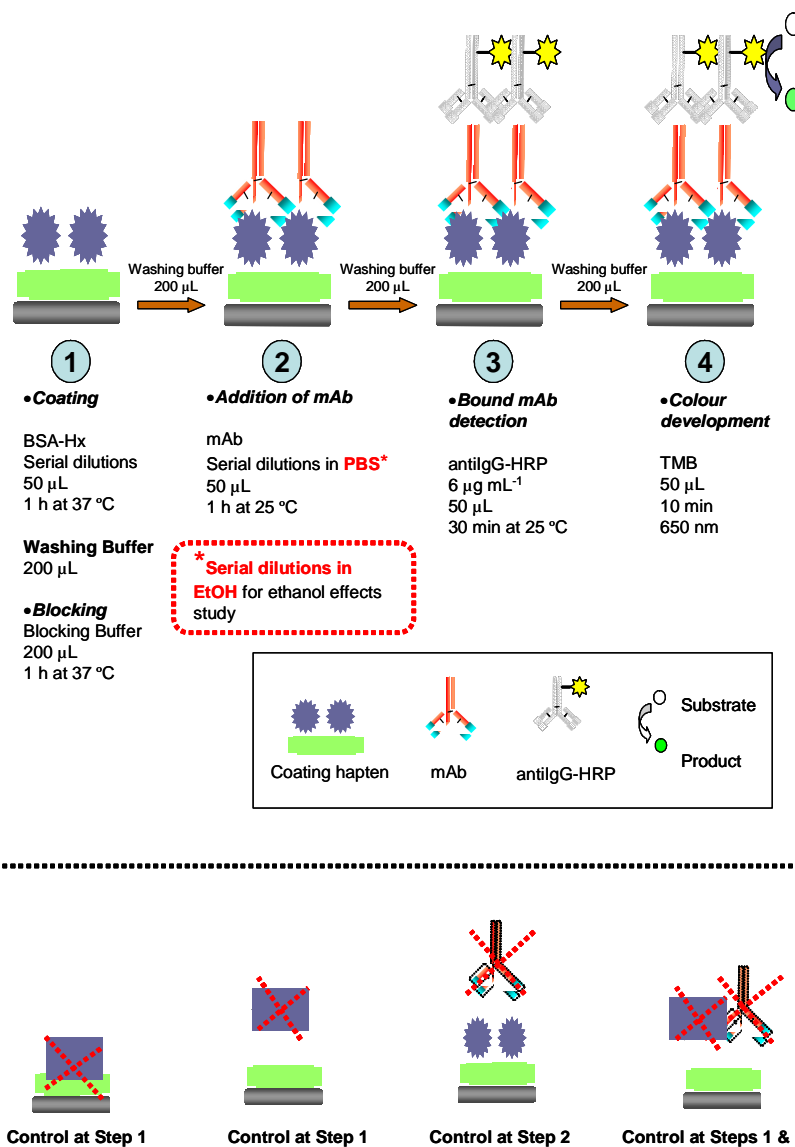


Fig. 2. 2: Schematic of indirect non-competitive ELISA (INCE), Procedures 1 to 3. Serial dilutions of MAb were carried out in PBS containing different EtOH percentages in the case of ethanol effects study (2.2.5.2)

INCE was carried out according to Fig. 2. 2. The study was implemented in step 2 by diluting the MAb in PBS solutions containing different EtOH percentages.

Chapter 2

Indirect competitive ELISA for 2,4,6-Trichloroanisole (TCA) detection

The final corrected absorbance (relative to controls) for every EtOH percentage (IC_{50} %EtOH) was referred to the one obtained when the MAb was diluted in the absence of EtOH (IC_{50} PBS). The percentage of Lost Signal was calculated according to:

$$\% \text{ Lost Signal} = \left(\frac{IC_{50 \text{ PBS}} - IC_{50 \% \text{ ETOH}}}{IC_{50 \text{ PBS}}} \right) * 100 \quad \text{Eq.2. 2}$$

2.2.5.4 Procedure 4: Indirect competitive ELISA (ICE) for pre-incubation time study

Fig. 2. 3 describes the steps followed for ICE. As detailed in the previously mentioned figure, a fixed MAb concentration of $6 \mu\text{g mL}^{-1}$ was used in all pre-incubation steps. TCA and MAb added concentrations diluted to half ($3 \mu\text{g mL}^{-1}$ MAb or 2×10^{-8} M MAb, MW 150 kDa [20] for conversion) in the pre-incubation, since they are added in the same volume. Aliquots to be added in the pre-incubation step were carefully selected according to the desired final antibody and analyte concentrations.

Controls description corresponds to the step at which the control was implemented; control steps 1b and 2 were considered to calculate corrected absorbance (Abs_i).

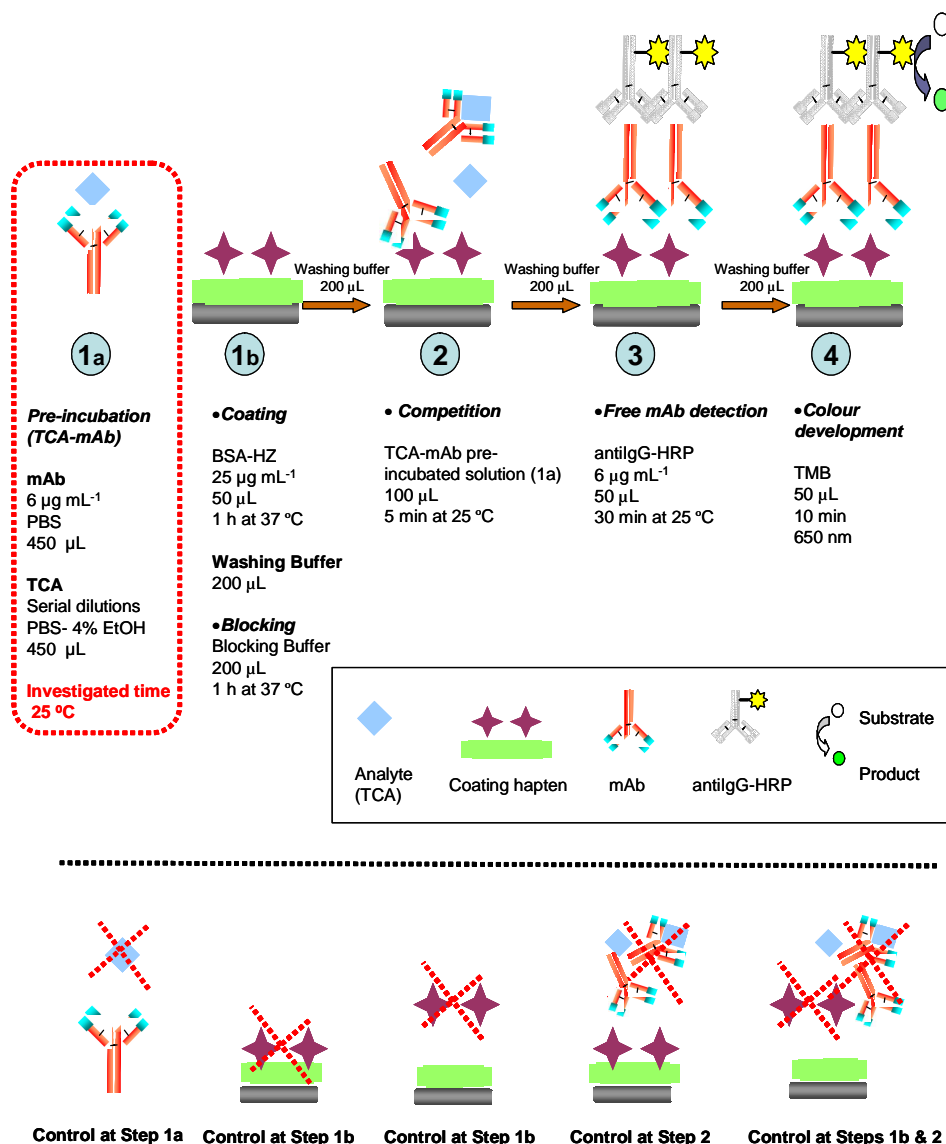


Fig. 2. 3: Schematic of indirect Competitive ELISA (ICE) for pre-incubation time study, Procedure 4.

Control columns for no competition (control at step 1a, Fig. 2. 3), *i.e.* aliquots of MAb pre-incubated in the absence of TCA in PBS 4 % EtOH, were included in every plate. From this control maximal absorbances were obtained, representing the total free MAb signal.

Chapter 2

Indirect competitive ELISA for 2,4,6-Trichloroanisole (TCA) detection

ICE results were normalized as percentage of free antibody (% free MAb) referred to the signal obtained when the antibody was not subjected to competition with TCA (Ab_{No competition}), the percentage was calculated as follows:

$$\% \text{ free MAb} = \frac{mAb_{\text{free (TCA)}}}{mAb_{\text{No competition}}} * 100 = \frac{Abs_{\text{(TCA)}}}{Abs_{\text{(No TCA)}}} * 100 \quad \text{Eq.2. 3}$$

where Abs_(TCA) is the corrected absorbance obtained from competition assay at a TCA concentration of the analyte and Abs_(No TCA) is the corrected absorbance obtained from competition assay in the absence of TCA.

2.2.5.5 Procedure 5: Optimized Indirect competitive ELISA (OICE)

The conditions selected for the optimized assay for the ICE are depicted in Fig. 2. 4. Also in the same schematic the steps where the Accelerated Aging tests were carried out (T1 and T2) are indicated.

Competition results were expressed as percentage of free MAb (%free MAb), according to Eq.2. 3.

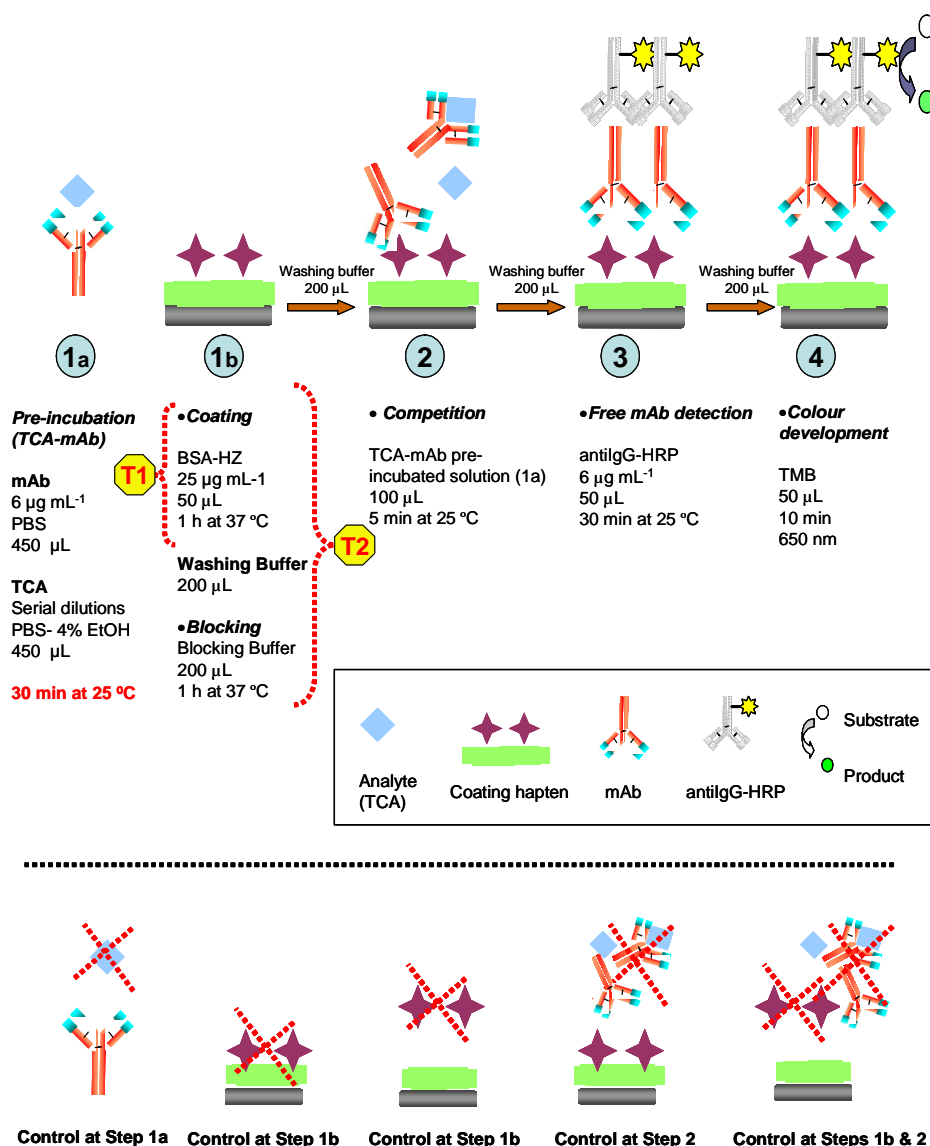


Fig. 2. 4: Schematic of optimized indirect competitive ELISA (OICE), Procedure 5. T1 (coating) and T2 (coating and blocking) depicts the steps where the Accelerated Aging test was carried out.

2.2.6 Accelerated Aging test

In order to test the stability of previously coated and blocked plates, Accelerated Aging test was performed.

Chapter 2

Indirect competitive ELISA for 2,4,6-Trichloroanisole (TCA) detection

The methodology for Accelerated Aging (AA) test followed American Society for Testing and Materials (ASTM) International regulation [21].

Two types of precoated plates were tested (step 1b Fig. 2. 4): only with coating (namely Treatment 1, T1) or both with coating and blocking steps (namely Treatment 2, T2). Once coating (T1) or coating and blocking (T2) of microtiter plates was completed, plates were washed, manually sealed and stored at the chosen temperature during the required Accelerated Aging Time (AAT). Table 2. 1 details the parameters of the experimental design of the AA test.

Under the experimental applied temperature (45 °C), the results obtained after the Accelerated Aging Time (ATT) of 1 to 4 weeks (1W, 2W, 3W and 4W) will correspond to a simulated lifetime of 5, 10, 15 and 20 weeks at 25 °C respectively. The post-aging testing was carried out following the corresponding steps of OICE Procedure 5 and comparing the results with data from the original plates not subjected to accelerated aging (No AA).

Table 2. 1: Accelerated Aging test. Experimental design according to ASTM F 1980-02

Q_{10}	T_{AA}	T_{RT}	AAF	Desired RT	AAT
2	45 °C	25 °C	4.92	5, 10, 15 and 20 weeks	1W, 2W, 3W and 4W

Q_{10} : Arrhenius reaction rate function states that a 10°C increase or decrease in temperature of a homogeneous process results in approximately, a two times or 1/2-time change in the rate of a chemical reaction namely Q_{10} . Q_{10} equal to 2 is a common and conservative means of calculating an aging factor [21]. T_{AA} : Selected Accelerated Aging Temperature (°C); T_{RT} : Ambient Temperature (°C). AAF (Accelerated Aging factor) = $\left[\frac{Q_{10}^{(T_{AA}-T_{RT})/10}}{1} \right]$. Desired RT: Desired simulated Real Time. AAT: Accelerated Aging Time to simulate a Desired RT; AAT = Desired RT/AAF

2.3 Results

2.3.1 Selection of monoclonal Antibody. Cross-reactivity study

The aim of these experiments was to select among the MAbs according to their cross-reactivity to TCA and TCP derivates in the coating. The interaction of the clones *vs.* the coating haptens was determined by investigation of the binding of serial dilutions of each MAb to microtiter plates coated with serial dilutions of different coating haptens. Cross-reactivity percentages calculated according to Eq.2. 1 ranged from less than 1 % to more than 100 % (Table 2. 2). The MAb obtained from the clone that showed less cross-reactivity was chosen for further experiments (clone 7, MAb).

Table 2. 2: Cross-reactivity percentages of the ten risen clones

Clone N ₀	1	2	3	4	5
% Cross-reactivity (n=5)	70.5 ± 9.1	0.5 ± 0.3	32.0 ± 8.0	109.0 ± 2.3	108.0 ± 3.0

Clone N ₀	6	7	9	10	11
% Cross-reactivity (n=5)	26.3 ± 1.6	0.3 ± 0.1	71.1 ± 1.1	91.0 ± 3.2	79.2 ± 9.1

A typical response of the interaction of low-cross-reactivity clones *vs.* BSA-HA, BSA-HPH or control wells is depicted in Fig. 2. 5.

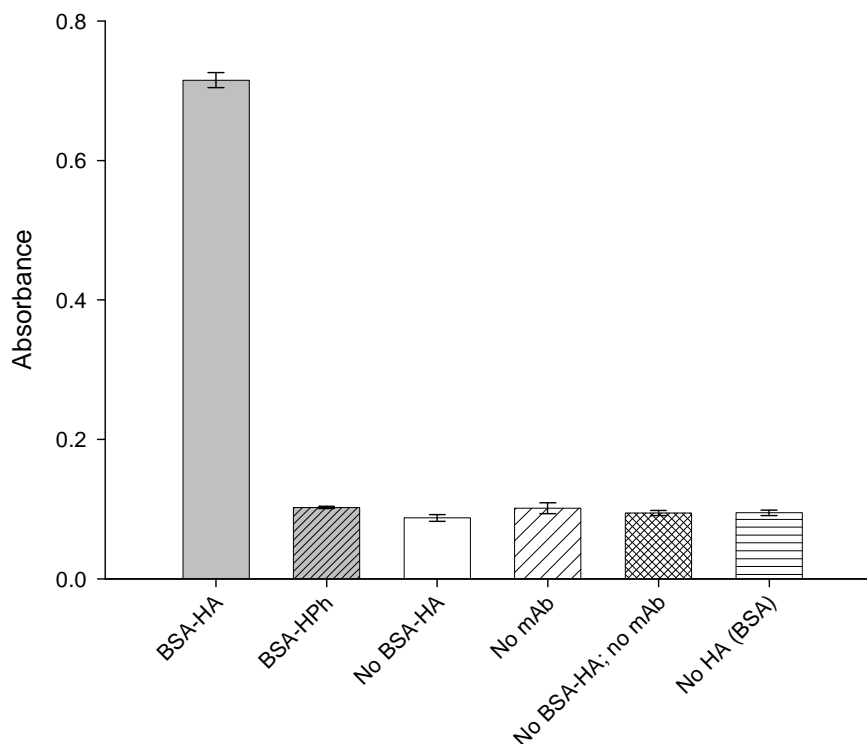


Fig. 2. 5: Signal generated (absorbance) by the interaction of low-cross-reactivity MAb obtained from clone with TCA or TCP derivates coating haptens and control wells.

Cross-reactivity results were also useful to estimate the appropriate coating hapten and antibody concentrations for future indirect competitive assays.

2.3.2 Effect of ethanol content in TCA samples

The effects of ethanol -needed for TCA solutions- in ELISA response were investigated by implementation of Procedure 3, where MAb solutions were prepared in the presence of different percentages of EtOH. Fig. 2. 6 demonstrates that, relative to the signal generated in absence of the solvent, the presence of less than 5 % EtOH does not significantly affect the generated signal. Hence TCA solutions were prepared with 4 %

EtOH, since the incubation with equal volume of MAb would result in 2 % EtOH final content. The percentage of lost signal (% Lost Signal) was calculated according to Eq.2. 2

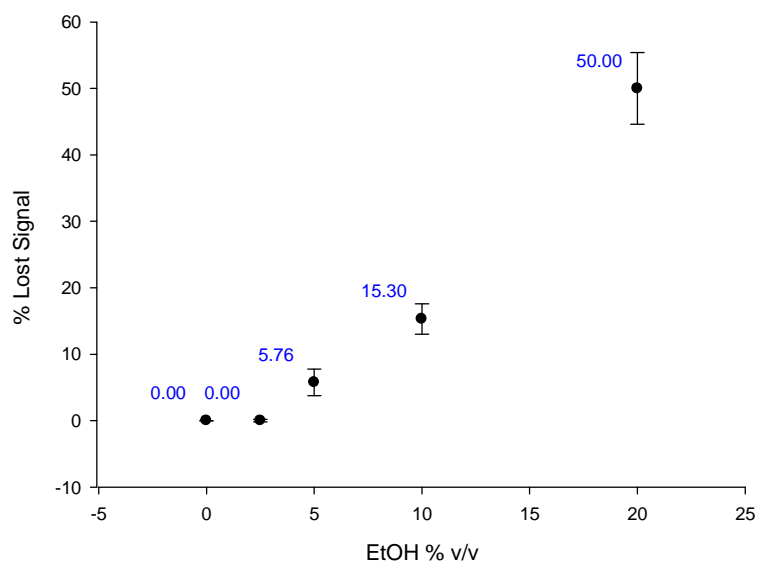


Fig. 2. 6: Effect of EtOH content in TCA samples, expressed as % Lost Signal relative to the signal obtained in absence of EtOH. The results (five replicates) were calculated according to Eq.2. 2.

2.3.3 Affinity Constant (K_{aff}) estimation

Once the MAb from the clone with lowest cross-reactivity was chosen and the adequate ethanol percentage was selected, the estimation of the affinity constants between MAbs and haptens was carried out.

2.3.3.1 MAb-coating hapten affinity estimation. Indirect non-competitive ELISA

Estimation of the MAb-coating hapten affinity constant was carried out by non-competitive ELISA. The constants were estimated according to literature [22-24] as detailed in the discussion section.

Chapter 2

Indirect competitive ELISA for 2,4,6-Trichloroanisole (TCA) detection

The estimated affinity constants (Table 2. 3) provided a range of one order of magnitude for choice of appropriate coating hapten.

Table 2. 3: Selected monoclonal antibody (MAB)-coating haptens affinity constant estimation

Coating hapten	BSA-HA	BSA-H1	BSA-HB	BSA-H3	BSA-HZ
Estimated MAb-coating hapten affinity constant* (M^{-1})	2.05×10^6	1.52×10^6	7.70×10^5	2.80×10^5	2.33×10^5

* The % error consisted in less than 2 % of the estimated affinity constant

The different affinities of the MAb for the coating haptens are demonstrated in Fig. 2. 7, where non-competitive ELISA was carried out using plates coated with same concentration ($25 \mu g mL^{-1}$) of coating haptens. According to the results, BSA-HZ is the coating hapten for which the MAb has the lowest affinity and BSA-HA being the hapten with the highest.

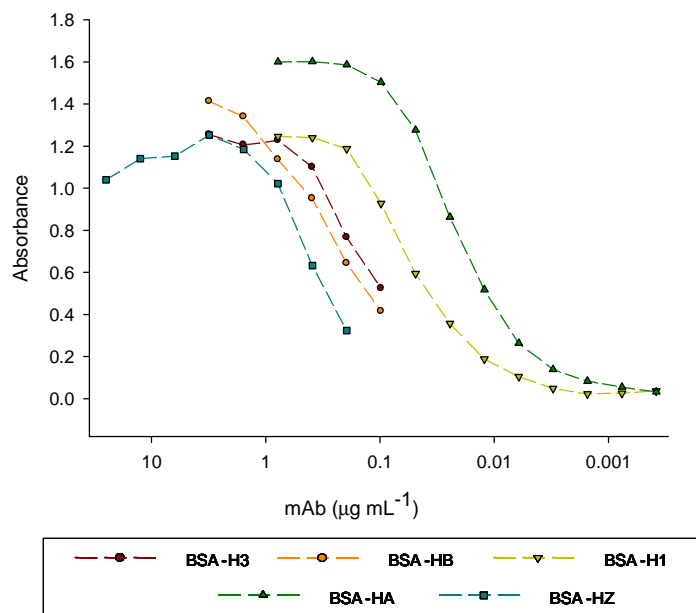


Fig. 2. 7: Non-competitive ELISA for serial dilutions of selected MAb on microtiter plates coated with different coating haptens ($25 \mu g mL^{-1}$). The figure illustrates corrected absorbance values vs. concentrations of the MAb.

2.3.3.2 MAb- compounds in solution affinity. Indirect competitive ELISA

Estimation of affinity constants of MAb with TCA, TCP and HA in solution were carried out by indirect competitive ELISA. As detailed in the discussion section according to literature [25].

The competition assays were carried out using the coating hapten with intermediate estimated affinity (BSA-HB, Fig. 2. 7). The estimated affinity constant, calculated from four replicates, are depicted in Table 2. 4.

Table 2. 4: Estimated affinity constants for HA, TCA and TCP

Estimated affinity constants (M^{-1})		
HA	TCA	TCP
$2.10 (\pm 0.71) \times 10^6$	$1.82 (\pm 0.58) \times 10^5$	$1.69 (\pm 0.44) \times 10^4$

According to the estimated affinity constants of the MAb with the analyte ($K_{\text{aff TCA}} 1.82 \times 10^5 M^{-1}$) and with the coating haptens ($K_{\text{aff BSA-Hx}} 2.05 \times 10^6$ to $2.33 \times 10^5 M^{-1}$), only competitors with affinity constants in the order of the analyte were available for the indirect competitive ELISA.

2.3.4 Selection of coating hapten towards indirect competitive ELISA for TCA determination

Thinking ahead in the development of an ICE for TCA detection matching human threshold, three coating haptens with affinity constants in the order of magnitude of

Chapter 2

Indirect competitive ELISA for 2,4,6-Trichloroanisole (TCA) detection

MAb-TCA (BSA-HB, BSA-H3 and BSA-HZ) were selected. The coating haptens were investigated using Procedure 4 and calculating preliminary limits of detection of TCA.

The obtained preliminary limits of detection were 416 ppb, 300 ppb and 2 ppb for BSA-HB, BSA-H3 and BSA-HZ respectively, which are expected from the estimated MAb-coating hapten affinity constant. The results demonstrated that regardless of the apparently insufficient difference between the affinity constants of MAb-TCA and MAb-coating haptens; the detection of the analyte of interest by competition was still possible.

Hapten Z coating (BSA-HZ) was selected to continue the improvement of the ICE for TCA detection.

2.3.5 Pre-incubation time effect

Previous work [12, 16, 26, 27] reported that on a competitive ELISA, the sensitivity of the immunoassay can be tuned by optimizing the time that the immunoreactions are allowed to take place. With the aim of improving the ICE limit of detection by changing the pre-incubation time, preliminary exploration of the competition assay for 1 ppm TCA by changing pre-incubation and competition time was carried out.

As detailed in Table 2. 5, the less percentage of free MAb was obtained in the case of 30 minutes of pre-incubation and 5 minutes of competition on plate. Competition times of less than 10 minutes (5 minutes in this study) agreed with the literature [28, 29] and seemed to demonstrate potential to enhance the TCA detection by changing the pre-incubation time.

Table 2. 5: Effect of pre-incubation and competition time on the percentage of free MAb (% free MAb) for 1 ppm TCA

Pre-incubation time (minutes)	Competition time (minutes)	% free MAb (6 replicates)
5	5	72 %
30	30	81 %
30	5	54 %
15	5	78 %

Accordingly, different pre-incubation times were explored maintaining the duration of the competing step in 5 minutes (step 2 in Fig. 2. 3). Fig. 2. 8 shows the performance of the indirect competition through different pre-incubation times. The exploration of a broad concentration range (1 ppt to 1 ppm) indicates a tendency of improvement of the competition up to 30 minutes after which a longer pre-incubation time does not mean a better detection (Fig. 2. 8 (a)). A closer examination of units to hundreds of ppt range also demonstrates the better performance for 30 minutes of pre-incubation in the lower range of concentrations (Fig. 2. 8 (b)). The sensitivity of the assay is also demonstrated in the same figure, since evidence of TCA detection in the range of units of ppt is shown. However, less reproducibility is observed for the lowest investigated concentration (1 ppt).

Pre-incubation time of 30 minutes was chosen as a compromise solution between good performance of the assay (according to percentage of free MAb relative to TCA concentration) and required experimental time.

Chapter 2

Indirect competitive ELISA for 2,4,6-Trichloroanisole (TCA) detection

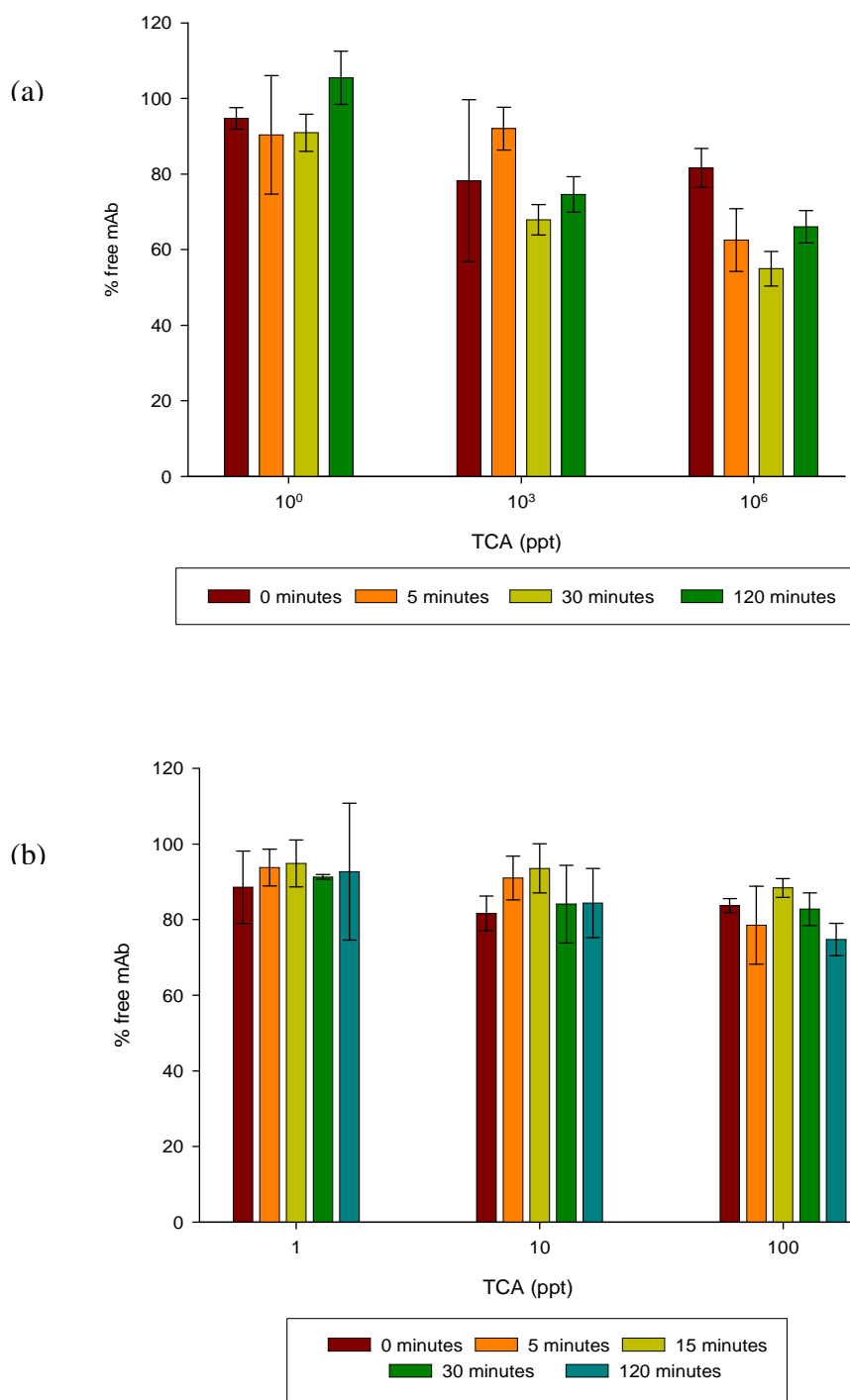


Fig. 2. 8: Pre-incubation time effect on the percentage of free MAb. (a) Pre-incubation of 1 ppt, 1 ppb and 1 ppm during 0, 5, 30 and 120 minutes. (b) Pre-incubation of 1 ppt, 10 ppt and 100 ppt during 0, 5, 15, 30 and 120 minutes

2.3.6 Optimized indirect competitive ELISA for TCA detection

Indirect competitive ELISA using previously selected BSA-HZ as coating hapten was carried out following the OICE procedure (Fig. 2. 4). The limit of detection obtained in preliminary experiments was enhanced by selection of the pre-incubation time (30 minutes) and further exploration of TCA concentrations below ppb range. The final detection of TCA resulted in a working range of 1 ppt to 1 ppm (Fig. 2. 9 (a)) which matches with the requirements of the human threshold for TCA.

The Limit of Detection (LOD) accomplished was $4.2 \pm 4.1 \times 10^{-1}$ ppt, obtained from the linear regression of [100- % free MAb] or [% bound MAb] vs. \ln [TCA ppt] for the ppt to ppb range in Fig. 2. 9 (b) and Table 2. 6.

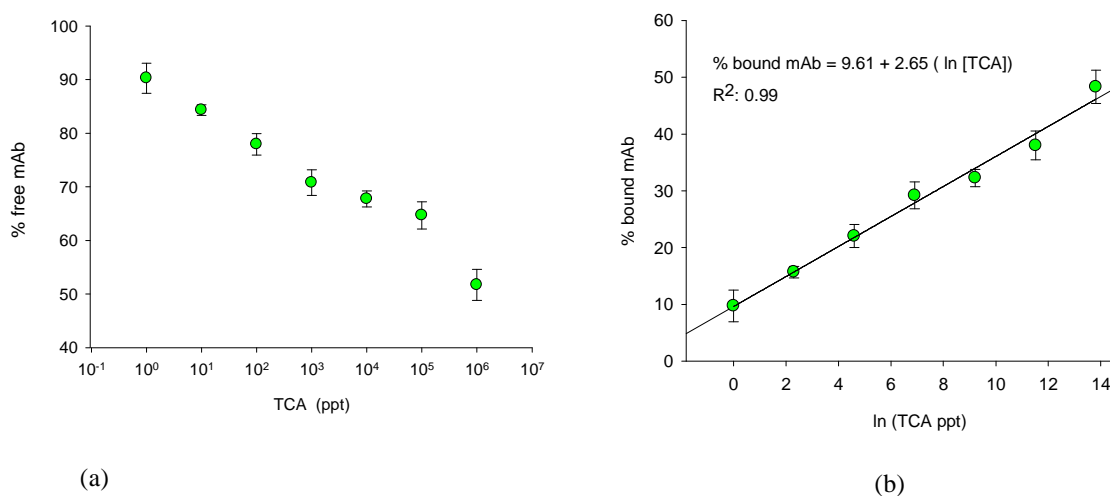


Fig. 2. 9: (a) Indirect competitive ELISA for TCA (4 % EtOH) detection. The figure illustrates the percentage of free MAb vs. TCA concentration in the competition step (1 ppt to 10⁶ ppt). Percentage of free MAb was calculated according to Eq. 2. 3 (b) linear regression results for LOD calculations.

Chapter 2

Indirect competitive ELISA for 2,4,6-Trichloroanisol (TCA) detection

Indirect competitive ELISA was also carried out for the detection of TCP using the optimized indirect competitive ELISA. The achieved limit of detection was 4 ppm (data not shown). Therefore, no cross-reaction is expected up to these concentrations of TCP.

Table 2. 6 : Linear regression parameters and blank standard deviation

Linear Regression (LR) for [(% bound MAb) = y ₀ + slope ln [TCA ppt])						y _{blank} = y ₀ + 3* S ₀	% Error Blank (n= 35)
y ₀			Slope				
Coefficient	Std error	t (95%)	Coefficient	Std error	t (95%)		
9.61	1.25 (Sb)	8.54	2.64	0.13	19.5	y _{blank} : 13.4 hence ; e ^(x blank) : 4.17 ppt	9.8 %

Direct competitive ELISA was investigated by HRP labelling the haptens (heterologous and homologous) and immobilizing the antibody. In order to study random and orientated immobilization of the antibody onto the microtiter plate, the immobilization was carried out directly in carbonate buffer or through anti-IgG specific to the Fc portion of the antibody. Nevertheless, no recognition was observed in this format for none of the immobilization procedures or labelled haptens. This results agreed with reported work [10].

2.3.7 Spiked water samples

Spiked water samples were prepared to simulate the detection of TCA in industrial boiling water as explained in the introduction. The spiked samples were prepared adjusting the pH and conductivity according to the developed immunoassay (pH 7.4 and 13.5 mS. cm⁻¹). Indirect competitive ELISA results (Fig. 2. 10) demonstrated what can be understood as a better performance of the immunoassay in the absence of EtOH, but at

Chapter 2

Indirect competitive ELISA for 2,4,6-Trichloroanisole (TCA) detection

the same time the some error increase can be notice. It seems that the water solubility factor plays decisive role in TCA dilutions, despite the fact that higher solubility of TCA in water have been reported (10 ppm [16] and 5.4 ppm [2]). Lower TCA concentrations and hence less solubility problems, together with absence of EtOH, could result in an immunoassay with higher sensitivity and lower limit of detection.

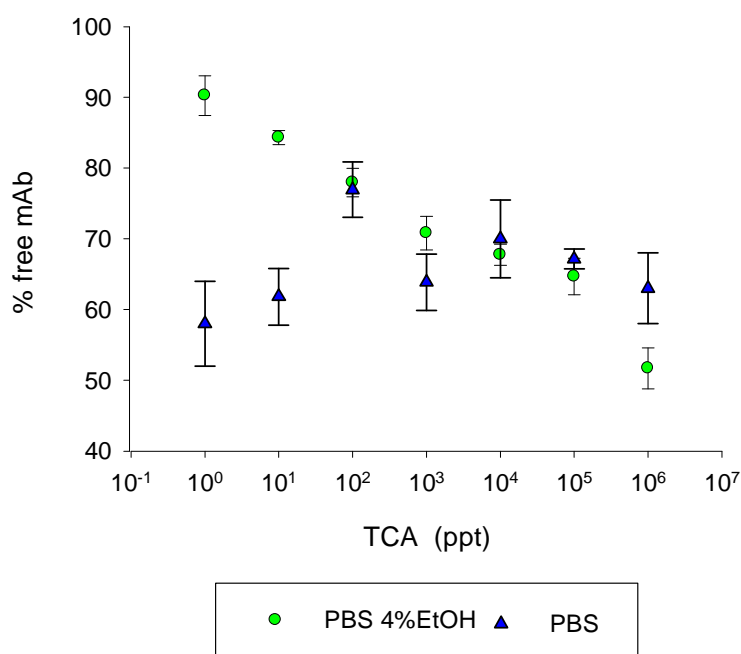


Fig. 2. 10: Indirect competitive ELISA in water samples spiked with TCA (absence of EtOH). The figure illustrates the % free MAb vs. TCA concentration in the competition step (10⁵ ppt to 1 ppt). Percentage of free MAb was calculated according to Eq.2. 3. The results are compared with the curve obtained with TCA samples prepared in PBS with 4% EtOH.

2.3.8 Matrix Effects

Spiked white wine samples were prepared to investigate the matrix effect. Wine conductivity ($3.2 \mu\text{S. cm}^{-1}$) and pH (pH 3.3) were adjusted to values according to the developed immunoassay (pH 7.4 and 13.5 mS. cm^{-1}). The EtOH content (12 % v/v) was also adjusted to requirements of the immunoassay, resulting in a 1 in 3 dilution of wine in PBS. Indirect competitive ELISA results (Fig. 2. 11) showed that the detection of TCA in white wine with the developed immunoassay might be possible; to confirm such suitability a broader sample of wines should be tested since wine matrix can vary from region to region [30]. The effect of the matrix could be strongest for smaller TCA concentrations. The suitability of the matrix after the dilution agrees with reported suggestions [14] and reported results [16].

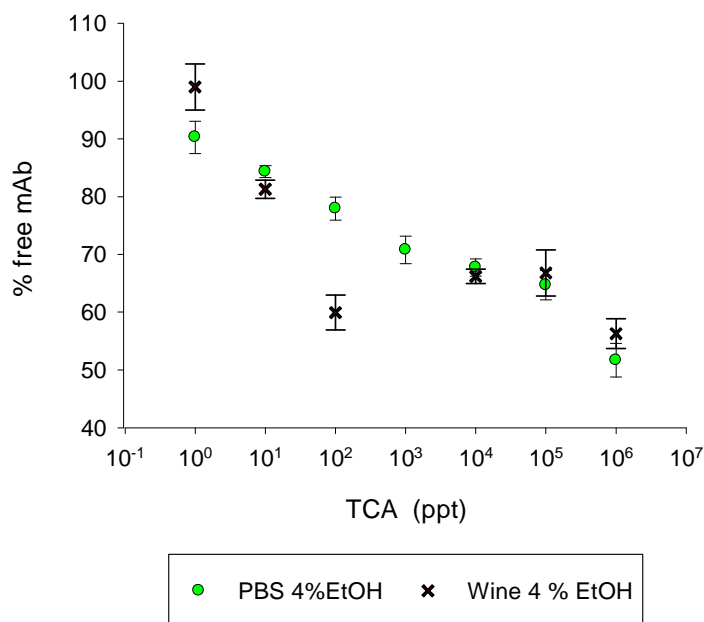


Fig. 2. 11: Indirect competitive ELISA in diluted wine samples spiked with TCA (4 % EtOH). The figure illustrates the % free MAb vs. TCA concentration in the competition step (10^6 ppt to 1 ppt). Percentage of free MAb was calculated according to Eq.2. 3. The results are compared with the curve obtained with TCA samples prepared in PBS with 4% EtOH.

2.3.9 Post-aging testing

Once the OICE with limit of detection similar to human threshold was achieved investigation to shorten the experimental time was carried out. Plates subjected to accelerated aging test were evaluated according to their performance in TCA detection. Indirect competitive ELISA (Procedure 5 at the corresponding stage) was carried out on plates affected by different treatments (T1 and T2) during the corresponding accelerated aging times (AAT). The results were compared with results coming from ELISA plates not affected by accelerated aging studies (No AA).

Fig. 2. 12 shows how every treatment affects differently the assay response (4 to 6 replicates). When only the coating (T1, Fig. 2. 12 (a)) was exposed to the AA test the detection of TCA becomes poorer and random compared to the recently prepared assay (No AA). On the other hand, when both coating and blocking (T2, Fig. 2. 12 (b)) undergone AA test, the detection curve (although with less reliability) is still sensitive to different TCA concentrations even after three weeks of AA test. In the fourth week, the assays lost sensitivity for both treatments Fig. 2. 12 (c). Showing mostly random results.

According to the post-aging test, Treatment 2 (previously coated and blocked plates) demonstrated reliable results for the first three weeks of accelerated aging conditions.

According to the ASTM, the AA test demonstrated the stability of microtiter plates pre-coated and pre-blocked during 10 to 15 weeks when stored at 25 °C.

These results indicate the possibility for an 80-minute assay for the detection of TCA using microtiter plates ready for the MAb-TCA incubation step (Fig. 2. 4).

Chapter 2

Indirect competitive ELISA for 2,4,6-Trichloroanisole (TCA) detection

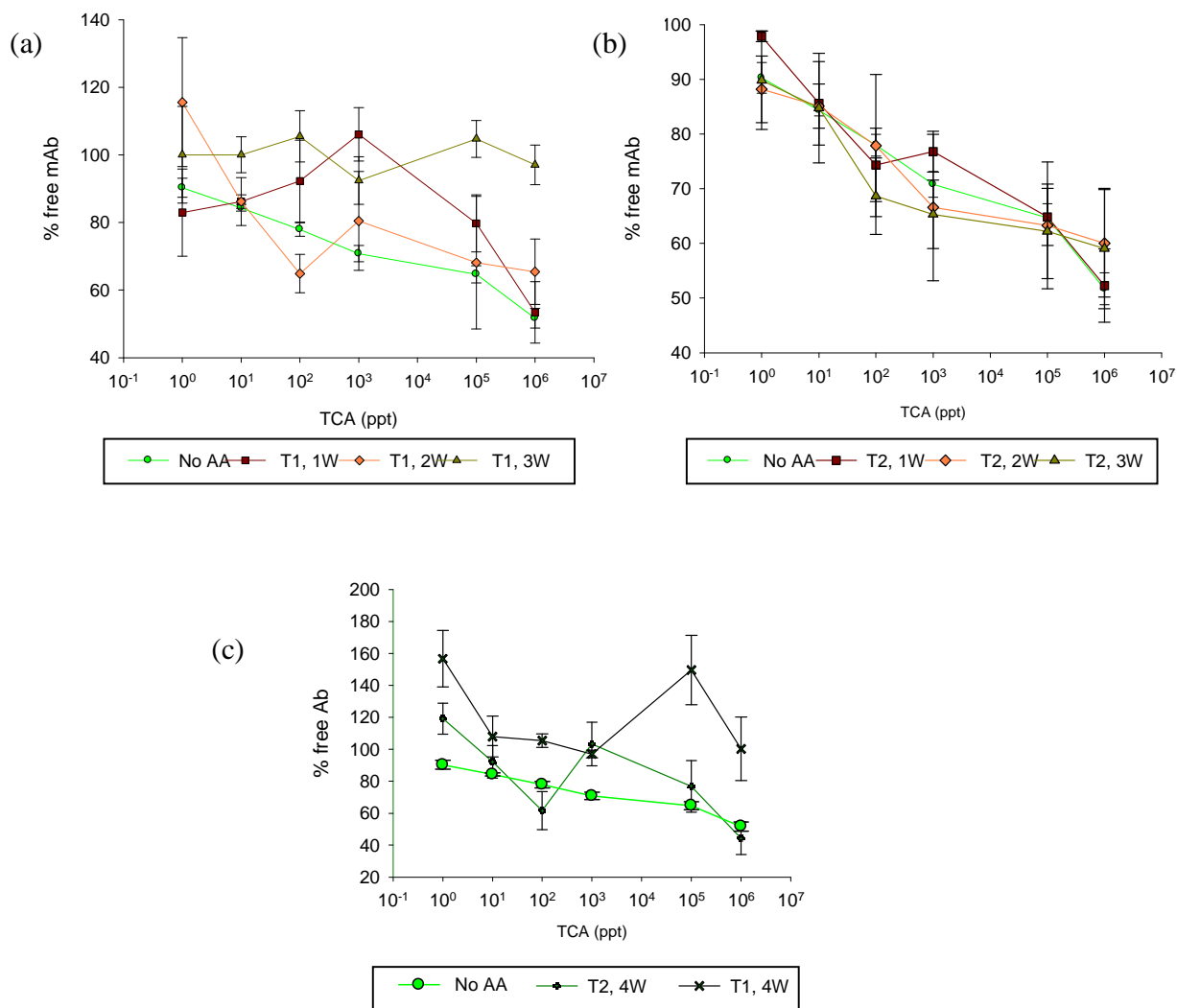


Fig. 2. 12: Post-aging testing. Indirect competitive ELISA on (a) Treatment 1 (coating subjected to AA test) during 1, 2 and 3 weeks, (b) Treatment 2 (coating and blocking subjected to AA test) during 1, 2 and 3 weeks and (c) Treatment 1 and Treatment 2 after 4 weeks of AA test.

2.4 Discussion

2.4.1 Immunogenic hapten selection

The selection of immunizing and coating haptens included a group of molecules obtained from the modification of the geometry and electronic distribution of the target analyte. The molecule with less heterology to the analyte, hapten A (Fig. 2. 1), kept TCA electronic distribution although with a more negative total charge (less positive charge in *-meta* position where the spacer arm was introduced) [18]. Haptens 1, B and 3 have higher heterology degree since the anisole group was blocked by the spacer arm. In hapten 3 also two chlorine atoms were removed or replaced by less electronegative group (-CH₃). Hapten Z presents the highest degree of heterology since it maintains the anisole group but does not contain chlorine groups. In contrast, hapten Z's spacer arm in *-para* position (alkyloxy group) could be an advantage for the immunorecognition since it leaves the anisole group free of steric hindrance.

Because of its high similarity with the analyte and based on a literature survey, HA was chosen as the immunogenic hapten (KHL-HA). Previous work [17, 18] also reported that HA could be the indicated for immunization dedicated to obtain antibodies against TCA, although further experiments orientated their work also to antibodies raised against haptens different from HA, which lacked the methoxy group [16].

In this work, Hapten A was selected as immunogen since it preserves all the functional groups of the analyte, despite the changes in electronic distribution (less positive charge in *-meta* position). The TCA detection through indirect competitive ELISA obtained

here, demonstrates the good performance of the antibodies produced with the chosen immunogen.

2.4.2 Coating hapten selection towards indirect competitive ELISA

Since the sensitivity of the competitive immunoassay is limited by the antibody affinity for the antigen in solution relative to the immobilized conjugate (coating hapten) [31], the coating hapten with lower estimated affinity constant (BSA-HZ) was selected for the development of the indirect competitive ELISA.

Galve *et al.* [27] demonstrated that, among a group of haptens with different heterology to trichlorophenol, the best indirect competitive immunoassay was accomplished by using the highest heterology in the coating hapten. The relative dissociation constant ratio to the homologous of the coating hapten was 246.4. Such ratio is far higher than the one available in this work ($K_{\text{aff BSA-HA (homologous)}}/K_{\text{aff BSA-HZ}} = 9$; $K_{\text{aff TCA (analyte)}}/K_{\text{aff BSA-HZ}} = 0.8$). It should be noted that regardless of the apparent insufficient affinity constants ratio, the developed ICE efficiently detects TCA. It is expected that the limit of detection could be improved using haptens with higher relative dissociation ratios. It is therefore possible, that a more suitable immunizing hapten could produce higher affinity MAbs. However, such attempts were not undertaken in this work.

2.4.3 Affinity Constant (K_{aff}) estimation

In the rational design of competitive immunoassay, the estimation of affinities of antibodies with antigens in solution and coating haptens is the key point for the selection of the competing antibody-analyte and antibody-coating hapten reactions.

Estimation of some affinity constants reported here were calculated by linearization of the data. Affinity constants are generally determined at equilibrium using Scatchard and Klotz plots [32]. Cases of non-linearity of Scatchard plots could suggest the antibody is a heterogeneous mixture with respect to its affinity, unless it is a monoclonal antibody [33]. Reported work compares linearized with non-linearized results finding out non-statistical differences between both methods under the evaluated experimental conditions [20]. Nevertheless some authors [34, 35] consider linearized plots as obsolete and suggest non-linear regression of data as more appropriate mainly when dealing with noisy data or when single binding can not be considered. Additionally, some researchers have reservations about solid-phase affinity methods to calculate affinity constants [23].

In this work the design of a competitive assay was done using estimated information of the competing immunoreactants by competitive and non-competitive ELISA.

2.4.3.1 Estimation of MAb-immobilized coating hapten affinity

Estimation of the MAb-coating hapten affinity constant was carried out by non-competitive ELISA. Non-competitive ELISA has been utilized to estimate [22-24, 36-39], have a qualitative approximation [40] or, independently of theoretical assumptions and corrections, have a relative value of the affinity of antibody-coating hapten [41].

The use of serial dilutions of antibody incubated in different coating hapten concentrations, results in a sigmoidal curve of absorbance vs. logarithm of total antibody added to the microtiter plates. Accordingly, the coating hapten – MAb affinity constants were estimated with a method for solid-phase affinity measurements that directly estimates the affinity constant from solid-phase binding of the antibody [22-24]. The

Chapter 2

Indirect competitive ELISA for 2,4,6-Trichloroanisole (TCA) detection

method uses serial dilutions of coating hapten and antibody for measuring the affinity constant using the Law of Mass Action and considers: 1) there are two identical antibody binding sites that have no cooperativity, 2) when absorbance approaches to a maximum value ($Abs_{100\%}$, upper plateau), the concentration of free Ag approaches zero and the total concentration of Ag (coated antigen) equals to the immunocomplex $[AbAg]$, 3) at any point of the sigmoidal curve, the absorbance vs. logarithm of concentration is assumed to be a direct reflection of the amount of antibody bound to the antigen in the well ($[AbAg]+[AbAg_2]$), that is, at 50 % of the maximal absorbance ($Abs_{50\%}$), the amount of antibody bound to antigen is half the amount of antibody bound at the $Abs_{100\%}$. Eq.2. 4 is an estimate of the affinity constant of the antigen-antibody interaction that is based on the previously detailed considerations:

$$K_{aff} = (n-1)/2 \left(n \left[Ab_{50\%}^{(b)} \right] - \left[Ab_{50\%}^{(a)} \right] \right); \quad \text{Eq.2. 4}$$

$$\text{with } n = \left[Ag^{(a)} \right] / \left[Ag^{(b)} \right] \quad \text{Eq.2. 5}$$

where $\left[Ab_{50\%}^{(a)} \right]$ and $\left[Ab_{50\%}^{(b)} \right]$ are the total MAb concentration at $Abs_{50\%}$ of two sigmoidal curves for the respective investigated coating hapten concentration $\left[Ag^{(a)} \right]$ and $\left[Ag^{(b)} \right]$.

2.4.3.2 Estimation of MAb- compounds-in- solution affinity

Estimation of affinity constants of MAb with TCA, TCP and HA in solution were carried out by indirect competitive ELISA. Friguet *et al.* [42], Stevens *et al.* [43] and Seligman *et*

Chapter 2

Indirect competitive ELISA for 2,4,6-Trichloroanisol (TCA) detection

al. [25] reported the use of indirect competitive ELISA that requires neither immobilization nor labelling of either investigated antigen and antibody. Through the mentioned reported work and more accurate linearization of the resultant equations[44], a simplified method was modified to adapt to real experimental situations of double binding sites, and relevance of coating antigen.

For the estimation of the affinity constants, the coating hapten concentration was kept low in order to diminish the influence of the solid-phase antigen in the calculated dissociation constant (K_D). The constant MAb concentration was such that the Ag concentrations were at least 10 times higher than the MAb concentration. According to literature [25], K_D can be calculated as follows:

$$\frac{Ag_0}{f} = \frac{K_D}{(1-f)} + Ab_0 \quad \text{Eq.2. 6}$$

$$f = \frac{[AbAg]}{[Ab_0]} \quad \text{Eq.2. 7}$$

From Eq.2. 6, K_D (and hence K_{Aff} from the reciprocal of K_D) can be estimated from the slope of the line produced by plotting Ag_0/f vs. $1/(1-f)$.

2.4.3.3 Equilibrium and kinetic constants

Since considering the simplest case for homogeneous ligands (antibody, Ab) which bind to a homogeneous population of receptors (antigen, Ag) that contain one binding site per antigen, it can be written [28, 34, 42, 44, 45]:

Chapter 2

Indirect competitive ELISA for 2,4,6-Trichloroanisole (TCA) detection



$$K_{aff} = \frac{k_{on}}{k_{off}} = \frac{[AbAg]}{[Ag^0 - AbAg][Ab^0 - AbAg]} \quad \text{Eq.2. 9}$$

where Ag^0 and Ab^0 are total initial concentrations of the antigen and the antibody respectively; $[AbAg]$ is the concentration of the antibody-antigen complex, K_{aff} is the Ab –Ag affinity constant, k_{on} and k_{off} are association and dissociation rate constants respectively.

Since K_{aff} , Ag^0 and Ab^0 are known (experimentally estimated or measured), Eq.2. 9 can be solved by the resolution of a quadratic equation. The results from the theoretical approximation are shown in Fig. 2. 13 :

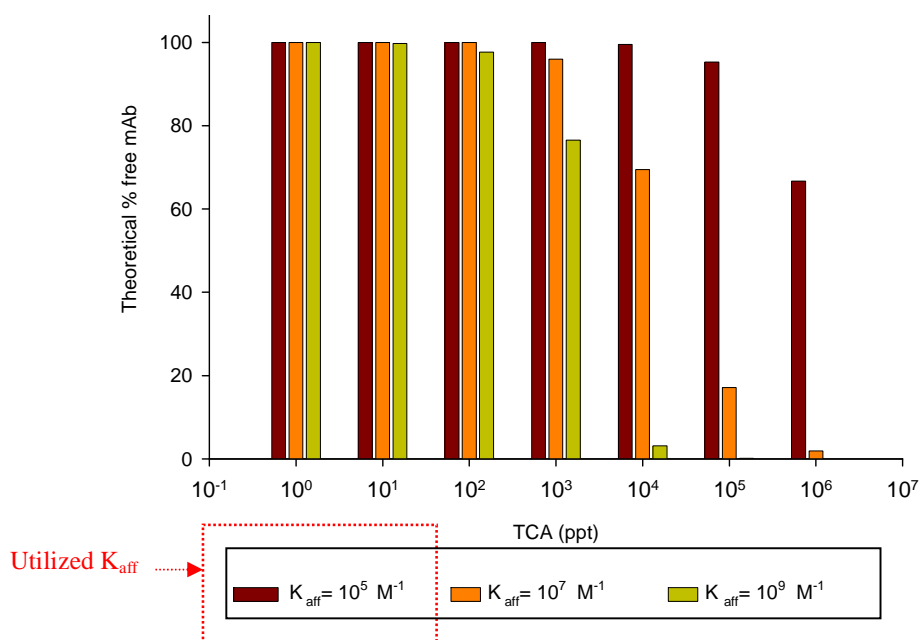


Fig. 2. 13: Theoretical percentage of free MAb (Theoretical % free MAb) for different K_{aff} ($10^5 M^{-1}$, $10^7 M^{-1}$, $10^9 M^{-1}$) and different Ag^0 (1ppt to 1 ppm or $5.0 \times 10^{-12} M$ to $5.0 \times 10^{-6} M$) and a fixed Ab^0 concentration ($2.0 \times 10^{-8} M$)

According to this approximation under the experimental conditions utilized in this work (K_{aff} in the order of 10^5 M^{-1}), the percentage of free antibody would be insignificant at equilibrium conditions, unless TCA (Ag) concentrations of 10^5 or 10^6 ppt were used (Fig. 2. 13).

It must therefore be coincidence of the following circumstances that allow detection limits of the order of magnitude observed. First, the concentration of MAb used ($2 \times 10^{-8} \text{ M}^{-1}$) during pre-incubation is very close to the end of the plateau observed in the checkerboard of optimization with the given coating hapten. Secondly, the slope of the checkerboard is very pronounced for this hapten. Thirdly the k_{off} is very small in absolute terms and therefore the associated [AbAg] complex is slow to dissociate. The two first conditions are met as shown in Fig. 2. 7. In order to obtain approximate values of k_{on} and k_{off} the analysis of Zhuang *et al.* [28] was used. Approximate values of k_{off} $6.30 \times 10^{-4} \text{ s}^{-1}$ and k_{on} $114 \text{ M}^{-1} \text{ s}^{-1}$ were obtained. Compared to typical values in the literature k_{off} (10^{-4} s^{-1} - 10^{-2} s^{-1}) and k_{on} ($10^3 \text{ M}^{-1} \text{ s}^{-1}$ - $10^8 \text{ M}^{-1} \text{ s}^{-1}$) [28, 46-49], it can be observed that an extremely low k_{off} and an unusually slow k_{on} assisted by the very short competition time conspired to achieve the low detection limits observed. The competition time was carefully optimized and Table 2. 5 shows the importance of this parameter. Higher concentrations of MAb during pre-incubations showed no sensitivity to TCA while lower concentrations did not produce enough signal for quantification (results not shown).

2.4.4 Accelerated Aging (AA) Study

The accelerated aging test was carried out to evaluate the stability and storage range of coated and blocked plates. The stable, pre-coated and blocked plates could be used in

order to obtain much shorter assay times since only the pre-incubation, incubation and reading steps would have to be carried out in less than 80 minutes. The obtained results demonstrated that indeed pre-coated and blocked plates are stable for at least 15 weeks at 25 °C. Although the regulation followed for these studies (ASTM International [21]) refers to sterile medical device packages, it is based on Arrhenius-type activation rate.

In choosing 45° C for the AA test the following considerations were taken into account: *i)* temperatures below 60 °C are recommended to avoid non-linear changes [21], *ii)* thermal denaturation of main components of the coating and blocking buffer are: BSA reversible partial unfolding occurs at 42 °C to 50 °C and thermal denaturation above 60 °C [50]; *iii)* Hapten Z melting point is 100 to 200 °C (according to the supplier); *iv)* irreversible unfolding of milk proteins occurs at 70 °C [51] and *v)* Non-Arrhenius behavior (non-linearity of $\ln K$ vs $1/T$) was only observed for unfolding/re-folding of proteins [52] and in polymeric systems [53].

In the AA study, the data obtained indicate that the previous coating and blocking of the plates could be stable for at least 15 weeks if kept at 25 °C. Some authors [54] evaluate the use of preservative solutions to test the stability of pre-coated ELISA plates demonstrating that the use of such preservative solutions (*e.g.* trehalose, 4 °C, plates coated with highly unstable proteins like thrombin), improve the stability of the pre-coated plates. In this sense, the use of preservative solutions can also be explored to increase the lifetime of the pre-coated and pre-blocked plates but was beyond the scope of this demonstration. Regarding the better performance of Treatment 2 (coated and blocked plates affected by AA test) compared to Treatment 1 (only coating of the plates affected by AA test), it can be proposed that there is a stabilization effect by means of

milk components (calcium, iron, magnesium, manganese, among others). Milk powder may contain stabilizing/preservative agents itself, which favour hydrophobic interactions that contribute to thermodynamic stability of the protein or simply do not affect negatively the non-covalent interactions (hydrogen bonds, hydrophobic forces and interaction between charged groups) that cumulatively contribute to stability of the native state [55].

Finally, the AA test demonstrated the feasibility of the production of microtiter plates ready to carry out an immunoassay for TCA detection in no more than 80 minutes. There is still the possibility of further reducing the total assay time by elimination of the second labelled antibody using labelled anti-TCA (labeled MAb). Preliminary studies for the ICE using labelled MAb were not successful. Further exploration of different labelling techniques and the use of a MAb with higher affinity would help to efficiently label the antibody and lead to a total assay time of less than 50 minutes including color development.

2.4.5 Achievements of the developed ICE

Developed Indirect Competitive ELISA have led to limits of detection in the ppt range; that is: a) 44 ppt [18], b) 10 ppt or 20 ppt [17] and c) 4.2 ppt in this thesis. Looking at the BRE utilized in such procedures, monoclonal antibodies were used in the cases (b) and (c). The monoclonal antibodies were raised against different haptens (Fig. 2. 14): HB and HC (procedure (b)) or HA (procedure (c)). Monoclonal antibodies are especially useful since they offer the possibility of standardized BRE. Unfortunately no information, for comparative purposes, of the K_{aff} utilized in case (b) above has been found.

The three mentioned works apply ICE for TCA detection, utilizing HC9 (a), HB or HC (b) and HZ (c) as coating haptens (Fig. 2. 14). Differences regarding the use of amplification of the signal by means of biotin-streptavidinHRP (b) or the use of pre-incubation prior to the competition step (c) were introduced in search of the optimal immunoassay.

Contributions of the ICE developed here and differences with the other reported works are the used immunizing hapten, the specially developed monoclonal antibody, a different coating hapten structure and the use of pre-incubation step of the competitors. Also the procedure developed here offers the advantage of a short experimental time; less than 80 minutes against more than 2 hours of other methodologies. The procedure showed stability-to-storage of the first steps of the ICE preparation with the potential of an experimental time of 50 minutes. In this case primary labelled antibody should be used instead of the second labelled antibody.

The use of immunosorbent solid phase extraction (IS SPE) opened the possibility of the detection of TCA in white wine with a limit of detection of 200 to 400 ppt for which procedure (a) is preceded by the IS SPE. The extraction technique requires a flux of 0.5 ml min^{-1} which could add more than 1 hr to the total experimental time [15]. Such extraction was not needed in this thesis.

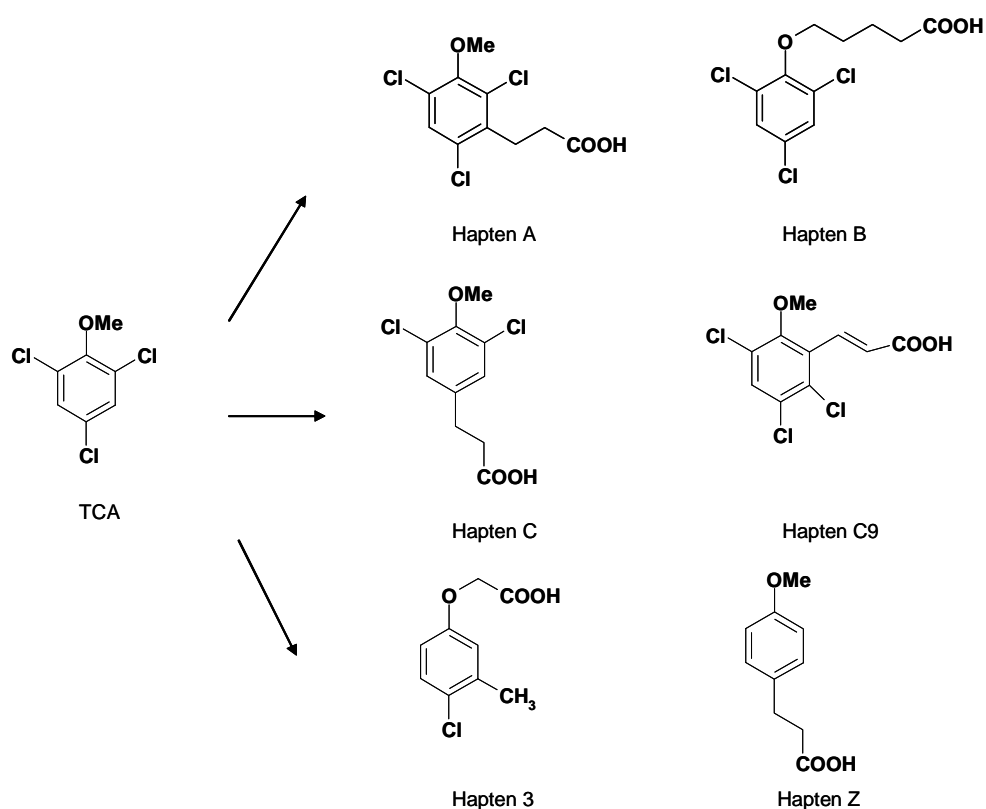


Fig. 2. 14: Chemical structures of TCA and derivated haptens investigated utilized in ICE

2.5 Conclusions

Characterization and selection of MAbS was carried out. In addition, the rational design of an indirect competitive ELISA for TCA detection was demonstrated. The basis of the immunoassays development lies on the study and selection of the possible combinations in the MAb-coating hapten and MAb-analyte competition system.

The monoclonal antibody raised for the design of this immunoassay demonstrated to be able to detect TCA under the experimental conditions investigated here.

Chapter 2

Indirect competitive ELISA for 2,4,6-Trichloroanisol (TCA) detection

The indirect competitive ELISA immunoassay that resulted from this work, demonstrated to be capable of detecting TCA solutions in a working range of 1ppt to 1 ppm, with a limit of detection of 4.2 ppt.

The assay can be carried out in a reasonably short experimental time (less than 80 minutes) and without the need of amplification of the signal.

Accelerated Aging studies demonstrated the stability to storage (15 weeks at 25 °C) of previously coated and blocked plates.

The immunoassay also demonstrated its potential applicability in wine matrix and water samples.

2.6 Bibliography

- [1] Lorenzo, C., Zalacain, A; Alonso, G.L., Salinas, M.R. *J. Chromatogr. A*, 2006, **1114**(2), p. 250-254.
- [2] Alzaga, R., Ortiz, L., Sanchez-Baeza, F., Marco, M.P., Bayona, J.M. *J. Agric. Food Ind.*, 2003, **51**, p. 3509-3514.
- [3] Perchiazzi, N., Ongarato, S., Bartolucci, G. *The reporter*, 2005, **15**, p. 12-14.
- [4] Riu, M., Mestres, M., Busto, O., Guasch, J. *Anal. Chim. Acta*, 2006, **563**, p. 310-314.
- [5] Jönsson, S., Uusitalo, I., van Bavel, B., Gustafsson, I.B., Lindström, G. *J. Chromatogr. A*, 2006, **1111**(1), p. 71-75.
- [6] Jaegger, L. L., Jones, A. D., Hammock, B.D. *Chem. Res. Toxicol.*, 1998, **11**, p. 342-352.
- [7] Shreder, K. *Methods- A Companion to Methods in Enzymology*, 2000, **20**(3), p. 372-379.
- [8] Singh, K., Kaur, J., Varshney, G., Raje, M., Suri, R. *Bioconjugate Chem.*, 2004, **15**, p. 168-173.
- [9] Ballesteros, B., Barceló, D., Sanchez-Baeza, F., Camps, F., Marco, M.P. *Anal. Chem.*, 1998, **70**, p. 4004-4014.
- [10] Galve, R., Sanchez-Baeza, F., Camps, F., Marco, M.P. *Anal. Chim. Acta*, 2002, **452**, p. 191-206.
- [11] Galve, R., Camps, F., Sanchez-Baeza, F., Marco, M.P. *Anal. Chem.*, 2000, **72**, p. 2237-2246.
- [12] Oubiña, A., Barcelo, D., Marco, M.P. *Anal. Chim. Acta*, 1999, **387**, p. 267 - 279.
- [13] Steward, M. W., Lew, A.M. *J. Immunol. Methods*, 1985, **78**, p. 173-190.
- [14] Moore, E., Pravda M., Guilbault, G.G. *Anal. Chim. Acta*, 2003, **484**(1), p. 15-24.
- [15] Sanvicens, N., Moore, E., Guilbault, G., Marco, M.P. *J. Agric. Food Chem.*, 2006, **42**, p. 9176-9183.
- [16] Sanvicens, N., Varela, B., Marco M.P. *J. Agric. Food Chem.*, 2003, **51**, p. 3932-3939.
- [17] Lauster, R., Sanvicens, N., Marco, M.P., Hock, B. *Anal. Letters*, 2003, **36**(4), p. 713-729.
- [18] Sanvicens, N., Sanchez-Baeza, F., Marco M.P. *J. Agric. Food Chem.*, 2003, **51**, p. 3924-3931.
- [19] Nickkova, M., Galve, R., Marco, M.P. *Chem. Res. Toxicol.*, 2002, **15**, p. 1360-1370.
- [20] Debbia, M., Lambin, P. *Transfusion*, 2004, **44**, p. 399-406.
- [21] F1980-02, *Standard Guide for Accelerated Aging of Sterile Medical Device Packages*, in *ASTM International*. 2002.
- [22] Beatty, J. D., Beatty, B. G., Vlahos, W. G. *J. Immunol. Methods*, 1987, **100**, p. 173-179.
- [23] Loomans, E. E. M. G., Roelen, A. J. M., Van Damme, H. S., Bloemers, H. P. J., Gribnau, T. C. J., Schielen, W. J. G. *J. Immunol. Methods*, 1995, **184**, p. 207-217.
- [24] An, L., Hu, J., Zhu, X., Deng, B., Zhang, Z., Yang, M. *Ecotoxicol. Environ. Safety*, 2007, **66**, p. 148-153.
- [25] Seligman, S. J. *J. Immunol. Methods*, 1994, **168**, p. 101-110.
- [26] Weller, M. G., Weil, L., Niessner, R. *Mikrochim. Acta*, 1992, **108**, p. 29-40.
- [27] Galve, R., Sanchez-Baeza, F., Camps, F., Marco, M.P. *Anal. Chim. Acta*, 2001, **452**, p. 191-206.
- [28] Zhuang, G., Katakura, Y., Omasa, T., Kishimoto, M., Suga, K. *J. Biosci. Bioeng.*, 2001, **92**(4), p. 330-336.
- [29] Hardy, F., Djavadi-Ohanian, L., Goldberg, M.E. *J. Immunol. Methods*, 1997, **200**, p. 155-159.
- [30] Peña-Neria, A., García-Vallejo, M.C. *Eur. Food Res. Technol.*, 2000, **210**, p. 445-448.
- [31] Plahk, L. C., Park, E. S. *J. Agric. Food Chem.*, 2003, **51**, p. 3731-3736.
- [32] Bobrovnik, S. A. *J. Biochem. Biophys. Methods*, 2003, **55**, p. 71-86.
- [33] Merrill, S. J. *J. Immunol. Methods*, 1998, **216**, p. 69-92.
- [34] Kubala, M., Plasek, J., Amler, E. *Eur. Biophys. J.*, 2003, **32**, p. 363-369.
- [35] Fuchs, H., Gessner, R. *Biochem. J.*, 2001, **359**, p. 411-418.
- [36] Zhang, W., Zhang, W., Tang, Y., Zhang, J., Liu, J.N. *Biotech. Letters*, 2006, **28**, p. 183-188.
- [37] Dmitriev, D. A., Massino, Y. S., Smirnova, M. B., Segal, O. L., Pavlova, E. V., Kolyaskina, G.I., Osipov, A.P., Egorov, A. M., Dmitriev, A. D. *Russian J. Bioorg. Chem.*, 2001, **27**(4), p. 232-240.
- [38] Orosz, F., Ovádi, J. *J. Immunol. Methods*, 2002, **270**, p. 155-162.
- [39] Liliom, K., Orosz, F., Horváth, L., Ovádi, J. *J. Immunol. Methods*, 1991, **143**, p. 119-125.

Chapter 2*Indirect competitive ELISA for 2,4,6-Trichloroanisole (TCA) detection*

-
- [40] Jang, M. S., Lee, S. J., Xue, X., Kwon, H., Ra, C. S., Lee, Y. T., Chung, T. *Bull. Korean Chem. Soc.*, 2002, **23**(8), p. 1116-1120.
- [41] Pedersen, M. K., Sorensen, N. S., Heegaard, P. M. H., Beyer, N. H., Bruun, L. *J. Immunol. Methods*, 2006, **311**, p. 198-206.
- [42] Friguet, B., Chaffotte, A. F., Djavadi-Ohanian, L., Goldberg, M.E. *J. Immunol. Methods*, 1985, **77**, p. 305-319.
- [43] Stevens, F. J. *Molec. Immunol.*, 1987, **24**(10), p. 1055-1060.
- [44] Bobrovnik, S. A. *J. Biochem. Biophys. Methods*, 2003, **57**, p. 213-236.
- [45] Quinn, J. G., O'Kennedy, R. *Anal. Biochem.*, 2001, **290**, p. 36-46.
- [46] Botus, D., Oncescu, T. *Rev. Chim.*, 2007, **58**(3), p. 323-327.
- [47] Morgan, C. L., Newman, D.J., Burrin, J.M., Price, C.P. *J. Immunol. Methods*, 1998, **217**, p. 51-60.
- [48] Hock, B., Seifert, M., Kramer, K. *Biosens. Bioelectron.*, 2002, **17**, p. 239-249.
- [49] Goldbaum, F. A., Cauerhff, A., Velikovskiy, C.A., Llera, A., Riottot, M.M., Poljak, R.J. *J. Immunol.*, 1999, **162**, p. 6040-6045.
- [50] Jackson, D. R., Omanovic, S., Roscoe, Sh. *Langmuir*, 2000, **16**, p. 5449-5457.
- [51] Anema, S., Lee, S., Klostermeyer, H. *J. Agric. Food Chem.*, 2006, **54**, p. 7339-7348.
- [52] Matagne, A. J., M., Chung, E., Robinson, C., Radford, Sh., Dobson, Ch. *J. Mol. Biol.*, 2000, **297**, p. 193-210.
- [53] Celina, M., Gillen, R.T, Assink, R.A. *Polymer Degradation and Stability*, 2005, **90**, p. 395-404.
- [54] Baldrich, E., Acero, J., Reekmans, G., Laureyn, W., O'Sullivan, C. *Anal. Chem.*, 2005, **77**, p. 4774-4784.
- [55] Whitford, D. *Proteins. Structure and Function*. 2005, England, Wiley.

CHAPTER 3

Mathematical Modelling of the Displacement Immunosensor

3.1 Introduction and aims

The importance of the prediction of immunosensor response resides in the possibility of facing a rational design of the immunosensor avoiding repeated experiments saving enormous effort, time and money. Designing a mathematical model involves putting together assumptions and knowledge about the system with experimental data. If the assumptions are correct and the model is adequately constructed, the predictions should be observed in the experimental work. Verifying the predictions does not prove that the assumptions are true, only that they may not be inconsistent with observations. Any model is a simplification of the system under study.

Computational models in immunology first appeared for the description of antibody-antigen interactions back in the seventies [1]. The affinity of an antibody has been broadly estimated by known early contributions of computational models to immunological methods such as Schatchard, Langmuir and Sips plots [2].

Assumptions like equilibrium conditions, small amounts of epitope to assure monovalency and fixed volume of reaction resulted useful for the development of a simple mathematical model between antibody-epitope in not competing reactions, the equations were based on the law of mass action and solved by a quadratic equation [3]. These authors reported that the intention of complicating the model by considering two epitopes crossreacting with one antibody, two different antibodies with a common epitope or polyvalence of antibody gave place to a mathematically complex model which had not been solved at the date of the publication. Same assumptions of monovalency, equilibrium conditions and the use of law of mass action were considered to model antibody-protein reactions with interest in the study of how antibodies adversely neutralize interferons and other biologically active proteins used clinically to treat patients [4, 5].

Mathematical modelling has become of great interest for clinical orientated investigators and pharmaceutical industries in the design of optimal vaccination strategies, and to produce effective drugs [6]. Mathematical model of the generation of antibodies in response to hepatitis B vaccines made great contributions to understand the protective immune memory generated by vaccine doses [7]. Half lives of therapeutic monoclonal antibodies as a contribution of the study of antibodies' permanence in patients was also

modelled [8]. In the other hand, the collection of real data coming from patients lead to the development of a mathematical model that helped to understand the effects of changing parameters in the antibody-targeted cancer tumor therapy targeting efficiency [9].

Mathematical models based on competitive binding have been reported for the study of two antibodies with multiple antigens and prediction of optimum mixed antibodies ratios, estimation of statistical parameters characterizing the competition assay and description of the interaction between polyvalent antigens to antibodies immobilized on liposomes [10-12].

A review of different works show some attempts to model a displacement sensor; a mathematical model was designed to describe the dose-response relationship of an optical displacement glucose sensor using fluorescence as signal generator [13]. The equations that describe the diffusion of glucose through a fiber membrane and the subsequent displacement reactions within the fiber lumen were solved numerically to predict the response time of the sensor. The authors support their mathematical modelling on local equilibrium assumption to describe the competing equilibrium reactions, finding that the competing binding constants did not affect the response time of the sensor. Deviations observed between the predictions of the model and the experimental data were attributed to the probably not application of the local equilibrium assumption.

Mathematical modelling of displacement based on the analysis of the equilibrium receptor-ligand reaction and mass balance equations have been reported [14-16]. Displacement was modeled assuming that the process of displacement of the sup-optimum antigen from the

immobilized receptor by the analyte may be approximated by a simple mechanism of two competitive binding reactions occurring in the solid phase. The authors solved the system of equations by a cubic algebraic equation and obtain the calibration curve of the sensor. The simulated immunosensor response was compared to hypothetical affinity system finding out that the mathematical model seemed to be sufficient to describe the behaviour of affinity sensors based on competitive displacement. The authors pointed out the concentration of the sub-optimum antigen initially loaded and the density of immobilized receptor on the solid phase as parameters that need to be considered in the design of affinity sensors. Regarding to the relative binding strength of both the analyte and the sub-optimum antigen toward the receptor, opposite opinions are found since the affinity constant ratios were considered as affecting [15] and not affecting the sensor response [13, 16].

Theoretical prediction for the displacement kinetics under different flow conditions [17, 18], and different Ab densities of solid phase immunoassays have been developed. The apparent dissociation rate constant was found to increase with an increase in the flow rate and decrease with an increase in the antibody density. In the absence of competitive unlabelled Ag (spontaneous dissociation) the dissociation rate constant increases as flow rate increases, suggesting a direct relation between dissociation and flow rate [19].

Chemometrics of immunological reactions have also been modelled. The limit of detection and range of quantification of competitive ELISA have been predicted by solving through Runge-Kutta method [20] the differential equations describing the change in the concentrations of an antigen-antibody complex and an enzyme conjugated antigen-antibody complex. The assumptions of the model relied on homogeneous binding and the numerical

predictions were based on rate constants defined as appropriated by previously reported competitive ELISAs [21].

The validity of developed techniques has also been predicted. The validity of a fully automated immunosensor river analyzer (RIANA) working under competition format was tested by modelling the immunoreactions taking place. Since the sensor was designed as simultaneous multi-detection of seven sulphonamides, the authors found hard to adequately describe the cross-reactivity and the behaviour of a mixture of polyclonal antibodies [22].

Modelling of ligand-receptor kinetics and the effects of diffusion on a cell surface receptor have also been investigated by mathematical modelling of the involved equations [23].

Effects like rebinding and diffusion limitation were investigated. Rebinding occurs because a ligand that dissociates from one receptor has a high probability of reacting with another receptor on the same surface instead of escaping into solution, probably slowing the rate of dissociation. At high receptor densities the forward kinetics of a reaction is also affected because of competition. The rate of binding could no longer be proportional to the number of free receptors on the surface but saturates with increasing receptor number as receptors compete for ligand and the reaction between ligand and receptor becomes diffusion limited. The authors finally suggested the use of low receptor densities to avoid rebinding and slow rate of dissociation.

Modelling has illuminated the relationship between various assay parameters such as reagent concentration and assay performance for different assay designs and can aid in assay optimization by predicting a set of parameters (concentration of specific binding

sites, concentration of labelled antigen, duration of incubations steps, type of the assay: displacement or competitive) that may give an optimum sensitivity [21, 24, 25].

The aim of this chapter is to demonstrate how the insights obtained from the mathematical modelling of the response of an equilibrium displacement electrochemical immunosensor, based on the displacement by the analyte of labelled antigens that are bounded to immobilized antibodies on the top of an electrode, allow the rational design of a displacement electrochemical immunosensor (DEI). The importance of parameters like surface to volume ratio and affinity constants ratio among other parameters were simulated. The predicted DEI behaviour will be contrasted with experimental data later in Chapter 4.

3.2 Materials and methods

3.2.1 Mathematical Model for displacement immunosensor

3.2.1.1 System description

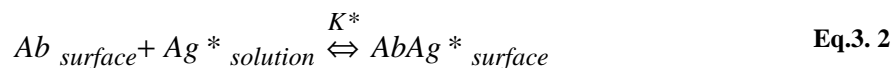
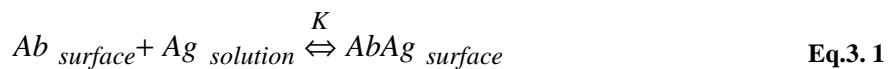
In biosensors working under displacement mechanism, the measurement of the analyte concentration is based on the displacement of sub-optimum molecules in a heterogeneous system. The sub-optimum molecules are initially bound to an immobilized ligand on some solid support. The addition of the analyte would generate the displacement of the sub-optimum away from the ligand and to the bulk liquid phase. In order to be able to follow the sub-optimum molecule concentration, the displaced molecule is generally labelled depending on the system of detection used giving place to a labelled sub-optimum

molecule. In this way, the analyte concentration is determined indirectly measuring the concentration of the labelled sub-optimum in the bulk solution or at the solid phase, depending on the system of detection.

Going more specifically to the Displacement Electrochemical Immunosensor (DEI) modeled in this thesis (Fig. 3. 1), the displacement system corresponds to the use of an antibody (Ab) as ligand immobilized on the surface of an electrode, the analyte (Ag) and the labelled sub-optimum antigen (Ag*). The concentration of the analyte will be followed by the decrease of the concentration of the labelled sub-optimum antigen on the electrode surface.

The modeled immunosensor based on displacement electrochemical immunoassay consists in the antibody previously immobilized (Ab_0) on the electrode surface and incubated with the labelled sub-optimum antigen (Ag^*_0) (Fig. 3. 1 a). The model refers to the use of such sensor, which after the incubation with the analyte or target antigen (Ag_0), shows a decrease of labelled sub-optimum antigen because of the displacement generated by the addition of the mentioned analyte.

The model focuses on the equilibrium that is reached after the incubation with the analyte which is the displacement step. The process consists of antibody - antigen reactions, one for the labelled sub-optimum antigen (Ag*) and the other one for the unlabelled target antigen or analyte (Ag) as described in Eq.3. 1 and Eq.3. 2 :



These are heterogeneous equilibrium reactions, since the antibodies are immobilized onto the surface.

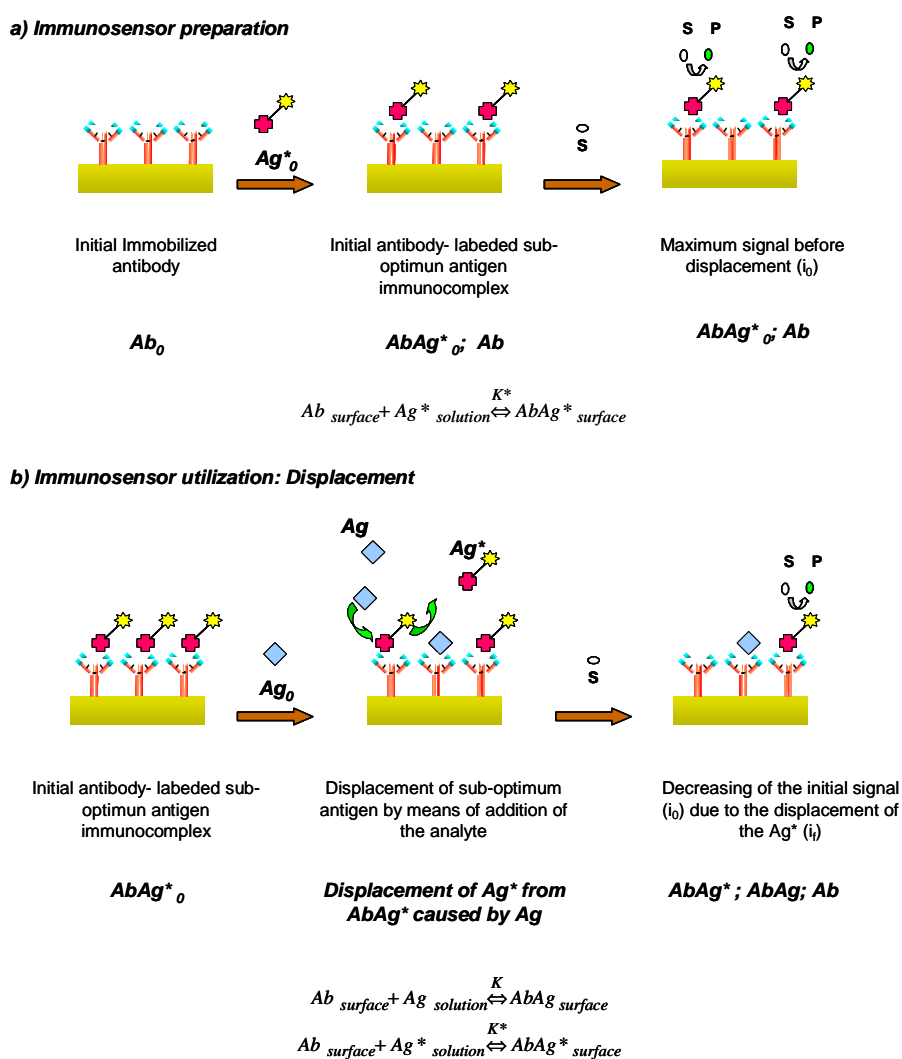


Fig. 3. 1: Schematics of modeled DEI. a) Immunosensor preparation by addition of labeled sub-optimum antigen on the immobilized antibody. b) Displacement of the labelled sub-optimum antigen by addition of the analyte.

3.2.1.2 Equations for equilibrium Mathematical Model (MM)

The process of the equilibrium model is described by the molar balance for the concentration of the species which are in the solution or on the surface. The equations of the molar balance are:

$$Ab_0 = Ab + AbAg + AbAg^* \quad \text{Eq.3. 3}$$

$$V \cdot Ag_0 = V \cdot Ag + S \cdot AbAg \quad \text{Eq.3. 4}$$

$$S \cdot AbAg^*_0 = V \cdot Ag^* + S \cdot AbAg^* \quad \text{Eq.3. 5}$$

$$K = \frac{AbAg}{Ab \cdot Ag} \quad \text{Eq.3. 6}$$

$$K^* = \frac{AbAg^*}{Ab \cdot Ag^*} \quad \text{Eq.3. 7}$$

where Ab_0 (nmol dm⁻²) is the total amount of immobilized antibody, Ab (nmol dm⁻²) is the amount of free antibody when the equilibrium is reached, $AbAg$ and $AbAg^*$ (nmol dm⁻²) are the amount of analyte and labelled sub-optimum antigen respectively that are bound to the antibodies when the equilibrium is reached, V (dm³) is the volume where the incubation with the analyte is performed, S (dm²) is the surface of the electrode, Ag_0 (nmol dm⁻³) is the initial concentration of the analyte in the solution, Ag (nmol dm⁻³) is the concentration in the solution of the analyte when the equilibrium is reached, $AbAg^*_0$ (nmol dm⁻²) is the

initial amount of labelled antigen that is bounded with the immobilized antibodies before the displacement, Ag^* (nmol dm^{-3}) is the concentration of the labelled antigen in the solution when the equilibrium is reached, K and K^* ($\text{dm}^3 \text{nmol}^{-1}$) are the equilibrium constants of the antibody for the analyte and the labelled sub-optimum antigen respectively. Equations Eq.3. 3 to Eq.3. 5 are equations for the molar balance of the different species of the system, equations Eq.3. 6 and Eq.3. 7 are the equilibrium expressions for the antibody antigen reactions. In this way, the system of equations has five equations Eq.3. 3 to Eq.3. 7 and five unknowns (Ab , Ag , Ag^* , $AbAg$, $AbAg^*$), the rest of the parameters (Ab_0 , $AbAg^*_0$, Ag_0 , V , S , K , K^*) are known or could be obtained experimentally.

The assumptions for this model are:

- Antibodies are immobilized as a monolayer.
- Local equilibrium assumption is introduced which assumes that the binding reactions take place instantaneously and equilibrium concentrations are reached. The local equilibrium assumption eliminates any reaction rate limitations in the response of the sensor. No cooperative and multivalent binding between antibody and antigens are considered [3, 13, 15, 16]
- Sub-optimum and target antigens compete for the same binding sites on the receptor protein and, in each case, the binding mechanism is bimolecular [3].
- Rebinding of the labelled sub-optimum is neglected since low densities of ligand (Ab) are considered [23].

For the mathematical solution of the system, it is also assumed:

- Initially all the antibodies have a labelled antigen bound (that is $Ab_0 = AbAg^*_0$)
- The antibodies-antigen binding is homogeneous and monovalent.

3.2.2 Expression of the predicted DEI response

The mathematical model (MM) simulates the changes of concentration of the species intervening in the immunosensor with the addition of different analyte concentrations, *i.e.* for the case of labelled immunocomplex the concentration of $[AbAg^*]$ before ($[AbAg^*_0]$) and after the addition of an specific TCA concentration ($[AbAg^*_{Ag=TCA}]$). The concentration of the labelled immunocomplex at any time is an indication of the signal that would be experimentally observed, the decrease of the concentration of the labelled immunocomplex would indicate the loss of the generated signal by means of displacement phenomenon.

The changes in the concentration of the labelled immunocomplex predicted by the MM, corresponding to the predicted response of the displacement immunosensor were expressed as percentage of loss of $[AbAg^*]$:

$$\% \text{ Loss } [AbAg^*]_{MM} = \left\{ \frac{[AbAg^*_0] - [AbAg^*_{Ag=TCA}]}{[AbAg^*_0]} \right\} * 100 \quad \text{Eq.3. 8}$$

where $[AbAg^*_0]$ and $[AbAg^*_{Ag=TCA}]$ are the predicted immunocomplexes concentration before and after the addition of TCA respectively.

3.2.3 Parameters and equation solving

Conditions were chosen or experimentally obtained to model the behaviour of the sensor in response to the presence of the analyte (Ag). The starting concentration of the species and equilibrium constant corresponded to the following parameters:

- Analyte (Ag) = TCA
- Sub-optimun labelled antigen (Ag*)= H3HRP
- Antibody (Ab)= monoclonal Ab (mAb) specific to TCA
- Affinity constants estimated by ELISA: K_{TCA} $1.82 \times 10^5 \text{ M}^{-1}$ ($1.82 \times 10^{-4} \text{ nM}^{-1}$); K_{H3} $2.80 \times 10^5 \text{ M}^{-1}$ ($1.82 \times 10^{-4} \text{ nM}^{-1}$)
- K_{TCA}/K_{H3}^* : 0.65
- Ab_0 : $0.2 \text{ nmoles dm}^{-2}$ (quantified through eSPR)

Equation solving of the Mathematical Model was accomplished using Matlab “The language of technical Computing” version 7.0, The MathWorks, Inc.

3.3 Results

3.3.1 Mathematical Model solution

The five non-linear equations system was solved using experimentally determined values for the parameters that have to be fixed (Ab_0 , $AbAg^*_0$, K , K^* , S , V) and applying the Newton-Raphson method programmed in MATLAB (Annex 3. I, Matlab Routine)

3.3.2 Predictions of the DEI behaviour

The objective of these calculations was to predict through the MM the predicted loss of labelled immunocomplex concentration Eq.3. 8 and hence the displacement phenomenon

caused by the addition of different concentration of analyte (TCA), these results would give an indication of what could be experimentally observed.

3.3.2.1 Effects of S/V changes in the DEI response

Since Ab_0 is intrinsic of the immobilization procedure, $AbAg^*_0$ is equal to Ab_0 according to the assumptions of the model and K and K^* are also intrinsic of the available immunosystem, the first parameters used to simulated the displacement response due to Ag_0 additions was V expressed as S/V ratio calculated according to a fixed chosen area.

In this sense, by changes in S/V (dm^{-1}) through changes in V (dm^3), the following simulated results were obtained:

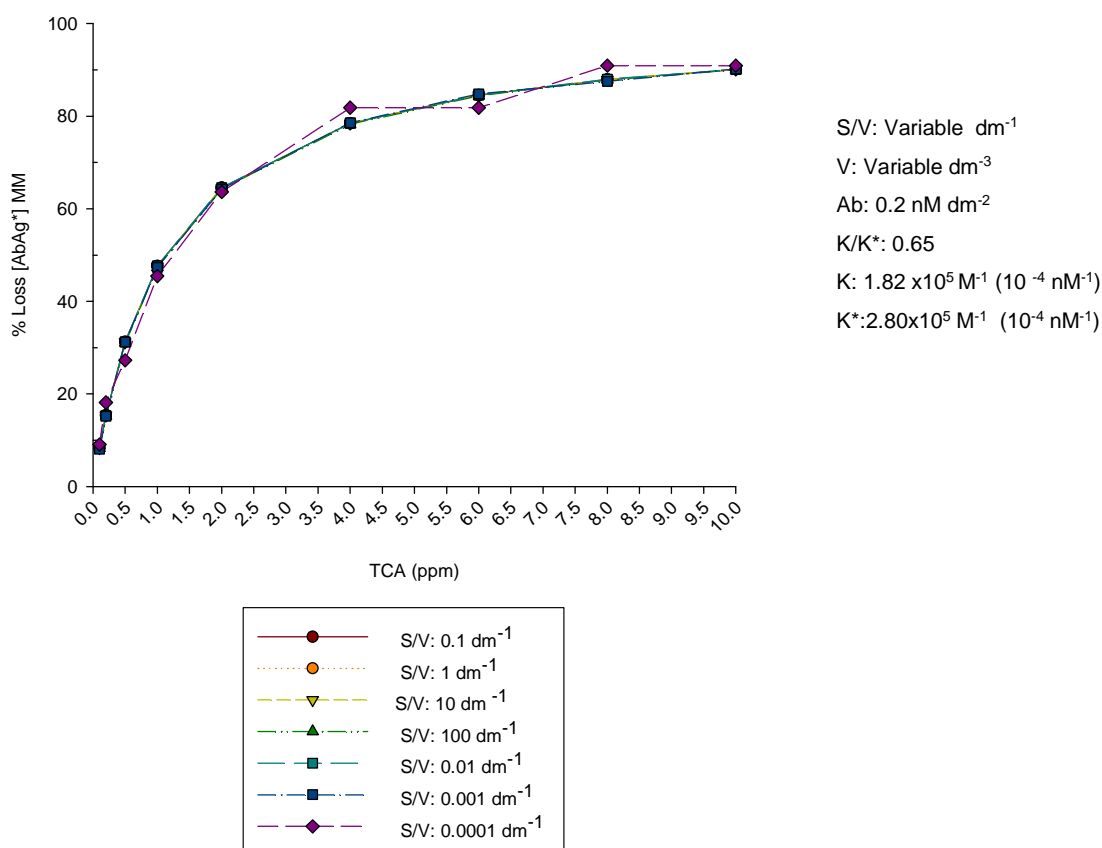


Fig. 3. 2: Mathematical modelling of the DEI depending on the S/V ratio. $Ab: 0.2 nMdm^{-2}$; $K/K^*: 0.65$; $K: 1.82 \times 10^5 M^{-1} (10^{-4} nM^{-1})$; $K^*: 2.8 \times 10^5 M^{-1} (10^{-4} nM^{-1})$

According to Fig. 3. 2, under the conditions that will experimentally be used as described in section 3.2.3, (addition of 0.1 to 10 ppm of TCA) the displacement phenomenon would provoke a loss of labelled immunocomplex between 8 % to more than 90 %. The simulated results seem to indicate that changes in the S/V ratio would not affect the displacement response with a K value in the order of 10^5 M^{-1} (10^{-4} nM^{-1}).

3.3.2.2 Effects of K^* and S/V changes in the DEI response

The objective of this study was to evaluate whether the mere immersion of the DEI in different buffer volumes would cause a decrease in the labelled immunocomplex concentration. Simulated data was obtained by changing the S/V ratio at different K^* for analyte concentration equal to zero ($A_g=0$).

According to the obtained results (Fig. 3. 3), the MM predicts almost total loss of labelled immunocomplex concentration for low K^* values in most of the S/V ratio values. These results hint the presence of inconsistencies in the MM when $A_g=0$ and K^* are low. Looking back at the displacement caused by addition of TCA (Fig. 3. 2) the signal was not totally lost even after simulating the addition of 8 ppm of TCA, also with a K^* value in the order of 10^5 M^{-1} (10^{-4} nM^{-1}). Opposite to the total loss of labelled immunocomplex observed for low K^* values, in the case of high K^* the MM predicts smaller losses of $[AbA_g^*]$ as S/V decreases. This kind of inconsistency or limitation of the MM to cover all possible cases has already been found, and reported that similar models' predictions were more realistic when high affinity constants were involved [26].

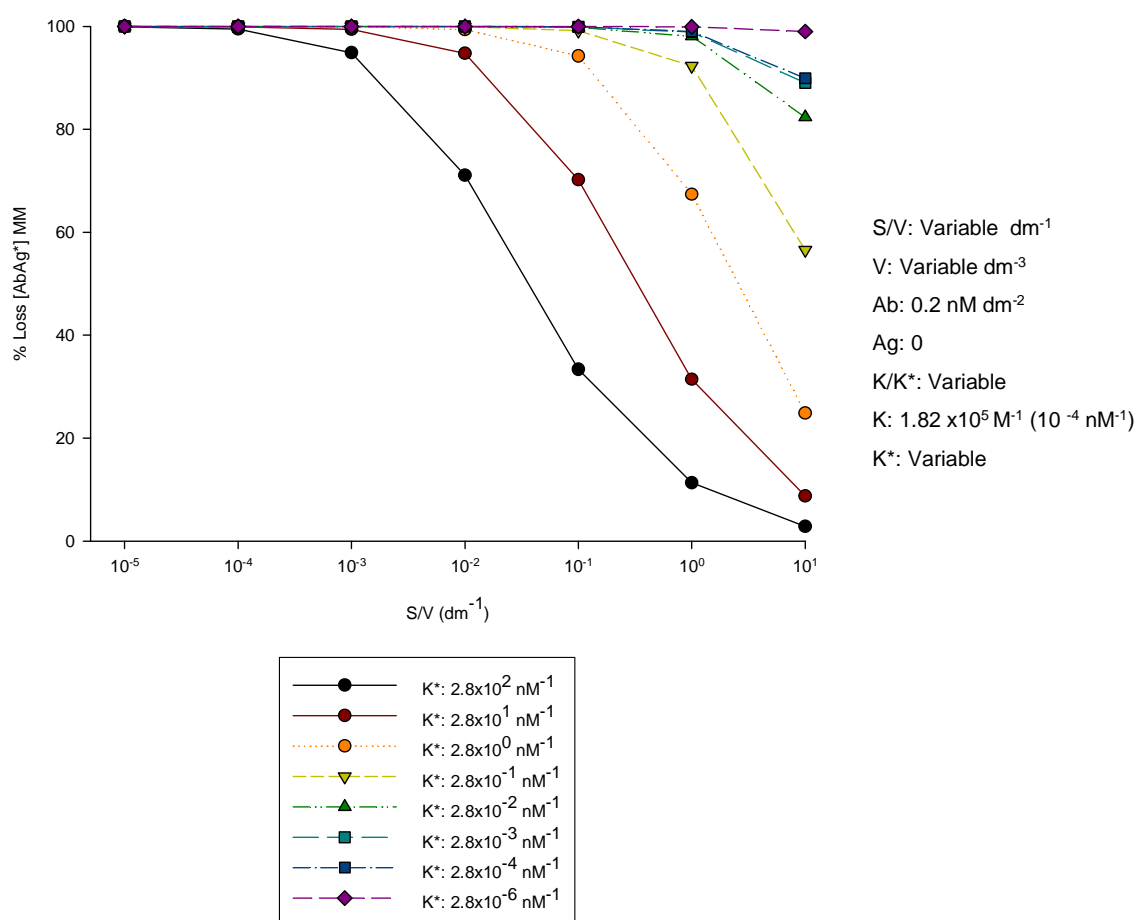


Fig. 3. 3: Effects of changes in S/V ratio in absence of added analyte (Ag=0). Ab: 0.2 nMdm⁻²; K/K*: Variable; K:1.82 x10⁵ M⁻¹ (10⁻⁴ nM⁻¹); K*:Variable

Thinking ahead in the reproducible manipulation and experimental replication of these predictions, and cautiously bearing in mind the information obtained from (Fig. 3. 3), a S/V ratio value of 0.1 dm⁻¹ was chosen as compromise between high S/V ratios (large loss of labelled immunocomplex predicted by the MM) and low S/V ratios (where the rebinding phenomena can damage the displacement).

3.3.2.3 Effects of higher and lower affinities (K and K^*) in the MM predictions

The objective of the simulations described in this section was to further explore the effect of introducing different K and K^* in the mathematical model.

In order to explore the MM prediction of the DEI behaviour for different ranges of K and K^* , simulations of the percentage of loss of $[AbAg^*]$ were calculated according to changes in S/V ratio for given Ag concentrations and K/K^* ratios. The simulations were divided in two groups: K and K^* ranging from $10^3 M^{-1}$ to $10^8 M^{-1}$ ($10^{-6} nM^{-1}$ to $10^{-1} nM^{-1}$; Fig. 3. 4) and ranging from $10^9 M^{-1}$ to $10^{14} M^{-1}$ ($10^0 nM^{-1}$ to $10^5 nM^{-1}$; Fig. 3. 5). Both cases were evaluated for K/K^* equal to: 0.00065, 0.065, 0.65 and 65.

As described in Fig. 3. 4 (a) for $Ag=0$, total washing of the signal is predicted unless K^* is in the range of $10^6 M^{-1}$ to $10^8 M^{-1}$ ($10^{-3} nM^{-1}$ to $10^{-1} nM^{-1}$). This situation does not agree with what is simulated for Ag different to zero (Fig. 3. 4 (b) to (d)) where for $[Ag] = 1$ ppm, 50 % loss of $[AbAg^*]$ is predicted and 90 % to 100 % loss of $[AbAg^*]$ is simulated for 10 ppm and 100 ppm respectively. The progress of the percentage of loss of $[AbAg^*]$ seems independent of S/V ratios or, depending if high affinity constants are investigated proportional to the same S/V ratio.

When higher K and K^* are investigated (Fig. 3. 5), the washing of the signal for $Ag=0$ (Fig. 3. 5; **Error! No se encuentra el origen de la referencia.** (a)) could be higher or lower depending of S/V ratio, even no washing is predicted for K^* in the order of $10^{14} M^{-1}$ ($10^5 nM^{-1}$). The loss of $[AbAg^*]$ increases as Ag increases from zero to 1 ppm depending on the

K/K^* ratio evaluated. Higher K/K^* ratio, and hence lower K^* , gives rise to a greater loss of $[AbAg^*]$.

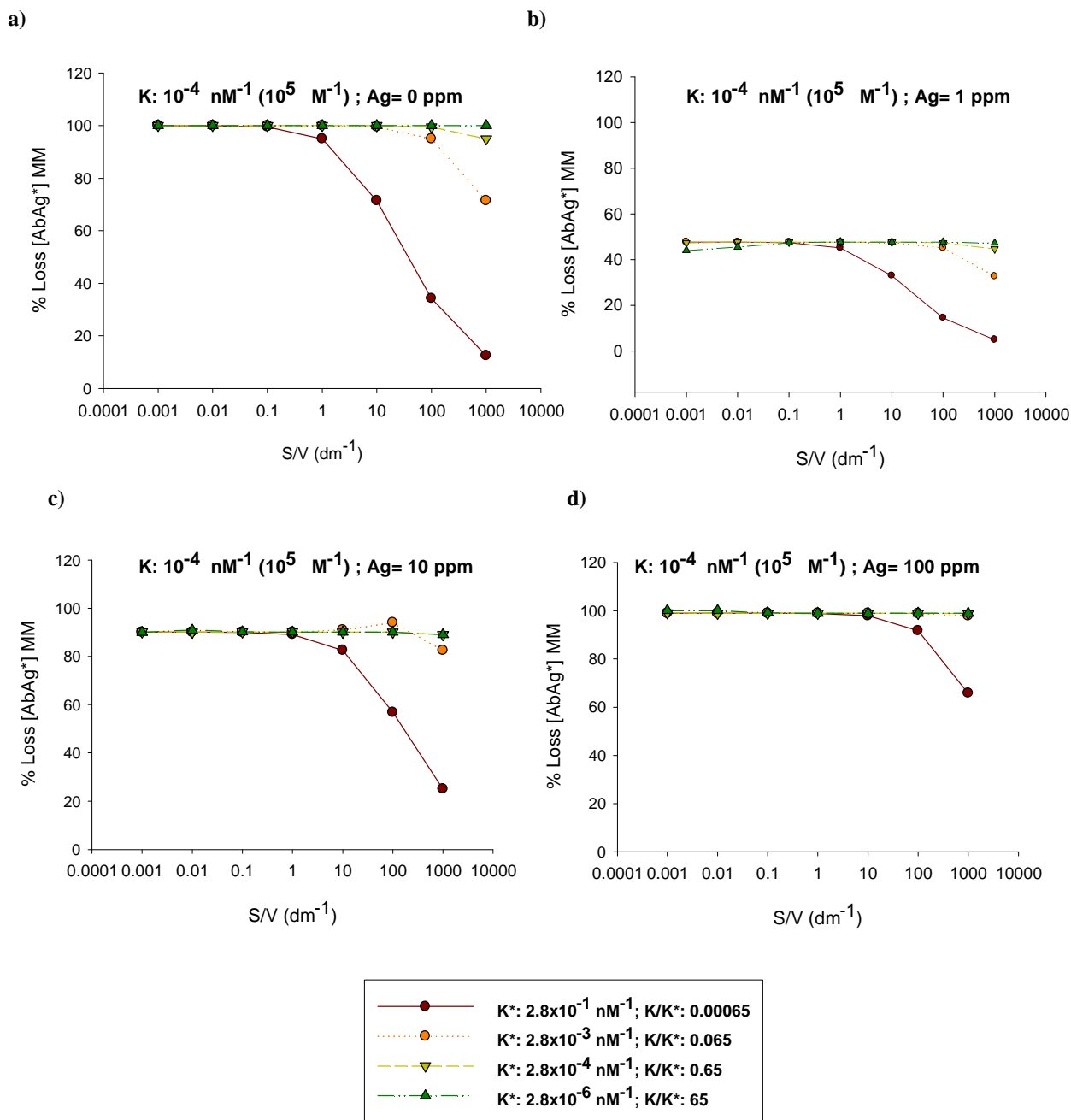


Fig. 3. 4: Simulated displacement response according to S/V and K/K^* ratios. K : $1.82 \times 10^{-4} nM^{-1}$; Ab : $0.2 nM dm^{-2}$; K/K^* : Variable; K^* : Variable.

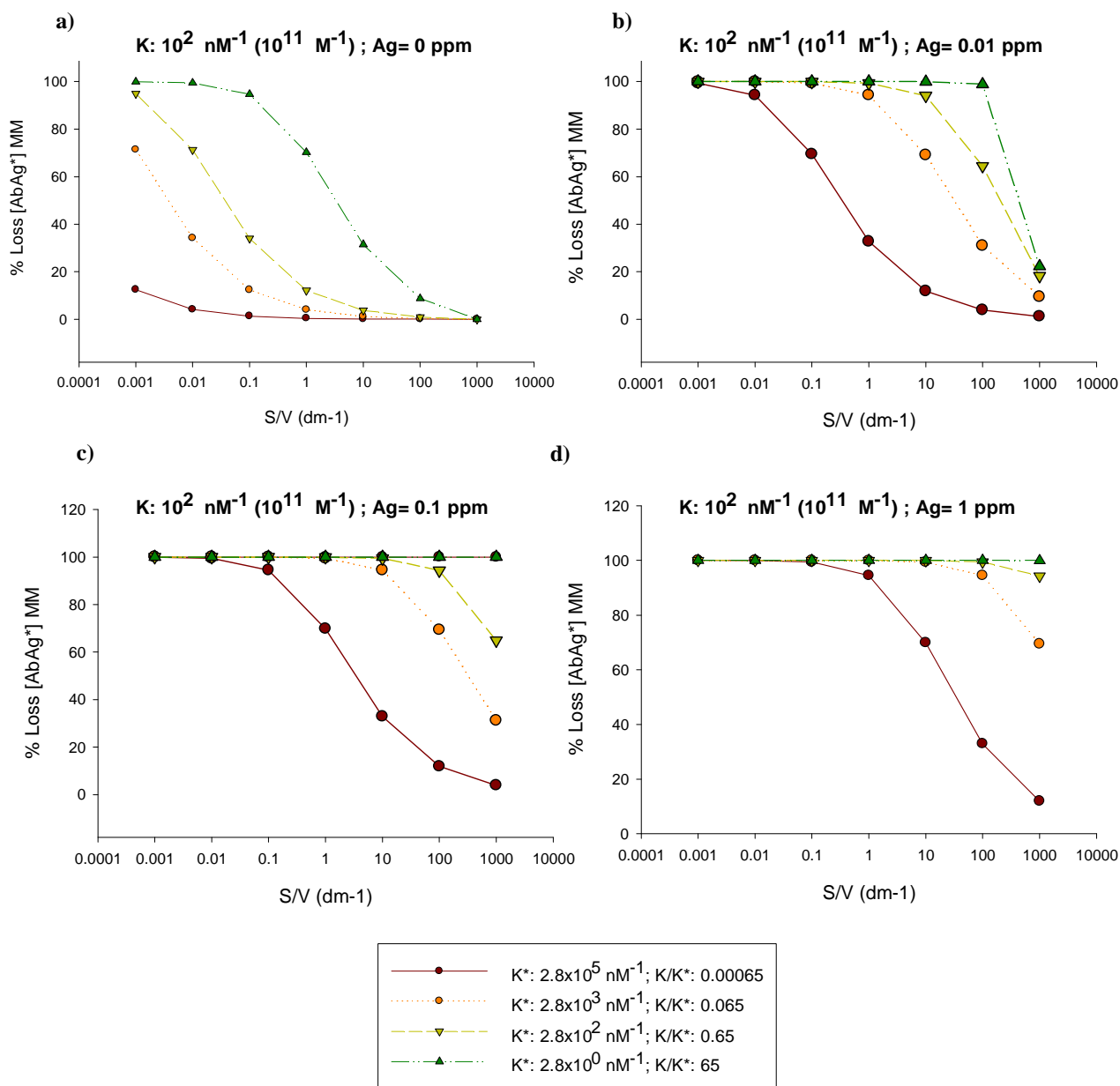


Fig. 3. 5: Simulated displacement response according to S/V and K/K* ratios. K: 1.82x10² nM⁻¹; Ab: 0.2 nMdm⁻²; K/K*: Variable; K*: Variable.

The results showed the dependence of the MM predictions on the affinity constants. The effects of S/V ratios seem to be associated only with high affinity constants.

3.3.2.4 Predicted DEI response

The predicted experimental results with S/V values equal to 0.1 dm^{-1} , as a compromise between high S/V ratios (large loss of labelled immunocomplex predicted by the MM) and low S/V ratios (where the rebinding phenomena can damage the displacement) (e.g.: electrodes of 0.5 mm diameter in 200 μl volume) are shown in Fig. 3. 6. The simulated results seemed to indicate that the range of operation of the displacement immunosensor would be in the order of units of ppm. The observation of this kind of response from the DEI will further be evaluated in Chapter 4.

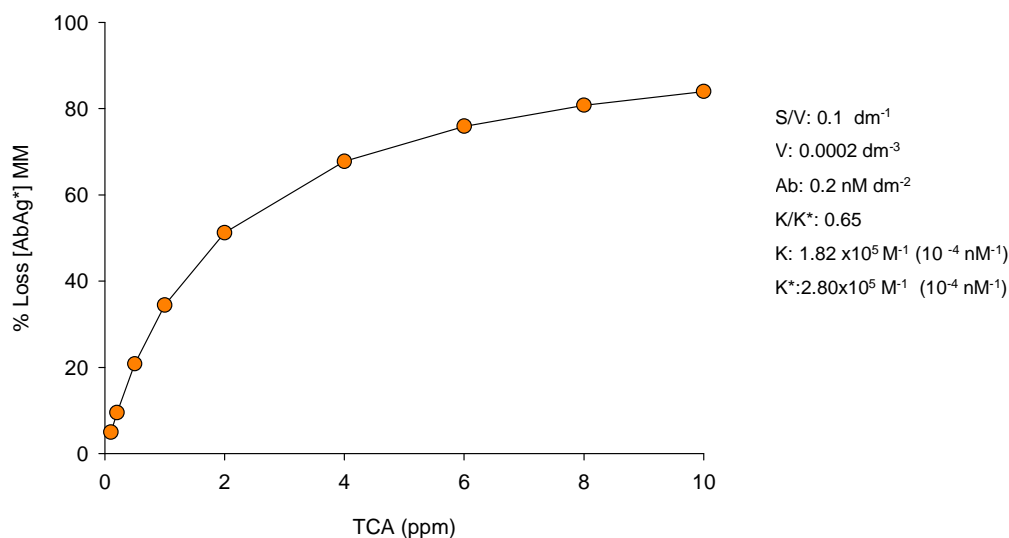


Fig. 3. 6: Predicted loss of signal upon addition of different [TCA] for the case of S/V ratio = 0.1 dm^{-1} .

3.3.2.5 Effects of K, K* and K/K* ratio in the DEI response

At this point the question of how the involved immunoreactions may limit the operation range of the immunosensor give rise to simulations to evaluate the impact of K, K* and K/K*. Simulations were carried out by changing the order of magnitude of both K and K*

keeping K/K^* equal to 0.65 (Fig. 3. 7 (a)) or changing the K/K^* by changing K (Fig. 3. 7 (b)). These changes were evaluated also using different concentrations of analyte.

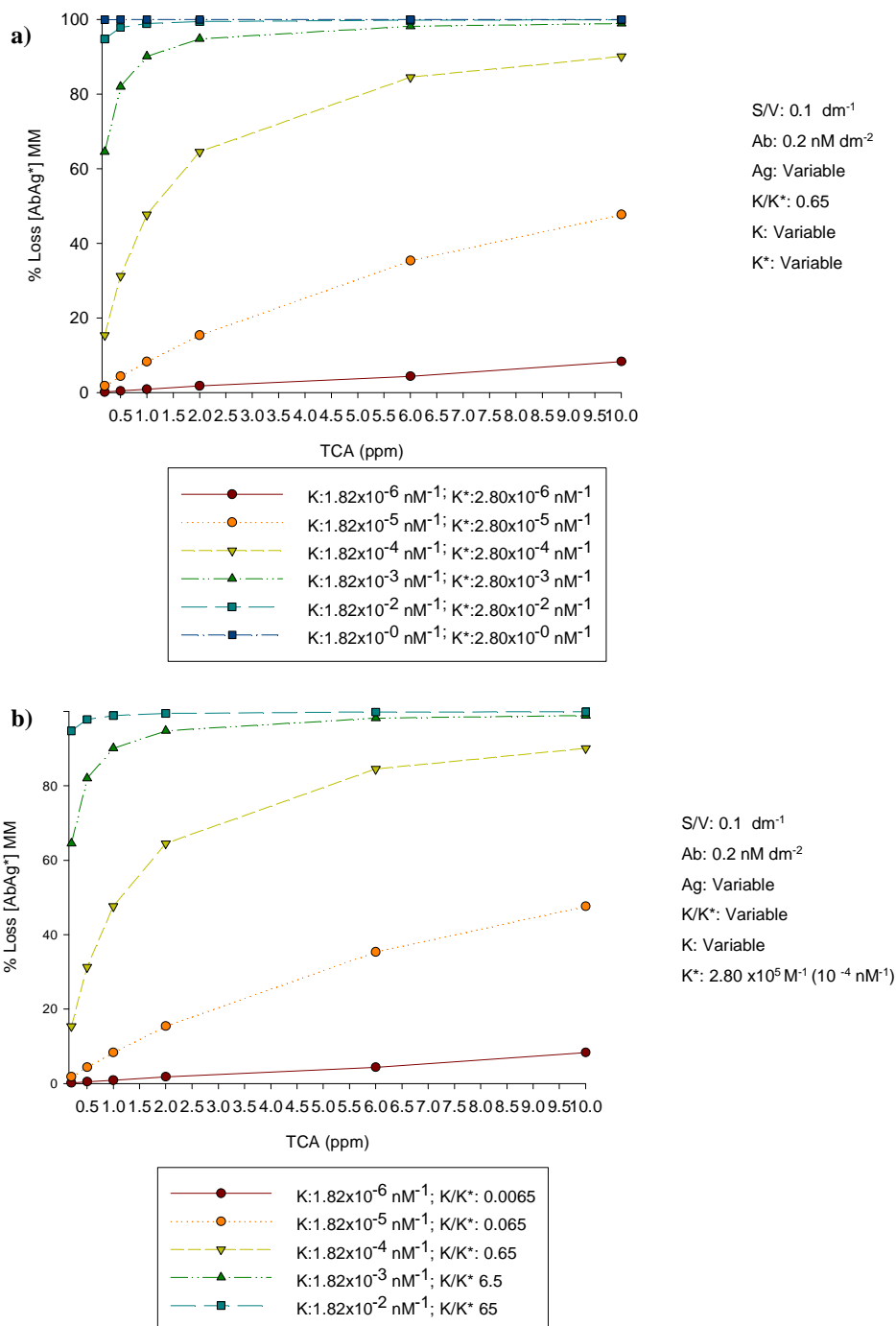


Fig. 3. 7: Predicted percentage of lost [AbAg*] depending in the affinity constants involved. a) Effect of the K and K^* keeping a K/K^* of 0.65. b) Effects of changes in the K .

According to Fig. 3. 7 (a) the same K/K^* ratio could generate different immunosensor behaviour depending on the implicated K and K^* , the used of K and K^* in the order of $10^5 M^{-1}$ ($10^{-4} nM^{-1}$) would generate displacement phenomenon in the order of ppm of TCA, smaller K and K^* would not generated displacement unless addition of TCA higher than 10 ppm are investigated. Better results could be obtained by increasing the order of magnitude of the affinity constants. For example, K and K^* values of $10^7 M^{-1}$ ($10^{-2} nM^{-1}$) and $10^9 M^{-1}$ ($10^0 nM^{-1}$) seem to generate total displacement of the signal in the range of units of ppm. Investigating the effects of varying K/K^* on the displacement response (Fig. 3. 7 (b)), it was observed that the difference between the two involved affinity constants is not as important as the affinity constant of the analyte (K), since for a fixed K value, the same displacement response would be observed independently of the difference with K^* .

3.3.2.6 Prediction of K needed to detect ppt of TCA

The objective of these simulations was to find out which affinity constants would be needed to develop a DEI able to detect TCA in the ppt range. In this sense, simulations were carried out keeping K^* constant (in the range of the experimental K^*) and once K was selected, the impact of K/K^* was evaluated by investigation of different K^* .

According to the simulated results (Fig. 3. 8 (a)), the use of use of K in the range of $10^9 M^{-1}$ ($10^0 nM^{-1}$) would allow the detection of TCA in units of ppt (human threshold). Regarding the K^* values required keeping constant a K of $10^9 M^{-1}$ ($10^0 nM^{-1}$), no significant differences were detected in the simulations obtained in the range of K/K^* from 0.65 to 6500 (Fig. 3. 8 (b)).

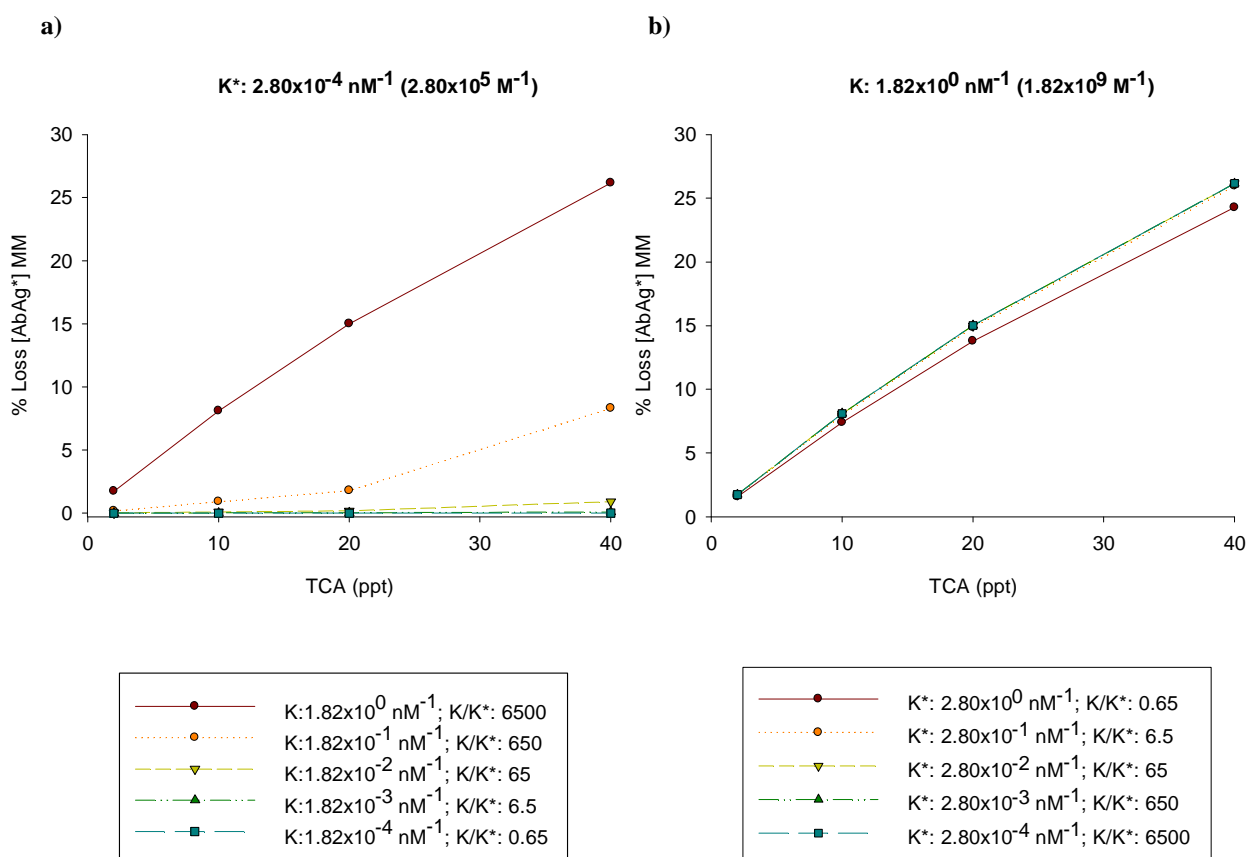


Fig. 3. 8: Simulated investigation of K and K^* needed for the detection of units of ppt of TCA.

The MM predicts that an experimental value of K of 10^9 M^{-1} (10^0 nM^{-1}) or higher may be required to achieve limits of detection of ppt, with a broad range of K/K^* ratios.

3.4 Discussion

3.4.1 Predicted DEI response

The MM predictions for the DEI response evaluated with real affinity constants values showed a displacement of 8% to 90% for TCA concentrations in the range of units of ppm. In contrast to this when the simulation was carried out for $A_g=0$, in total absence of analyte, the MM predicts some dependence of loss of signal with S/V ratios for high K^* or total washing of the signal for low K^* . It has to be noticed that the predictions tried to simulate a system were spontaneous binding and unbinding processes between an antibody and its antigen that could take place driven by thermal motion [27]; the unbinding of the antigen could lead to irreversible dissociation of the labelled antigen, depending on the volume where the electrode is immersed for displacement experiments, giving rise to a loss of labelled antigen concentration not associated to the specific displacement caused by TCA addition; a process namely here “washing effect”.

The MM predictions, considering they do not account for rebinding effects, can be interpreted as correct.

Low K^* constants along with not considering rebinding processes would mean a weak binding of the labelled antigen to the antibody, which can justify the observed washing effect. It also has to be kept in mind that previous works of similar mathematical models dealing with low affinity constants have reported a certain lack of realism in the correlation between predicted behaviours and experimental observations.

3.4.2 Predicted DEI range of detection

With regard to the detection of TCA in the human threshold range, the MM predicts that K values of 10^9 M^{-1} (10^0 nM^{-1}) or higher are needed. The MM also highlights the importances of the high K values over K/K* ratios. Although the MM predicts that the choice of K/K* would not affect the DEI response, it is noteworthy that K/K* ratio should be a compromise between avoiding long time DEI response [15] (higher K*) and controlling the an increasing washing effect associated with a decreasing K*.

An example of the need to reach favourable compromise between high and low K*, is the displacement of chymosin from a synthetic receptor ($K = 1.4 \text{ M}^{-1}$) immobilised to agarose by pepsin which took 30 min, while displacement of pepsin from pepstatin-agarose ($K = 1.5 \text{ M}^{-1}$) by pepsin took 90 h.

The K/K* cannot be altered easily and must be examined before constructing the sensor. A compromise should be made between the sensitivity and the response time when choosing the protein/receptor pair in constructing an affinity sensor.

3.4.3 Validity of the developed MM

The validation of the MM treated here depends on its level of accuracy to mimic experimental results.

The assumptions, or boundary conditions, of the model analyzed here have been considered valid in previous works that is, approximation of competition assay to a simplified system of two reactions competing [16], the simulation of the system considering equilibrium conditions [3, 13, 15, 16], ligand homogeneity [15, 21, 22] and, bimolecular binding [3, 23]. Before assessing the suitability of the MM for the experimental case treated later in Chapter 4, there are aspects that may damage the symbiosis of the MM with the real

situation. Antibody heterogeneity coming from random attachment during the covalent coupling of ligand immobilization would mean the non applicability of the homogeneous binding [28] or also masking of potential sites by bound ligand in case of crowded immobilization would indicate the non applicability of the chosen model and the need of a more complex approximation.

Discrepancy of the MM predictions depending on the evaluated range of K and K^* has been previously foreseen in reported work [26] where the authors estimated that the model best fit the experimental results for high affinity constants.

3.5 Conclusions

A mathematical model for a displacement immunosensor under equilibrium conditions has been developed. The model relays on the assumptions of local equilibrium, homogeneity and monovalency of the antibodies. The MM predicts that the available system with estimated affinity constants of K_{TCA} : $1.82 \times 10^5 \text{ M}^{-1}$ and K_{H_3} (K^*): $2.80 \times 10^5 \text{ M}^{-1}$, K/K^* ratio of 0.65 ($K_{TCA}/K^*_{H_3}$) and initial boundary conditions of $0.2 \text{ nmoles dm}^{-2} \text{ Ab}_0$ and S/V equal to 0.1 dm^{-1} , will theoretically undergo displacement with additions of TCA in the order of hundreds of ppb to units of ppm.

The MM predicts the presence of washing effect of the signal for K^* $2.80 \times 10^5 \text{ M}^{-1}$. The predictions were more realistic in the case high K^* .

Regarding to increasing the sensitivity of the DEI, the selection of K is indicated as the main parameter, although a compromise for the K/K^* ratio has to be established to combine rapid response time and avoidance of washing effects.

According to the MM predictions, in order to be able to detect TCA in the human threshold range, K affinity constant in the order of 10^9 M^{-1} (10^0 nM^{-1}) and higher may be required, keeping in mind the K/K^* compromised ratio mentioned before.

3.6 Bibliography

- [1] Van Emon, J. *Immunoassay and other Bioanalytical Techniques*. 2007, London, Taylor and Francis Group, LLC.
- [2] Merrill, S. J. *J. Immunol. Methods*, 1998, **216**, p. 69-92.
- [3] Holland, T., Holland, H. *J. Microscopy-Oxford*, 2004, **214**, p. 1-6.
- [4] Kawade, Y., Finter, N., Grossberg, S.E. *J. Immunol. Methods*, 2003, **278**(1-2), p. 127-144.
- [5] Chou, T. C. *Pharmacol. Reviews*, 2006, **58**(3), p. 621-681.
- [6] Castiglione, F., Liso, A. *Immunopharmacol. Immunotoxicol.*, 2005, **27**(3), p. 417-432.
- [7] Wilson, J. N., Nokes, DJ., Medley, G.F., Shouval, D. *Vaccine*, 2007, **25**(18), p. 3705-3712.
- [8] Gurbaxani, B. *Clinical Immunol.*, 2007, **122**(2), p. 121-124.
- [9] Green, A. J., Johnson, C.J., Adamson, K.L., Begent, R.H.J. *Phys. Medicine Biol.*, 2001, **46**(6), p. 1679-1693.
- [10] Glass, T. R., Ohmura, N., Morita, K., Sasaki, K., Saiki, H., Takagi, Y., Kataoka, C., Ando, A. *Anal. Chem.*, 2006, **78**(20), p. 7240-7247.
- [11] Hayashi, Y., Matsuda, R., Maitani, T., Imai, K., Nishimura, W., Ito, K., Maeda, M. *Anal. Chem.*, 2004, **76**(5), p. 1295-1301.
- [12] Hendrickson, O. D., Zherdev, A.V., Kaplun, A.P. Dzantiev, B.B. *Molec. Immunol.*, 2002, **39**(7-8), p. 413-422.
- [13] Clark, H. R., Barbari, T.A., Rao, G. *Biotechnol. Prog.*, 1999, **15**, p. 259-266.
- [14] Selinger, J., Rabbany, S. *Anal. Chem.*, 1997, **69**, p. 170-174.
- [15] Chen, J. P., Hsu, M.S. *J. Chem. Tech. Biotechnol.*, 1996, **66**, p. 389-397.
- [16] Chen, J. P. *J. Chem. Tech. Biotechnol.*, 1993, **56**, p. 273-277.
- [17] Wemhoff, G. A., Rabbany, S. Kusterbeck, A., Ogert, R., Bredehorst, R., Ligler, F. *J. Immunol. Methods*, 1992, **156**(2), p. 223-230.
- [18] Rabbany, S., Kusterbeck, A., Bredehorst, R., Ligler, F. *Sens. Actuators B*, 1995, **29**, p. 72-78.
- [19] Rabbany, S., Piervincenzi, R., Kusterbeck, A., Bredehorst, R., Ligler, F. *Anal. Letters*, 1998, **31**(10), p. 1663-1675.
- [20] Ralston, A., Rabinowitz, P. *A first course in numerical analysis*. Second ed. 2001, Mineola, NY., Dover Publications, Inc.
- [21] Choi, D. H., Katakura, Y., Matsuda, R., Hayashi, Y., Ninomiya, K., Shioya, S. *J. Biosci. Bioeng.*, 2007, **103**(5), p. 427-431.
- [22] Tschmelak, J., Kumpf, M., Proll, G., Gauglitz, G. *Anal. Letters*, 2004, **37**(8), p. 1701-1718.
- [23] Goldstein, B., Dembo, M. *Biophysical J.*, 1995, **68**, p. 1222-1230.
- [24] Jackson, T. M., Ekins, R.P. *J. Immunol. Methods*, 1986, **87**, p. 13-19.
- [25] Taylor, R. F., Schultz, J.S. *Handbook of Chemical and Biological Sensors*. First Ed. ed. 1996, Bristol, U.K., Institute of Physics Publishing Ltd.
- [26] O'Connor, T., Gosling, J.P. *J. Immunol. Methods*, 1997, **208**(2), p. 181-189.
- [27] Kulin, S., Kishore, R., Hubbard, H.B., Herlmerson, K. *Biophysical J.*, 2002, **83**, p. 1965-1973.
- [28] O'Shannessy, D. J., Winzor, D.J. *Anal. Biochem.*, 1996, **236**, p. 275-283.

3.7 Annex. Example of Matlab routine

```
clear all; clc; close all;
global Ab0 Ag0 V AbAgp0 S k kp

Ab0=0.2; %nmol/dm^2
Ag0=50000; %nmo/dm^3
V=0.002; %dm^3
AbAgp0=0.2; %nmol/dm^2
S=1.96e-5; %dm^2
k=182; %dm^3/nmol
kp=280; %dm^3/nmol

n=5;
u=[0 0 0 0 0];
e=1e-12;
e1=1e-5;
g=sistem(u);
w=1;
iter=0;
while w==1
    for i=1:n
        u1=u;
        u1(i)=u(i)+e1;
        g1=sistem(u1);
        for j=1:n
            J1(j,i)=(g1(j)-g(j))/e1;
        end
    end
    du=J1\(-g');
    u=u+du';
    g=sistem(u);
    if max(abs(g))<e
        w=0;
    end
    iter=iter+1;
end
u
results=[u(3),1-u(3)/AbAgp0,V,S/V,k,k/kp,Ab0,Ag0,Ag0/5000,u(1:2),u(4:5)]

f_path=cd;
f_name='\results.txt';
f_id=fopen([f_path,f_name],'a');
for i=1:length(results)
    fprintf(f_id,'%1.10f',results(i));
    fprintf(f_id,'%s',' ');
end
fprintf(f_id,'\n');
```

System for Matlab

```
function g=sistem(u);
global Ab0 Ag0 V AbAgp0 S k kp

Ab=u(1);
AbAg=u(2);
AbAgp=u(3);
Ag=u(4);
Agp=u(5);

g(1)=Ab + AbAg + AbAgp - Ab0;
g(2)=AbAg*S + Ag*V - Ag0*V;
g(3)=AbAgp*S + Agp*V - AbAgp0*S;
g(4)=Ab*Ag*k - AbAg;
g(5)=Ab*Agp*kp - A
```

CHAPTER 4

Strategy for Displacement Electrochemical Immunosensors Development: the 2,4,6-trichloroanisole (TCA) case

4.1 Introduction and aims

4.1.1 Introduction

Biosensors have been under continuous evolution over more than three decades. Throughout their existence and continuous adaptation to science and life requirements, biosensors have been criticized and equally praised [1]. Over all discussions, biosensors development is no doubt a powerful tool for diagnostics, and has no competition when speed, portability, selectivity and specificity are required [2]. Biosensors can have relative low cost of construction and storage, potential for miniaturization, ease of automation, portable equipment for fast analysis and monitoring in platforms of raw material reception or quality control laboratories [3].

The definition of biosensor [4], focused in a Bio-Recognition Element (BRE), points towards the fundamental need of using an effective BRE-target interaction. In the case of immunosensors such interaction is characterized through the antibody-antigen affinity constant, which strongly affects the performance of an immunoassay [5]. The challenge rises when the production of such antibody leads to a low antibody- antigen affinity constant, then only a rational design of the immunosensor would overcome the low affinity and make the immunosensor efficient. Non-specific adsorption phenomenon has to be specially watched, since it is one of the main factors that define the detection limits of electrochemical bioaffinity assays [6, 7].

4.1.2 Non-Specific Adsorption (NSA) and strategies to control it

The control of NSA phenomenon and the development of strategies to maximize the specific adsorption phenomenon are of great relevance in this work. As detailed in Chapter 2, the utilized immunoreactants are characterized by low affinity constants hence rational design of the immunosensor is due. It should be also kept in mind that NSA has been reported as one of the main factors affecting the sensitivity of an immunoassay, specially in the case of low concentrations of analyte [8]. The lowest limit of detection of an immunoassay has been reported to be determined not only by the binding constant of the antibody but also by the NSA of the assay [7].

4.1.2.1 Adsorption of proteins. The interface that is formed between two phases usually has a higher standard free energy than the bulk phase. In this sense, the interface is apt to be

thermodynamically stabilized by adsorbing any substances different from the solvent molecules [9].

Protein adsorption is known to be the net result of various complex interactions between and within all components of the system including the solid surface, the protein, the solvent and any other solutes present. The whole process combines electrostatic attraction and repulsion, hydrophobic and hydrophilic interaction, hydrogen bonding or dipole attraction [10-12]. All these inter- and intramolecular forces would contribute to a decrease of the Gibbs energy during adsorption [13]. The orientation of proteins during the adsorption process could be either horizontally, vertically or as a mixture of both [9, 14].

The adsorption of proteins to solid–water interfaces is considered as a multistep process. The first steps would be determined by long-range interactions where surface properties such as hydrophobicity, distribution of charged groups, ion concentrations and pH play important roles. In next steps, structural rearrangements in the protein molecule and dehydration effects become more important making the adsorption process often irreversible [9, 11].

The adsorption process involves the transfer of a protein molecule from solution to the sorbent surface. Despite the diversity of experimental procedures and great effort of literature, general conclusions regarding to the interfacial behaviour of proteins are considered difficult to make [12] and nature of chemical bonds is still considered as poorly understood at the molecular level [15].

Regarding the effects that determine the amount of adsorbed protein, the literature [12, 13]

lists:

i) effects of electric charge: repulsion and attraction forces that take place depending on surface and protein charges which, at the same time depend on pH. The pH of the solution have been reported to affect the protein adsorption depending on the pI of the protein and the net charge of the surface [10].

ii) effects of hydrophobicity: hydrophobic interaction has been reported to play an important role in protein adsorption, hydrophobic surfaces are assumed as “stickier” than hydrophilic ones [9, 16]. As example, IgG demonstrated to adsorb on hydrophobic surfaces three times more than on hydrophilic surfaces [16].

iii) effects of surface energetic: related to the search of stabilizing effects by the system [12, 16].

iv) influence of temperature: different adsorption results have been reported depending on the temperature and the entropy of the system [12].

v) time: the amount of adsorbed protein would increase with time until reaching a plateau. The increase of both time and protein concentration seem to contribute to larger amount of adsorbed molecule. Time and protein concentration would also define the orientation of the adsorbed molecule as horizontal, vertical or a mixed of both [10].

The adsorption phenomenon results as the combination of different factors, in this sense, it has been reported that although hydrophobicity determines much of the amount of adsorbed protein, as well as the protein layer thickness and the refractive index layer, other effects like electrostatics could also contribute to the adsorption phenomenon [16, 17].

4.1.2.2 Adsorption of proteins on metals. Proteins have been reported to specifically adsorb to metallic surfaces. An example of such specificity have been evaluated on gold, titanium and indium-tin oxide (ITO) surfaces through the exploration of two different proteins containing greater number of cysteine groups or greater number of lysine groups [11]. The authors found that the protein with higher cysteine groups adsorbed preferably to gold since sulfur groups would form S bridges on gold.

Regarding to the widely utilized as enzyme-labelling, horseradish peroxidase (HRP), reported work on the enzyme aminoacids revealed as predominant components 16 % of aspartic acid and 13 % of leucine. The presence of cysteine was found to be 3 % and of lysine 1.6 % [18]. According to this information, HRP would content low percentage of residues that would form S bridges with gold but, on the other hand, it has an important component of aspartic acid/aspartate. The acid character of the H⁺ of aspartic acid would give negative density surroundings depending on the pH utilized solutions, which is also a factor contributing to the increase of NSA.

4.1.2.3 Effects of protein adsorption on electron transfer: Adsorption of proteins can play a negative role in electron transfer. Reported work investigating the adsorption of human serum albumin (HSA) and immunoglobulin G (IgG) on gold electrode, demonstrated the adsorption of the molecules on the gold electrode surface and their blocking effect on the electron transfer. Total blocking of the electron transfer was detected for protein concentrations in the order of μM of HSA and IgG on gold electrodes with incubation times of 10 minutes [10].

4.1.2.4 Construction of protein resistant surfaces. In order to control the adsorption phenomenon, protein resistant surfaces have been constructed and reported. Self-assembled monolayers (SAMs) with oligo(ethylene glycol)_n (OEG) with n=3 to 6 have been mentioned as the most protein resistant surfaces available since they “hydrophilize” hydrophobic surfaces. OEG adequacy as protein adsorption barrier is generally attributed to hydrophilicity, flexibility, chain mobility and high steric exclusion volume in water [17, 19-24]. Nevertheless OEG_n tends to get oxidized [16, 25] and for this reason, the bibliography have investigated alternatives to OEG_n by studying protein adsorption resistance of gold surfaces modified with SAMs containing different functional groups. The reported functional groups shared by SAMs that satisfactory resisted protein adsorption were [22, 25]:

- i)* polar groups,
- ii)* accepting H groups,
- iii)* groups without net charge,
- iv)* groups without H donor groups,

being the last one proposed as key structural element in protein-resistant surfaces. The formation of bound water at the interface has been proposed also as main factor to avoid NSA [21].

Surfactants and proteins have been reported as blocking agents of NSA [19, 21, 25, 26].

4.4.2.5 Self-assembled monolayer (SAM)s formation. Organothiols (RSH) spontaneously arranges themselves on gold surfaces as self-assembled monolayer with the sulfur atoms bound to the gold. Although it has been reported that the thiolate (RS-) form dominates the initially formed Au-S bond, how RSH goes to RS- is not sufficiently know and may involve other reactions [27, 28], including radical reactions [29]. Two important parameters in SAM formation are incubation time and alkanethiol solution concentration. Thin and less organized layers have been detected for short exposures. Longer adsorption times with more concentrated solutions give more dense molecular packing and vertical orientation of the molecules on the surface. SAMs layer thickness have been reported in a range from 2 Å to 12 Å [30, 31].

SAMs have been prepared on a variety of electrode materials such as silicon, silver, copper, gold and platinum. Assemblies based on thiols on gold are the most extensively studied SAMs [30, 32-34] because of the high stability of Au in different environments and the easy preparation of clean gold surfaces [35]. On the other hand, alkanethiols assembled on copper and silver are more difficult to work with because of the sensitivity and stability of these systems to air exposure and long exposure to the solution containing the thiol [36].

The modification of metal electrodes surface with SAMs requires special attention since long alkyl chains of highly packed SAM layer would block the approach of electrochemically active species to the electrode surface, even suppressing their reactions at the electrode [37]. However, if the alkylchains of the SAM are relatively short, electron tunnelling across the SAM, penetration of electroactive species through defects in the SAM, or both, allow electrochemical reactions to occur at the electrode. As example, total blocking of the electrochemical signal have been reported for 10 mM of 4-aminothiophenol on Pt electrodes during 24 hrs incubation [32].

The coexistence of thiol SAMs and Cu plays an important role in the development of this work; hence thiol SAM formation on Cu merits an overview:

4.1.2.6 SAM on Cu. Even though some difficulties could be found during their preparation, SAMs on Cu have been widely proposed as barrier for water and ions that cause Cu corrosion [31, 38]. Cu has three oxidation states that can exist in different proportions depending on the corrosion conditions. Metallic Cu^0 is oxidized to Cu^{+1} and Cu^{+2} upon exposure to air forming oxidized species like Cu_2O , CuO and $\text{Cu}(\text{OH})_2$. In terms of substrate preparation, it is demanding to remove as much of the native oxide from Cu surface as possible to have a successful SAM formation. Irreproducibility in SAM quality on Cu surfaces has been attributed to the presence of a chemically complex $\text{Cu}^0/\text{Cu}^{+1}/\text{Cu}^{+2}$ oxides giving rise to heterogeneous surface morphology and reactivity [36, 39].

The formation of SAMs on Cu have been reported on single-crystal and polycrystalline Cu, nevertheless single-crystal surfaces are recommended because of their uniform composition

and atomic structure that are more appropriated to obtain reproducible results [40, 41]. Best results of SAMs formation on Cu were obtained using toluene as solvent [33].

Investigation of the Cu-SAM, Ag-SAM and Au-SAM bond stability have been reported through the electrochemical analysis of the peak potential (E_p) for the electrodesorption of an *n*-alkanethiolate [33]. The electrochemical desorption of SAM from Cu surface was reported as shifted 0.6 V in the negative direction with respect to the corresponding E_p value of Au and Ag. Hence SAMs on Cu were proposed to be more stable than those formed on Au surfaces, indicating high stability of SAMs on Cu surfaces. This observation was investigated considering electronic configuration of the metals as $nd^{10} (n+1) s^1$ where $n=3$ for Cu, 4 for Ag and 5 for Au (Cu $3d^{10} 4s^1$, Ag $4d^{10} 5s^1$ and Au $5d^{10} 6s^1$ valence shells) [42-44] and utilizing combined Auger Electron Spectroscopy (AES) with quantum density functional theory (DFT). The authors found that:

The barrier for electrochemical desorption of an alkanethiolate molecule from the metal surface (E_{ed} , Eq.4. 1) would involve the energy needed to introduce an electron in the alkanethiolate-metal system (E_{e-}), the energy needed for the desorption of the thiol (E_{des}) and substrate-solvent ($E_{Me-solv}$) energies.

$$E_{ed} = E_{e-} + E_{des} + E_{Me-solv} \quad \text{Eq.4. 1}$$

It was reported that the adsorption energies, which at the same time are opposite to the desorption energy ($E_{ads}=-E_{des}$), decreases with the investigated metal as follows: Au >Cu >Ag. On the other hand, the energy needed to introduce an electron in the S-Me binding

decreases as $Au > Ag > Cu$. Hence the energy required for the electrochemical desorption (Eq.4. 1) of Cu would be higher compared to Au; this observation is in agreement with other reported data where the stronger chemisorption interaction on the Cu surface was explained in terms of the atomic properties of Cu and Au, *i.e.*, the differences in a radial distribution of the valence $(n+1) s$ atomic orbitals. Radial distribution of the Cu 4s orbital is smaller than that of the Au 6s orbital; the size of the Cu 4s orbital would be more compatible with that of the S valence orbitals. Thus, the Cu 4s orbital can overlap with the S orbitals more effectively than the Au 6s orbital [35].

4.1.2.7 SAM on Cu UPD: Underpotential deposition (UPD) has been explored with the purpose of obtaining controlled composition at molecular level of mixed SAMs. UPD is an electrochemical process where a single metal adlayer is electroplated onto metal. The process is driven by the formation of substrate- adatom interactions that are stronger than the adatom-adatom interactions that form during bulk electrodeposition making the preparation of adlayers easy and with coverages no greater than a monolayer [45].

The combination of SAM formation and metal UPD has been reported for the optimization of gold substrates. The procedure consisted in the application of a non-complete Pb UPD monolayer that was followed by the first SAM formation with an alkanethiol that would occupy the Pb-free gold sites, next the Pb stripping would create vacant sites in the alkanethiol adlayer available to immobilize a second functionalized thiol, giving rise to the formation of a mixed SAM with a defined composition ratio [46].

Another strategy of metal UPD and SAMs consists in the metal deposition after the SAMs formation; the feasibility of such strategy on gold surface has been previously demonstrated [37, 47]. The reported work found that depending on the deposited metal, the SAM monolayer would not be damaged and would even undergo stabilizing effects. In the cited literature, SAMs on gold electrode were formed and next the investigated metal was deposited to be further stripped and finally proceed with the reductive desorption of thiols in order to evaluate SAM integrity. Except for the case of Bi, other metals like Cu, Ag, Tl, Pb and Cr demonstrated to be adequate to be underpotentially deposited and stripped without damaging the SAM. The UPD of metal was reported to be successful for alkylchain length of the thiol shorter than 8 carbons (C8).

UPD reactions on the SAM-coated electrode require that the metal ions penetrate through the SAM to make direct bonding between metals atoms of the electrode substrate and metal atoms deposited. Negative shifting of the cathodic deposition and positive anodic shifting of the stripping of metals have been proposed as indication of the blocking effect of SAMs hydrophobic environment [47].

The study of the metal UPD on SAM stability demonstrated also translocation of the metal directly bound to the SAM (*e.g.*; SAM/Ag(UPD)/Au) [37, 48]) and also stabilization of the SAM in the case of Cu [45, 47] that would agree with reported work on Cu-SAM and Au-SAM desorption energies previously cited here (section 5.1.2.6). Cu UPD was reported as reversible on gold electrode coated with SAM of short alkanethiol without any significant

loss of thiol molecules [47]. In this sense, UPD of metals would provide means to design the metal surfaces covered with SAM with molecular or atomic level control.

Attempts to directly form SAMs on Cu UPD monolayer have been unsuccessful because of the Cu UPD monolayer tendency to get oxidized by air and to be corroded by thiol solution [36, 47].

4.1.3 Displacement phenomenon

Immunosensors operating on a displacement methodology could result in reagentless, labelless and fast responding devices. Displacement immunoassays are based on the use of a labelled sub-optimum antigen (Ag^*) that binds to the antibody (Ab) and forms an immunocomplex ($AbAg^*$) that produces an easily discernible signal (Fig. 4. 1). These labelled sub-optimum antigens are displaced during the detection step by the displacing antigen that is normally the analyte of interest (Ag). If the signal of the label is produced in the absence of other substrates (S), then displacement is the key point to reagentless and labelless immunosensors. It is obvious that the antibody-antigen affinity constant plays a limiting role in the success of this methodology.

Examples of displacement strategies in the literature involve immobilization of the sub-optimum antigen on supporting elements (column, hollow fiber, biochips) to further detect the displacement by optical, piezoelectric and colorimetric methods [49-52]. In particular, electrochemical detection of the displacement phenomenon has been accomplished using indirect detection [53, 54], direct detection in flow [55] or batch systems [56].

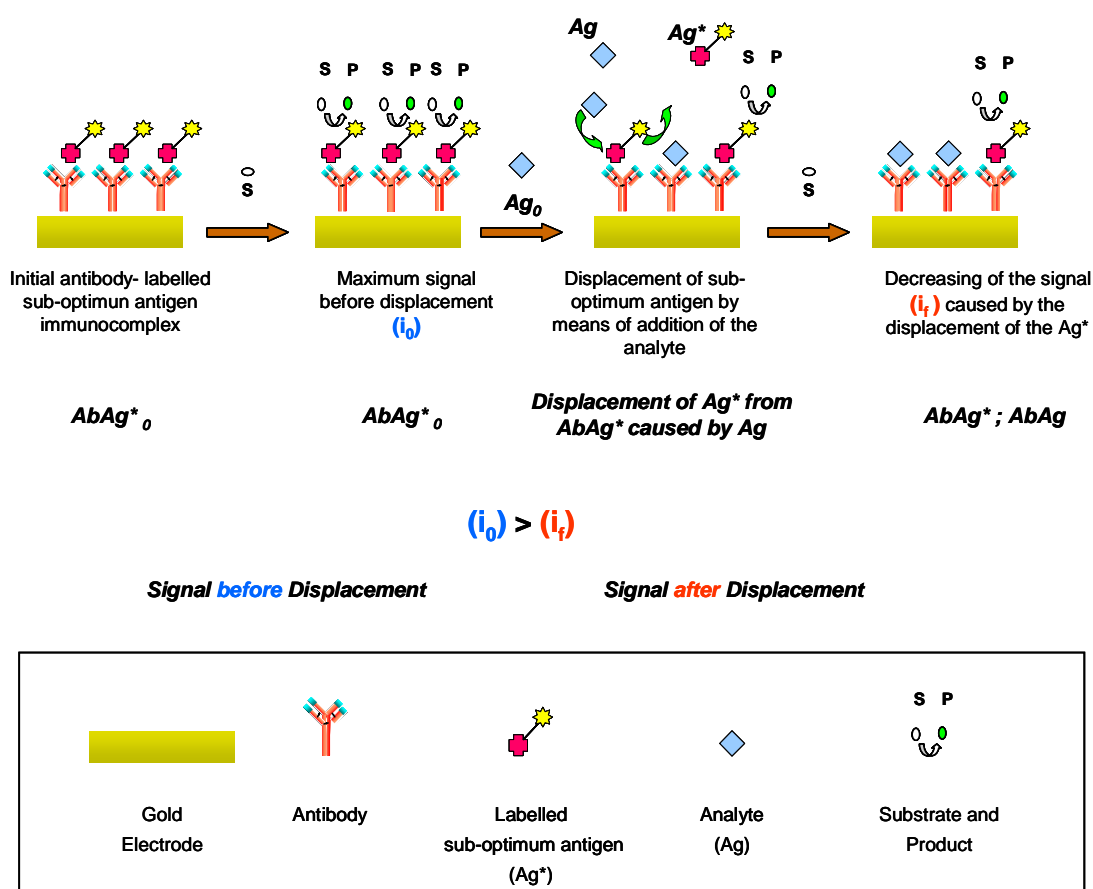


Fig. 4. 1: Schematics of Displacement Phenomenon

Electrochemical biosensors have advantages when compared with other transducers. They can be operated in turbid media and they do not depend on detectable heat changes, in contrast with optical or thermal biosensors. Electrochemical biosensors combine the specificity of biological recognition layers with the inherent advantages (sensitivity, speed, miniaturization, linearity) of electrochemical transduction [57]. They are easy to handle and low cost [58]. Electrochemical biosensors work with potentiometric, capacitive and amperometric transducers, but due to their fast detection, broad linear range and low detection limit, amperometric transducers are preferred [59].

4.1.4 TCA detection

As explained in Chapter 1, the literature related to TCA detection in wine could be divided as follows: 65 % detection with gas chromatography, 15 % utilizing immunoassays and 4 % with the application of electrochemical bioanalytical devices. The use of chromatography and immunoassays (ELISA) techniques allowed satisfactory detection limits matching the human threshold [60-63]. Nevertheless some aspects of these techniques like the need of sample preconcentration [64] or the use of still not fully automated routine analysis (ELISA) [65], could turn into disadvantages. Here is where advantages of biosensors gain importance; it has been reported the electrochemical immunosensing of TCA using polyclonal antibodies achieving limits of detection in the ppt range under direct competitive assay [66].

In this work, the concepts of electrochemical displacement immunosensing are applied to the detection of 2,4,6-trichloroanisole (TCA) using an specially raised against TCA monoclonal antibody (mAb) as BRE and horseradish peroxidase labelled 3-chloro-2-methylphenoxyacetic acid (H3 in Fig. 4. 2) as chosen sub-optimum antigen (Ag*, H3HRP).

Consequently, the aim of this chapter is to illustrate electrochemical displacement principles through the detection of 2,4,6-trichloroanisole (TCA), demonstrating also: *i*) the feasibility for the construction of immusensors with low antibody-target affinity constant; *ii*) the reduction of non-specific adsorption (NSA) *via* Underpotential Deposition of Cu (Cu

UPD) [37, 47, 67], *iii*) the use of electrochemical displacement towards labelless and reagentless detection.

4.2 Materials

4.2.1 Chemicals

The analyte 2,4,6-trichloroanisole (TCA, 99%) was purchased from Sigma-Aldrich Chemical Co. (Spain). The sub-optimum antigen 3-chloro-2-methylphenoxyacetic acid (Hapten 3, H3) was synthesized as described in the literature [68].

As detailed in Chapter 2, anti-TCA monoclonal antibody clones were obtained from *Antibodyshop* (Denmark) and selected according to cross-reactivity. The selected clone (mAb) was purified and kept at 4 °C. The antibody to TCA affinity constant estimated by ICE was $1.82 \times 10^5 \pm 5.85 \times 10^4 \text{ M}^{-1}$.

2,4,6-trichlorophenol (TCP 98%), 3-(4-methoxyphenyl) propionic acid (Hapten Z, HZ), horseradish peroxidase (HRP), hydrogen peroxide (H₂O₂), potassium hexacyanoferrate (II) trihydrate, potassium hexacyanoferrate (III), strontium nitrate, 3-mercaptopropionic acid (MPA), thioctic acid (TA), 11-mercaptoundecanoic acid (MUA), copper (II) sulfate pentahydrate, 1-ethyl-3-[3-(dimethylamino)propyl carbodiimide hydrochloride (EDC), N,N-dicyclo-hexylcarbodiimide (DDC), N-hydroxi-succinimide (NHS) and ethanolamine were obtained from Sigma-Aldrich Chemical Co. (Spain), as well as solvents and salts for buffer preparations (PBS pH 6.5, acetate-acetic buffer pH 8.5, citrate Buffer pH 4.8).

Hydrogen peroxide, TCA and enzyme solutions were prepared daily. Deionised water purified in a Milli-Q system (Millipore, Bedford, MA, USA) was used to prepare solutions.

All reagents were of analytical grade, unless stated otherwise.

4.2.2 Instrumentation and Apparatus

All electrochemical measurements were performed in a standard three-electrode cell with a platinum mesh counter electrode and Ag/AgCl reference electrode (*Bioanalytical System, IN, USA*). The working electrodes consisted in sputtered gold electrodes (SGE) of 3 mm of diameter (Institut für Mikrotechnik, Mainz) or epoxy resin sealed disk gold electrodes of 0.5 mm of diameter (DGE). The cleaning procedure of working electrodes consisted in UV/ozone treatment (SGE) or polishing with alumina slurries (1 μm), sonication, cyclic voltammetry in 2 M H_2SO_4 and final UV/ozone treatment (DGE).

Electrochemical measurements were carried out with a PGSTAT10 potentiostat interfaced with the AUTOLAB Electrochemical Workstation software (Ecochemie, Utrecht, The Netherlands).

Impedance measurements were carried out in a CHI 660 A electrochemical workstation (CHInstruments, USA).

Sonication was conducted in a Branson bath type sonicator, model 2510 (Branson, Soest, Netherlands). UV/ozone cleaning was carried out using a temperature controlled UV surface decontamination system PSD-UVT Ultra-Violet/Ozone probe and surface decontamination with temperature controlled heated stage (Novascan, USA). Pumping of solutions was carried out using a Peristaltic Pump P-1 (Amersham Biosciences, USA).

Absorbance measurements for activity assays were collected using Hewlett Packard UV-Vis Spectrophotometer 8453/G1103A with Deuterium discharge lamp and diode array detector, interfaced with a PC. Measurements of pH were obtained with a CyberScan 2000 pH meter (Eutech Instruments, Netherlands).

The characterization of bioconjugates was carried out using matrix assisted laser desorption ionization-time-of-flight mass spectrometry (MALDI TOF) on a stainless steel plate with a Voyager DE-STR High Performance from MALDI-TOF Mass Spectrometer.

4.2.3 Conjugation of HRP to Hapten 3 (H3HRP)

The conjugates were prepared by the N-hydroxysuccinimide (NHS) and N,N-dicyclo-Hexylcarbodiimide (DDC) conjugation protocol [69]. Formation of such esters may be achieved by the reaction of a carboxylate with NHS in the presence of a carbodiimide. Hapten 3 was conjugated to HRP using this protocol. The conjugates were characterized through MALDI-TOF analysis. Activity of the enzyme was analyzed according to SIGMA Enzymatic Assay of horseradish peroxidase [70].

4.2.4 Immuno-electrodes

4.2.4.1 Analyte and sub-optimum antigen

According to the Mathematical Model (MM) described in this thesis, the decisive factor in the performance of a Displacement Electrochemical Immunosensor (DEI) is the antibody to analyte affinity constant (K). Less significance has the K/K^* ratio, where K^* is the antibody to displaced sub-optimum antigen affinity constant. It could be considered that, in a range of available sub-optimum antigens, the selection of the sub-optimum antigen should be done in the sense of avoiding total loss of signal due to displacement of the sub-optimum only caused by the buffer solution (low K^*) and on the other hand, avoiding long time response and even null displacement (high K^*).

Among the available K/K^* ratios depending on the K^* estimated by ELISA (see Chapter 2, section 2.3.3); that is K/K^* ratio equal to 0.089 (HA); 0.12 (H1), 0.24 (HB), 0.65 (H3) and 0.78 (HZ), H3 and HZ were chosen for the DEI development. The selection considered the low available K values, hence the use of too high K^* values in the range of selection were avoided.

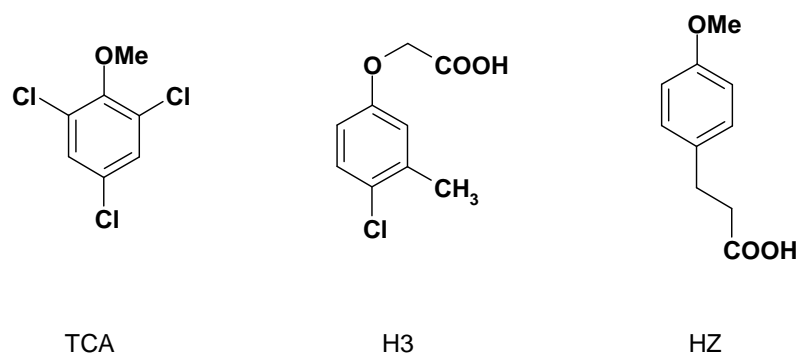


Fig. 4. 2: Schematic of the analyte (TCA) and first selection of sub-optimum antigens (H3 and HZ).

Following experiments of electrochemical detection of prepared immunoelectrodes (see section 5.2.4.2 for immunoelectrodes preparation description) with HZHRP demonstrated non-reproducible and almost not detectable current (data not shown). In this sense, H3HRP was finally selected for the DEI development.

4.2.4.2 Preparation of Immunoelectrodes

The following procedure (Fig. 4. 3) describes an optimized immobilization methodology for the preparation of immunoelectrodes.

After the final UV/ozone treatment the electrodes were immersed in ethanol for 10 minutes in order to remove the resulting gold oxide monolayer [71-74]. Electrodes were immersed in the thiol solution immediately after.

i) Thiol based self-assembled monolayer (SAM): Different thiols (thioctic acid (TA); 3-mercaptopropionic acid (MPA) and 11-mercaptoundecanoic acid (MUA)) were investigated depending on chain length and gold-sulfur (Au-S) anchoring possibilities. Thiol SAMs were investigated through reductive thiol stripping in 0.5 M KOH [37, 75]. Due to its better performance, overnight incubation in 100 mM of 3-mercaptopropionic acid in ethanol was selected for SAM formation after that, the electrodes were rinsed with ethanol and dried with N₂.

ii) Cu deposition: A Cu monolayer was deposited via Underpotential Deposition (Cu UPD) by reductive linear sweep voltammetry (0.2 to -0.1 V vs. Ag/AgCl at 5 mV s⁻¹) in an electrochemical cell containing 5 mM CuSO₄ in 0.5 M H₂SO₄.

iii) MPA Esterification: After Cu UPD, the electrodes were immersed during 30 minutes in 400 mM 1-ethyl-3-[3-(dimethylamino)propyl carbodiimide (EDC) and 200 mM N-hydroxysuccinimide (NHS) solution prepared in purified milliQ water [29].

iv) Antibody (mAb) Immobilization: After the ester formation, the electrodes were immersed in solution of 10 µg mL⁻¹ mAb pH 4.8 Citrate Buffer solutions for 60 minutes. Covalent attachment have been reported to increase the stability of the immobilized protein layer and decrease the extent of denaturation upon immobilization [76].

v) *Free ester groups blocking*: The electrodes were immersed in a solution of 1 M ethanolamine pH 8.5 during 20 minutes.

vi) *mAb–H3HRP immunobinding*. *Fully assembled immunoelectrode*: The Au-S-Cu-mAb modified electrodes were immersed in a solution of H3HRP for 30 minutes to complete the immunoelectrode assembling (Au-S-Cu-mAb-H3HRP)

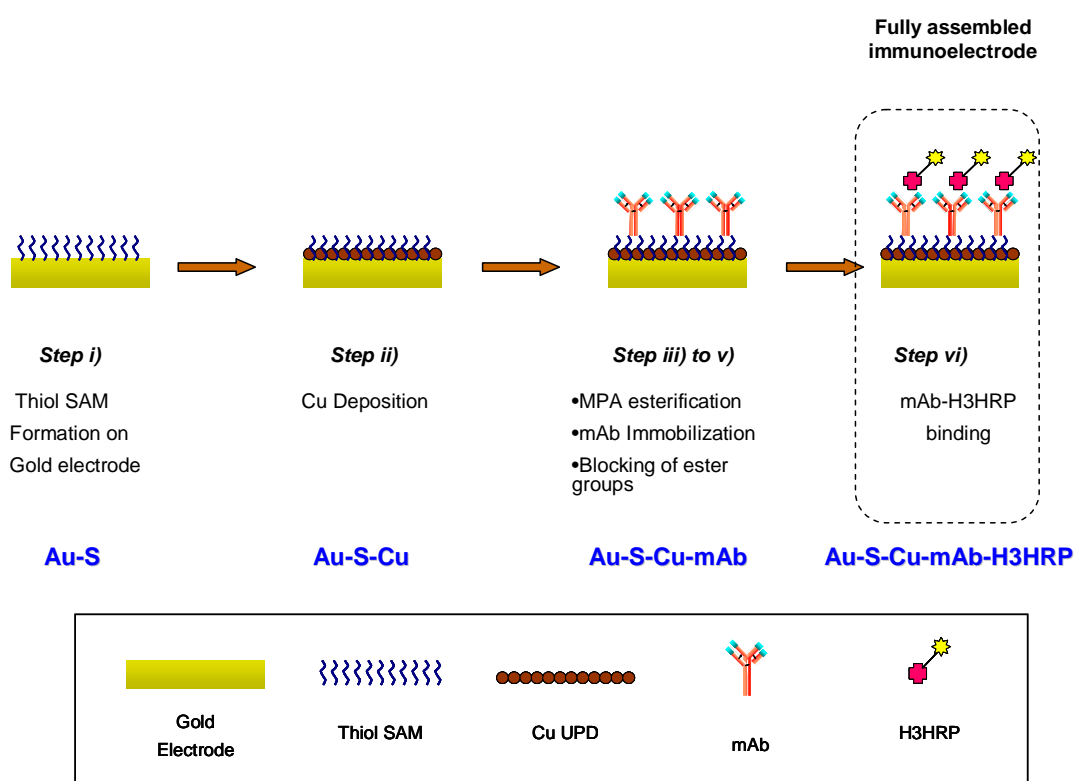


Fig. 4. 3: Schematic of the fully assembled immunoelectrode

Immunoelectrodes preparation steps were also monitored by Electrochemical Impedance Spectroscopy measurements.

4.2.5 Electrochemical measurements

Electrochemical experiments were carried out *on-line* or in *batch* conditions. In both cases, displacement was carried out in a volume adequate to keep an S/V ratio of 0.1 dm^{-1} following the MM studies (see Chapter 3, section 3.3.2.2).

On-line experiments were carried out in a three electrode cell using SGE electrodes as working electrode, containing 5 mM $\text{K}_4\text{Fe}(\text{CN})_6$ in 0.5 M $\text{Sr}(\text{NO}_3)_2$ as mediator solution (M). Investigated solutions (substrate (S), analyte and buffer) were added through one of the inlets of the cell and mixed by bubbling N_2 through an additional inlet. The solutions were renewed by pumping freshly prepared M solution always maintaining a constant surface of electrode to volume (S/V) ratio. The applied potential was 0.15 V vs. Ag/AgCl. The substrate concentration was kept 0.5 mM H_2O_2 .

Batch experiments were carried out in a three electrode cell using DGE electrodes as working electrode, containing 5 mM $\text{K}_4\text{Fe}(\text{CN})_6$ in 0.5 M $\text{Sr}(\text{NO}_3)_2$ as mediator solution (M). The applied potential was 0.1 V vs. Ag/AgCl under static conditions (not stirred). An *ON/OFF* procedure was used to record the sensor response upon addition of substrate. The substrate addition was carried out under stirring to ensure homogenization, while the readings were done under static conditions. Displacement step was carried out using the chosen S/V ratio apart from electrochemical measurements. The substrate concentration was kept 0.5 mM H_2O_2 .

Electrochemical impedance measurements were performed in the presence of equimolar concentrations, 1 mM of $[\text{Fe}(\text{CN})_6]^{3-}$ and $[\text{Fe}(\text{CN})_6]^{4-}$ as redox probe in 100 mM $\text{Sr}(\text{NO}_3)_2$ at the formal redox potential, using a sinusoidal ac potential perturbation of 5 mV, in the

frequency range 10^5 Hz to 1 Hz. The impedance spectra were plotted in the form of Nyquist plots (Z_{re} vs Z_{im}).

4.2.6 Displacement studies procedures

The expected goal of displacement experiments is to observe a net loss of signal in electrodes incubated with the analyte of interest as evidence that the displacement phenomenon had have place (Fig. 4. 4).

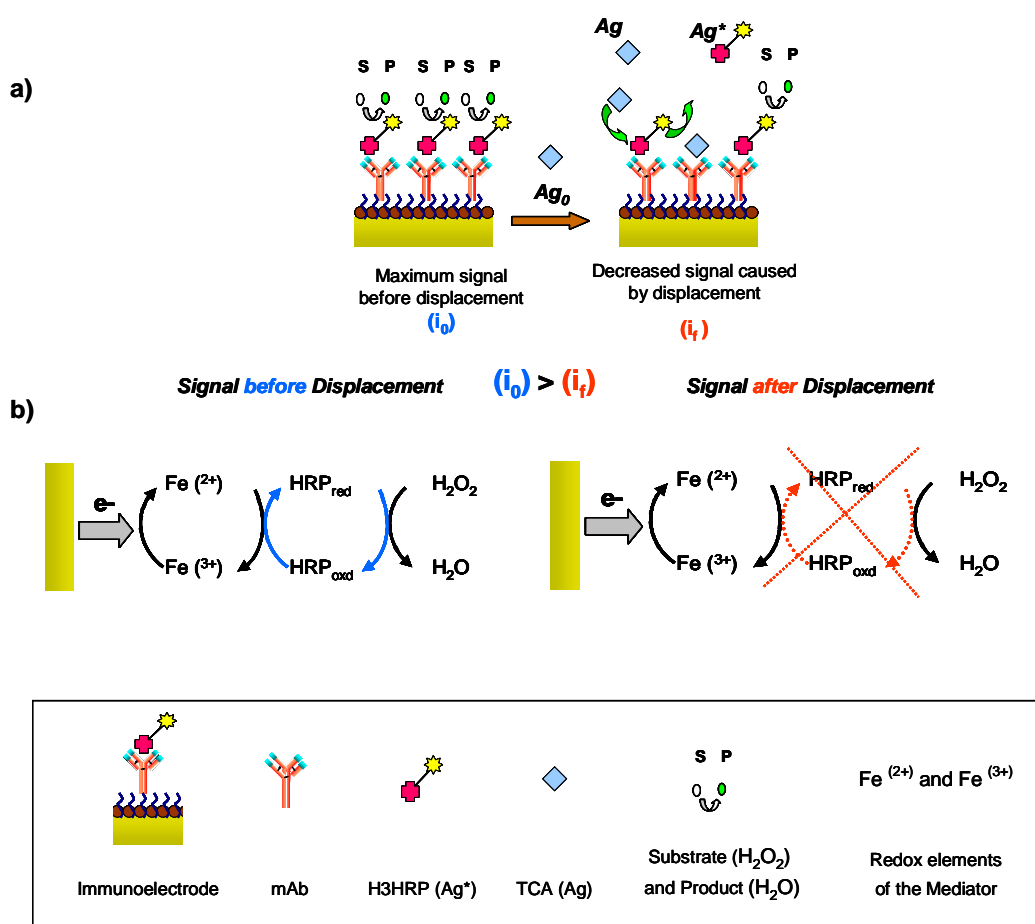


Fig. 4. 4: Displacement of labelled sub-optimum antigen (H3HRP) upon analyte addition. a) Schematic of the displacement phenomenon. b) Schematic of the generation and loss of cathodic current

4.2.6.1 Displacement Electrochemical Immunosensor (DEI) for TCA detection. On-line experiments

The optimized procedure followed in on-line experiments of the DEI is described in Fig. 4.

5 (a). The procedure can be divided into five main steps:

1) Mediator baseline: generation of a baseline by the introduction of the immunoelectrode (**Au-S-Cu-mAb-H3HRP**) in the three electrode cell containing mediator (M) solution.

2) Initial cathodic current: Generation of an initial cathodic current by means of addition of the substrate (S) that reacts with the enzyme (H3HRP) on the immunoelectrode.

3) TCA addition: beginning of the displacement phenomenon with the addition of the analyte (TCA, Ag).

4) Regeneration: regeneration of the mediator solution (M).

5) Final cathodic current: New addition of substrate (S) to detect the remaining cathodic current and calculation of the displaced current.

Investigated control immunoelectrodes (Fig. 4. 5 (b)) evaluated the loss of current generated from non-specifically adsorbed (NSA) labelled sub-optimum and the loss of signal due to buffer effects that is: (i) NSA on fully assembled electrode mimicking mAb protein with other IgG (NSA IgG); (ii) NSA in absence of mAb (NSA no mAb); (iii) NSA

on Cu modified surface (NSA Au-Cu); (iv) NSA on fully assembled electrode without Cu UPD (NSA no Cu) and (v) loss of current due to buffer effects (washing effect).

Control (iv) that represents immunoelectrodes without Cu UPD were prepared only for punctual comparative studies with Cu UPD modified electrodes and hence they were not applicable for the estimation of net current displacement (% NDC)

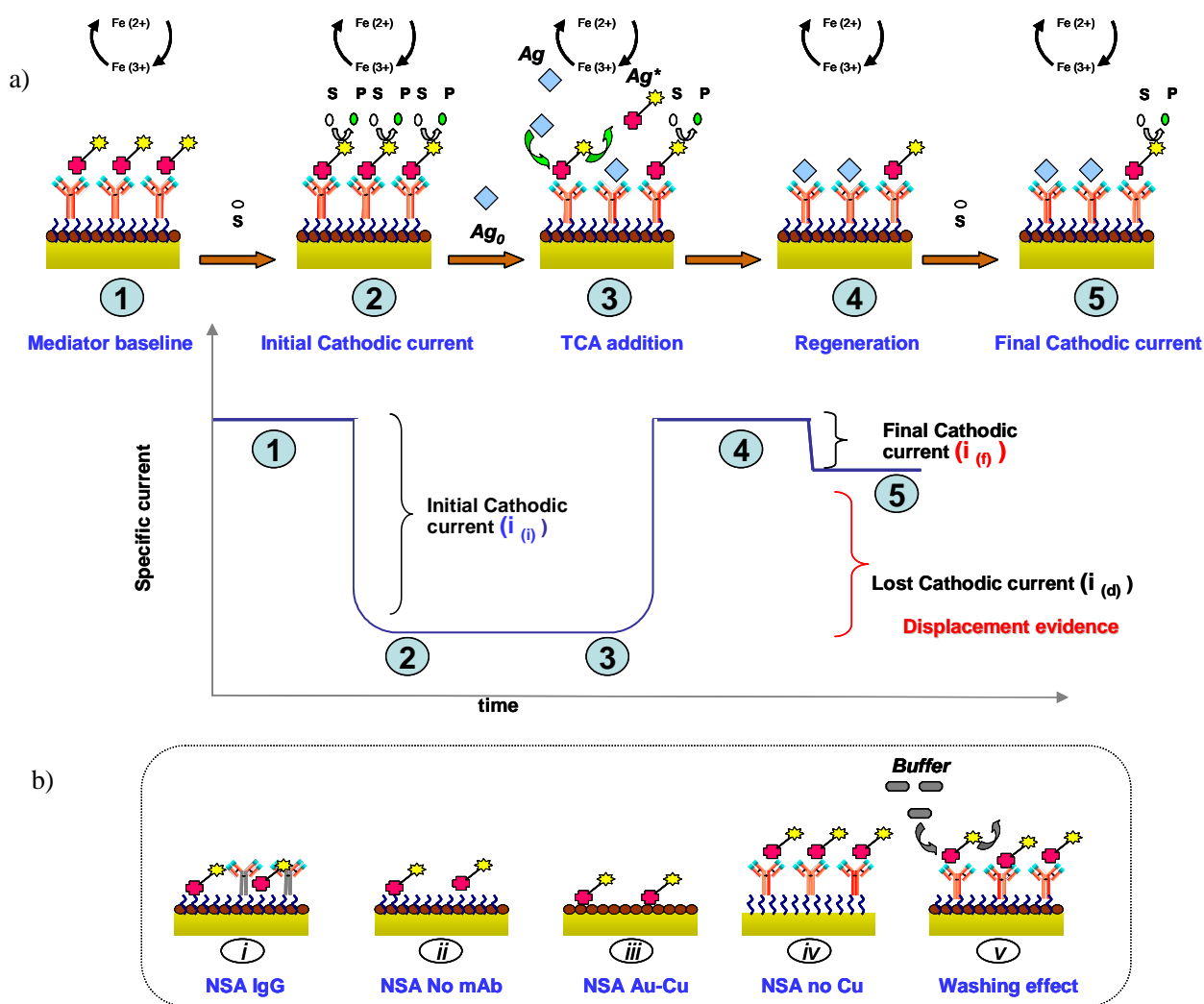


Fig. 4. 5: Schematics of the procedure followed for on-line experiments of Electrochemical Displacement (a). b) Control electrodes architectures. All the steps were carried without moving any component of the electrochemical cell.

All the steps were carried only changing solutions through injection or pumping. No electrochemical cell component was removed or replaced during the DEI measurement. Recording the current progress during these steps, the percentage of displaced current was calculated as follows:

$$\% DC_{TCA} = \frac{i_{(i)} - i_{(f)}}{i_{(i)}} * 100\% = \frac{i_{(d)}}{i_{(i)}} * 100\% \quad \text{Eq.4. 2}$$

where $i_{(i)}$ and $i_{(f)}$ are the immunoelectrode current before and after the displacement step (Fig. 4. 5) and $i_{(d)}$ is the displaced lost current.

Considering - if observed - the displacement of controls electrodes, the Net Displaced Current due to TCA displacing effect ($\% NDC_{TCA}$) was calculated according to:

$$\% NDC_{TCA} = \% DC_{TCA} - \% DC_{Control\ electrodes} \quad \text{Eq.4. 3}$$

where $\% DC_{Control\ electrodes}$ represents the lost of current observed for any of the control electrodes ((i) to (iii) and (v) , Fig. 4. 5). Since opposite to control (v) , controls (i) to (iii) did not demonstrate significant loss of the initial current because of the addition of TCA, the percentage of lost current due to non-specific effects or washing effects was mainly represented by the loss of current only in the presence of buffer ($\% DC_{Buffer, Ag=0}$), hence Eq.4. 3 can be writing as:

$$\% NDC_{TCA} = \% DC_{TCA, Ag=Ag_i} - \% DC_{Buffer, Ag=0} \quad \text{Eq.4. 4}$$

where % DC_{TCA, Ag=Ag_i} and % DC_{Buffer, Ag=0} represent the loss of current due to the addition of any concentration of TCA (Ag= Ag_i) or due to the addition of a Buffer solution (Ag= 0) representing the lost of current caused by other phenomenon different from TCA displacement, namely here “*washing effect*”.

Consequently, the relevance of the buffer loss of signal effects (Ag= 0) was considered and TCA displacement experiments (Ag ≠ 0) were complemented with equivalent buffer control experiments, calculating the Net Displaced Current (% NDC_{TCA}).

It is important to clarify here that the volumes added at displacement step always corresponded to less than 0.001 % of the total cell volume, avoiding in this way effects of dilution.

4.2.6.2 Displacement Electrochemical Immunosensor (DEI) for TCA detection. Batch experiments

The optimized procedure followed in batch experiments of the DEI is described in Fig. 4. 6.

The followed optimized procedure was divided in three experimental stages:

- 1 - Determination of the cathodic current generated by the immunoelectrode (Au-S-Cu-mAb-H3HRP) upon addition of substrate, prior to the interaction with TCA solution ($i_{(i)}$).
- 2 - Incubation in TCA or PBS solutions ($S/V=0.1 \text{ dm}^{-1}$) during 10 minutes..
- 3 - Determination of the current upon substrate addition after the interaction with TCA solution ($i_{(f)}$) and estimation of the displacement of the signal.

Data obtained in batch displacement experiments were processed in terms of percentage of Net Displaced Current (%NDC_{TCA}) according to Eq.4. 4. The investigated control electrodes followed what is described in section 4.2.6.1.

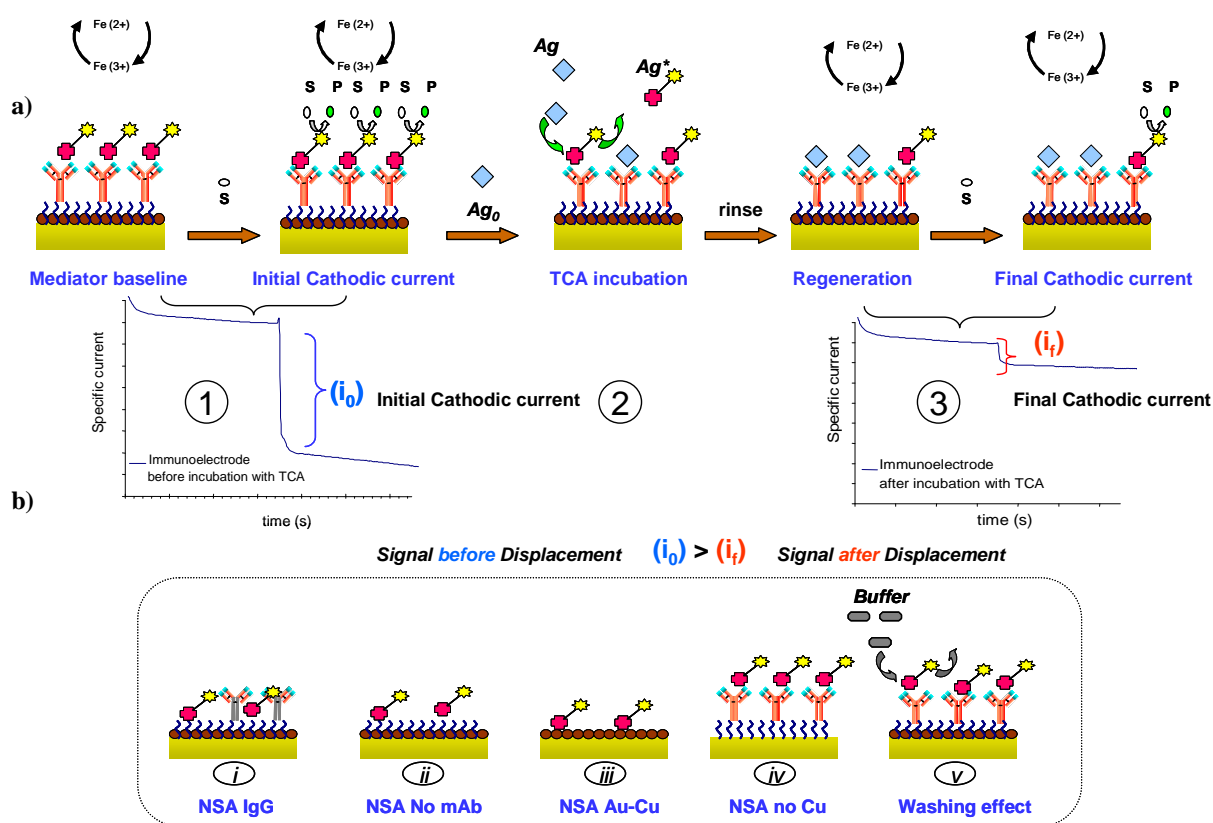


Fig. 4. 6: Schematics of procedure followed for Batch experiments of Electrochemical Displacement (a).
 b) Control electrodes architectures.

4.3 Results

4.3.1 Optimization of the electrode modification procedure

4.3.1.1 Thiol selection for self-assembled monolayer (SAM) formation

Thiols with different chain length and anchoring possibilities were investigated that is, thioctic acid (TA), 3-mercaptopropionic acid (MPA) and 11-mercaptoundecanoic acid (MUA) in Fig. 4. 7.

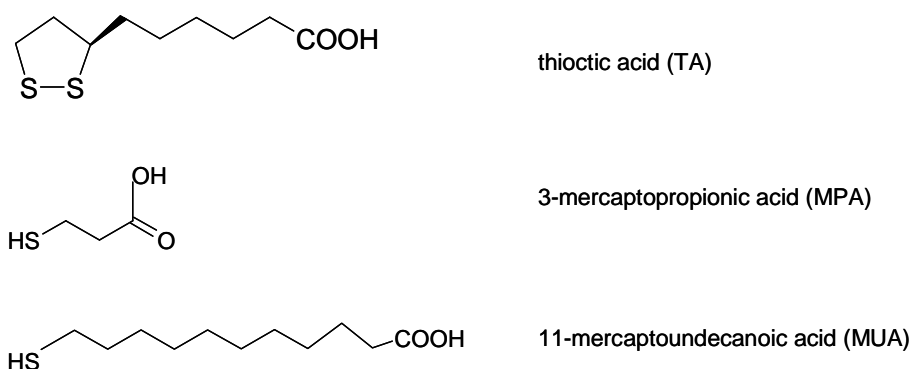
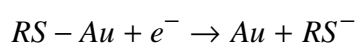


Fig. 4. 7: Structures of thiols investigated for SAMs formation on gold surface

Time of incubation and concentration of thiol solutions are considered the two main factors in SAM formation [77, 78]. In this sense, different incubation times and thiol concentrations were investigated. The SAM formation was quantified after rinsing and shaking for 2 minutes in ethanol in order to consider covalent attachment only. The characterization of the SAMs on gold electrode was carried out according to the reductive desorption of the monolayer and for the more widely proposed expression [27]:



Eq.4. 5

Thiols can be desorbed by reduction of the RS-Au bond at negative potentials [26, 75, 78]. SAM modified electrodes were submerged in 0.5M KOH. The reduction peak of thiolated monolayer obtained from cyclic voltammetry [26] (50 mV s⁻¹ from -0.4 V to -1.1 V vs. SCE) was used to calculate the surface coverage according to:

$$\text{Thiol Surface Coverage (mol cm}^{-2}\text{)} = \frac{Q}{nFA} \quad \text{Eq.4. 6}$$

where Q is the total charge (C), n the number of electron transferred, F is the Faraday's constant (96485.4 C mol⁻¹) and A is the electrode area (cm²).

Gold electrode active area was calculated using cyclic voltammetry technique (0.5 M H₂SO₄, 20 mV s⁻¹ from -0.2 V to 1.8 V vs. SCE) utilizing the gold oxide reduction peak area [79].

In SAM formation results (Fig. 4. 8) it is possible to observe that overnight incubations of the gold surface in thiol solution reached higher surface coverage. Regarding to the concentration of the solution, 10 mM of MPA or TA always generated the smallest coverage for the same incubation time. The use of 100 mM of thiol did not reach significantly different coverage compared to 1000 mM solutions. Considering the standard deviations in Fig. 4. 8, overnight incubation seemed to indicate a more homogeneous behaviour among electrodes. No significant differences were observed in the use of TA and MPA, that agrees with other authors [26, 75]. Reported work demonstrated that the increase of surface coverage, whose surface coverage magnitude agrees with the one reported here

and other literature (10^{-10} - 10^{-9} mol cm⁻²) [37, 47, 80], started to level off at 10 hours of incubation and in a concentration of 250 mM of all investigated solutions [26].

Together with surface coverage and stability of the SAM, the formed monolayer should demonstrate no insulation of the electrode surface, since the final detection of the immunoelectrode will be through electrochemical measurement. In this sense, MUA was discarded for the SAM formation since it was observed that in some cases it insulates the electrode surface and consequently hindered the reading of the electrochemical processes taking place on the immunoelectrode. This last observation agrees with other reported work with the difference that the response of their final immobilized surface was carried out using impedance [81]. The blocking of electron transfer due to adsorbed and immobilized protein has been broadly reported [10, 82-84]

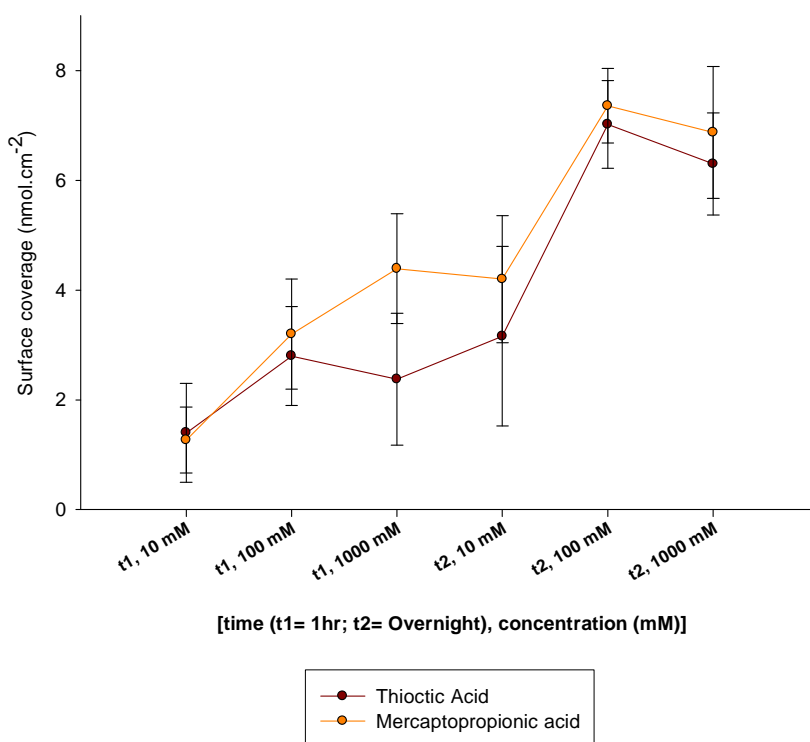


Fig. 4. 8: Effect of time and thiol solution concentration on SAM formation

Once MUA was discarded, MPA was selected for SAM formation since even though its performance was similar to TA, the double anchoring of the molecule could generate some steric effects hindering the covalent immobilization of proteins on TA gold modified electrodes [76]. Also parallel study of underpotential deposition of Cu deviated the work to MPA since shorter alkyl chains contribute to better Cu depositions [37, 47].

4.3.1.2 Preliminary study of NSA control by Cu

Thinking ahead in the application of Cu as NSA barrier on gold electrodes, the physical adsorption of HRP and HRP-labelled molecules on gold and copper sheets was investigated. Accordingly, clean metal sheets of the same geometric area (18 mm²) were incubated during 3 hours in HRP solutions containing the same enzymatic activity and protein concentration.

The evaluation of adsorbed HRP molecules was carried out through UV-Vis spectrophotometry using TMB (3,3',5,5'-tetramethylbenzidine liquid Substrate). Higher adsorption of HRP on gold compared to copper sheets was observed (Fig. 4. 9 (c)). No significant differences in the adsorption of HRP compared to H3HRP were detected (Fig. 4. 9 (a)). On the other hand, the contribution of proteins conjugated to HRP (IgG HRP) to the increase of the amount of adsorbed protein was observed (Fig. 4. 9 (b)). All the results were compared to non-incubated clean sheets (Fig. 4. 9 (d)).

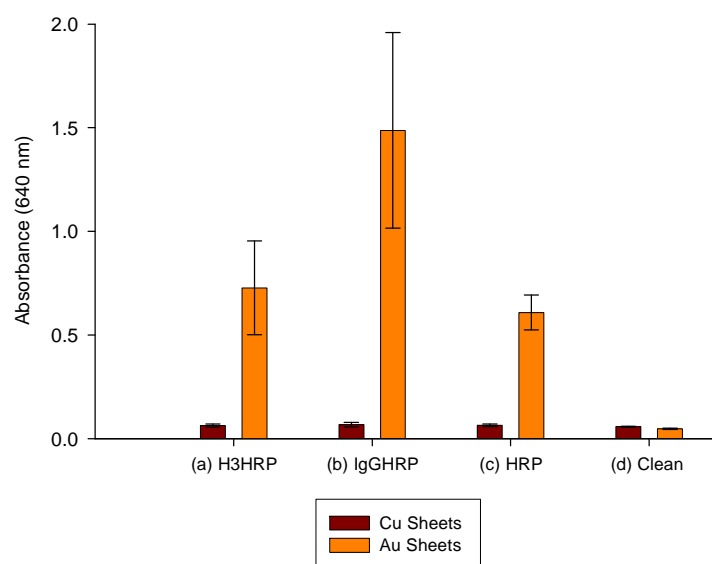


Fig. 4. 9: HRP and HRP molecules physical adsorption on Cu and Au sheets.

Complementary to this, the physical adsorption of horseradish peroxidase (HRP) solutions on bare and Cu underpotentially deposited gold electrodes was investigated. The electrodes were incubated during 3 hours in HRP solutions. Fig. 4. 10 demonstrates the higher HRP physical adsorption of the enzyme in absence of Cu UPD.

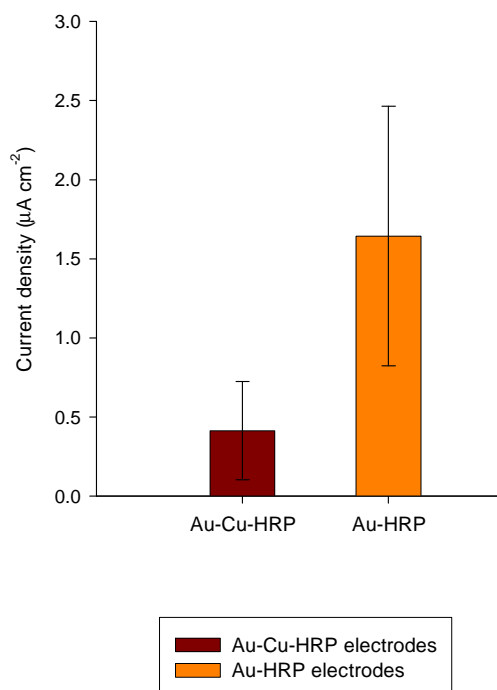


Fig. 4. 10: Signal observed in gold and Cu UPD modified gold electrodes after incubation with HRP 0.5 mM H₂O₂ in 5 mM K₄Fe(CN)₆ in 0.5 M Sr(NO₃)₂ . 0.1 V vs. Ag/AgCl Applied Potential.

4.3.1.3 Effects of Cu UPD on modified electrode

The effects of Cu as surface modifier were tested sequentially in the electrode modification procedure. The aim of these experiments consisted in the evaluation of the efficiency of Cu UPD as non-specific adsorption (NSA) barrier, demonstrating the capability of Cu UPD modified electrodes to generate a cathodic current in presence of H3HRP significantly different to the one observed for control electrodes since an efficient NSA barrier would give more relevance to the Specific Adsorption phenomenon (SA).

Different steps of the electrode modification were tested using chronoamperometry. The current densities obtained by replicates (n=5) for every group of electrodes are plotted in Fig. 4. 11.

Modified Electrodes without Cu deposition

The electrochemical response observed in **Au-H3HRP** electrodes demonstrated once again the evidence of Non-Specific Adsorption of H3HRP on Bare Gold Electrodes. On the other hand, the higher response observed for **Au-S-mAb-H3HRP**, demonstrated the contribution of the Specific Adsorption (SA) to the electrochemical response. The **Au-S-mAb-H3HRP** response resulted in average 22% higher compared to **Au-H3HRP** (Fig. 4. 11 (a)).

Modified Electrodes with Cu deposition

The electrochemical response observed in **Au-S-Cu-H3HRP** electrodes, showed that there is still evidence of Non-Specific Adsorption of H3HRP. However, the improvement of the SA signal when Cu is underpotentially deposited is demonstrated, since not only the **Au-S-Cu-mAb-H3HRP** electrodes response resulted higher when compared to **Au-Cu-H3HRP**, also the electrochemical response resulted in average 58% higher when compared to **Au-Cu-H3HRP** response (Fig. 4. 11 b).

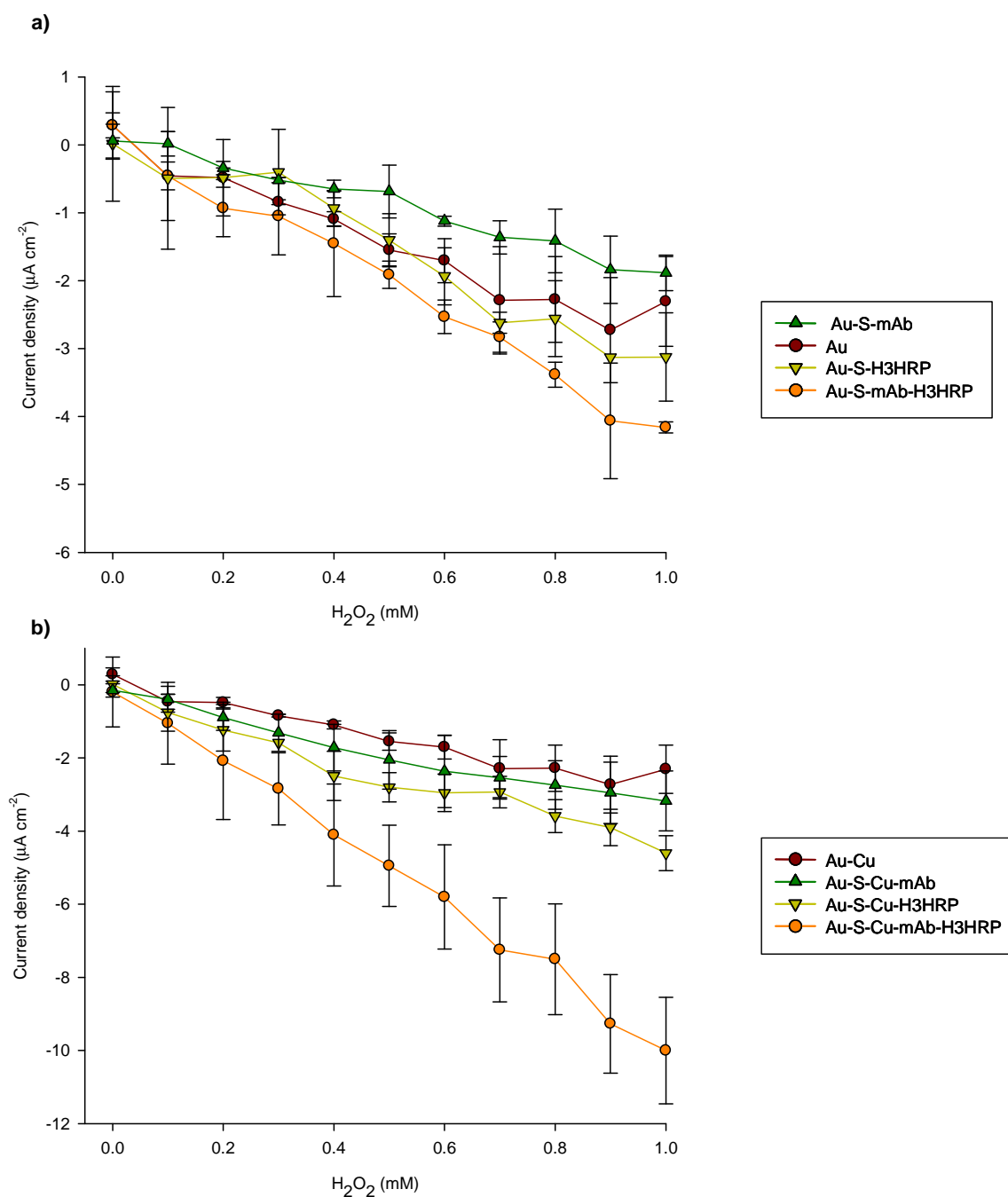


Fig. 4. 11: Current density observed for modified electrodes. a) Electrodes without Cu UPD; b) Electrodes with Cu UPD. Additions of 0.1 mM H_2O_2 up to 1.0 mM H_2O_2 . 2 ml 5 mM $\text{K}_4\text{Fe}(\text{CN})_6$ in 0.5 M $\text{Sr}(\text{NO}_3)_2$. 0.1 V Applied Potential. Measurement under static conditions. Current densities were calculated utilizing active electrode area determined according 5.3.1.1

Looking at the higher net current density observed for **Au-S-Cu-mAb-H3HRP** the effect of controlled NSA of molecules seems obvious, since comparing **Au-s-mAb-H3HRP** (no Cu UPD) with **Au-s-Cu-mAb-H3HRP** (Cu UPD) responses, it can be noticed that the electrochemical signal for the case of Cu deposited electrodes is higher. This could suggest that due to the blocking effect of the Cu, the decrease in NSA has a corresponding increase in the SA.

The demonstrated capability of Cu UPD to act as NSA barrier orientated the immunoelectrodes preparation to the use of such metal as blocking agent. Cu UPD was carried out by linear sweep voltammetry (5 mV s^{-1} , 0.2 to -0.1 V vs. Ag/AgCl) in an electrochemical cell containing 5 mM CuSO₄ in 0.5 M H₂SO₄.

4.3.1.4 Effect of Cu UPD on displacement experiments

The objective of these experiments was to study the effects of Cu UPD modified immunoelectrodes in the displacement step. An efficient performance as NSA controller should allow the detection of significant net loss of signal due to the addition of TCA.

Displacement batch experiments were carried out on immunoelectrodes with (Au-S-Cu-mAb-H3HRP) and without Cu deposition (Au-S-mAb-H3HRP). As a starting concentration selected from the MM results, 2 ppm TCA was used in the displacement step.

The obtained results depicted in Fig. 4. 12, demonstrates the positive contribution of Cu UPD for the detection of displacement phenomenon since a net loss of signal of 29% was observed for **Au-S-Cu-mAb-H3HRP** electrodes. This indicates that at least a 29% of the

loss of signal is not merely attributed to the washing effect by buffers but to the effective displacement of H3HRP by TCA.

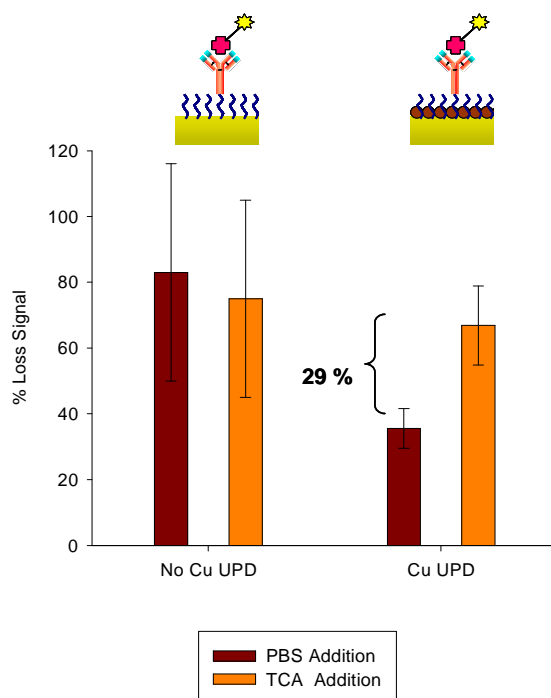


Fig. 4. 12: Au-s-mAb-H3HRP immunoelectrodes and Au-s-Cu-mAb-H3HRP immunoelectrodes incubated in 2 ppm TCA or PBS (n=5 for each case). Substrate concentration: 0.5 mM H₂O₂. Static measurements. Applied Potential: 0.1 V vs. Ag/AgCl.

In this way the contribution of Cu UPD to the detection of displacement phenomenon was demonstrated. The control of non-specifically adsorbed molecules increases the chances of specific binding occurrence consequently increasing the component of specifically attached molecules, molecules that will undergo displacement by means of TCA. In the case of not controlled NSA phenomenon the initial current will have an important component of non-specifically adsorbed molecules which, although they contribute to the initial current they do not undergo displacement. The loss of current in these cases would have an important contribution of detachment of NSA molecules caused by phenomena independent from

TCA displacement and hence the loss of current observed with TCA addition would not be easily distinguishable from buffer effects.

In the case of **Au-s-mAb-H3HRP** electrodes, no evidence of significant displacement effects was observed, since the loss of signal could not be differentiated between incubations with or without TCA (Fig. 4. 12).

4.3.2 Displacement on optimized immunoelectrodes

4.3.2.1 Displacement Electrochemical Immunosensor (DEI). On-line Experiments

Once immunoelectrode preparation was optimized regarding to NSA barrier and experimental conditions of immunoelectrodes fabrication, the displacement phenomenon was further explored.

Analyte concentrations that according to the mathematical model would provoke displacement of the signal higher than 50 % were chosen as starting point.

Fig. 4. 13 depicts the results obtained when 4 ppm of TCA were used as displacing agent in on-line experiments. The percentage of displaced current of fully assembled immunoelectrodes (**Au-S-Cu-mAb-H3HRP**) with addition of TCA in the displacement step was calculated according to Eq.4. 2 and resulted 58.4 ± 5.7 % (n= 3 replicates). Control experiments depicted in Fig. 4. 5 ((i) to (iii) and (v)) were also carried out. Since control (iii) gave no significant loss of current, it was not plotted.

Experiments using (i),(ii) and (v) control immunoelectrodes gave a loss of current of 12.5 ± 5.7 % (**Au-S-Cu-IgG-H3HRP**), 20.4 ± 2.2 % (**Au-S-Cu-No IgG-H3HRP**) and 31 ± 10.5

% (Au-S-Cu-IgG-H3HRP with addition of PBS in the displacement step) respectively.

According these control experiments, 28 % of the lost current observed in the DEI could be considered as Net Displaced Current due to TCA displacing effect.

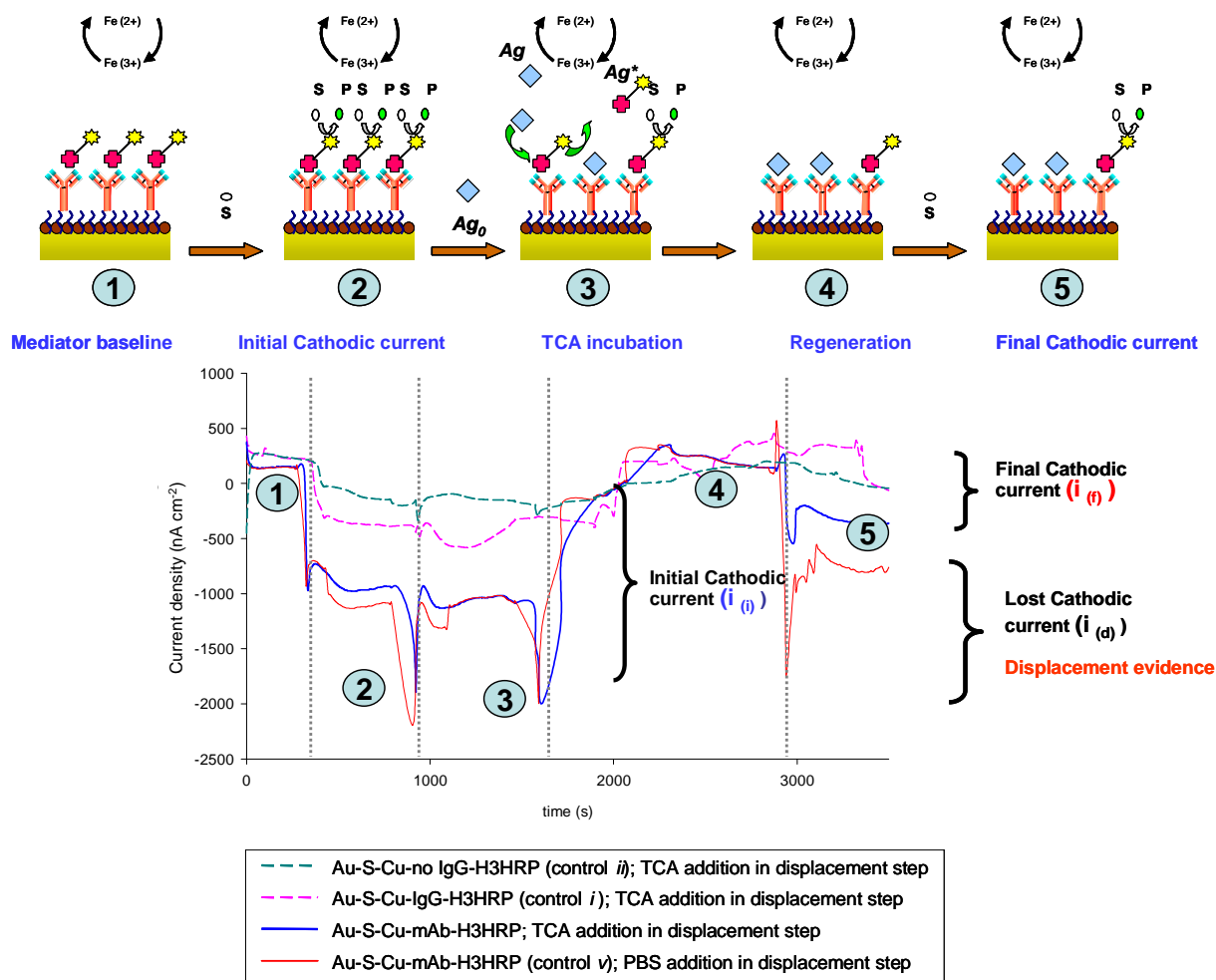


Fig. 4. 13: Signal observed in on-line experiments for TCA detection and controls. Current densities were calculated utilizing active electrode area determined according 5.3.1.1

Once the displacement phenomenon was demonstrated with on-line experiments and in order to avoid background noise, difficulties of manipulation and to reach homogeneous conditions more easily, batch experiments were investigated from this point onwards.

4.3.2.2 DEI Limit of Detection

The relevance of buffer displacement effects or washing effect (Fig. 4. 5, Control v) was further investigated.

The observed loss of current due to buffer effect (S/V ratio= 0.1 dm^{-1}) calculated as %DC_{TCA} was $29 \pm 6 \%$ ($n=20$). This percentage of lost current defined hence the Limit of Detection (LOD) [85] as:

$$LOD = \% DC_{(Ag \neq 0)} - \% DC_{(Ag = 0)} \geq 18\% \quad \text{Eq.4. 7}$$

Accordingly, only percentages of net displacement current higher than 18 % were considered as specific displacement phenomenon.

4.3.2.3 DEI range of operation

Batch experiments were carried out according to the procedure described in Fig. 5.6 . The investigated range of TCA concentration consisted in hundreds of ppb to units of ppm according to the predictions of the mathematical model. Net displaced current percentage (%NDC_{TCA}) was calculated as described in Eq.4. 4.

The obtained displacement results were contrasted with those predicted by the MM (Fig. 4. 14). The observed loss of current could be attributed to specific displacement phenomenon (Eq.4. 7) in the range of 0.2 ppm to 4 ppm.

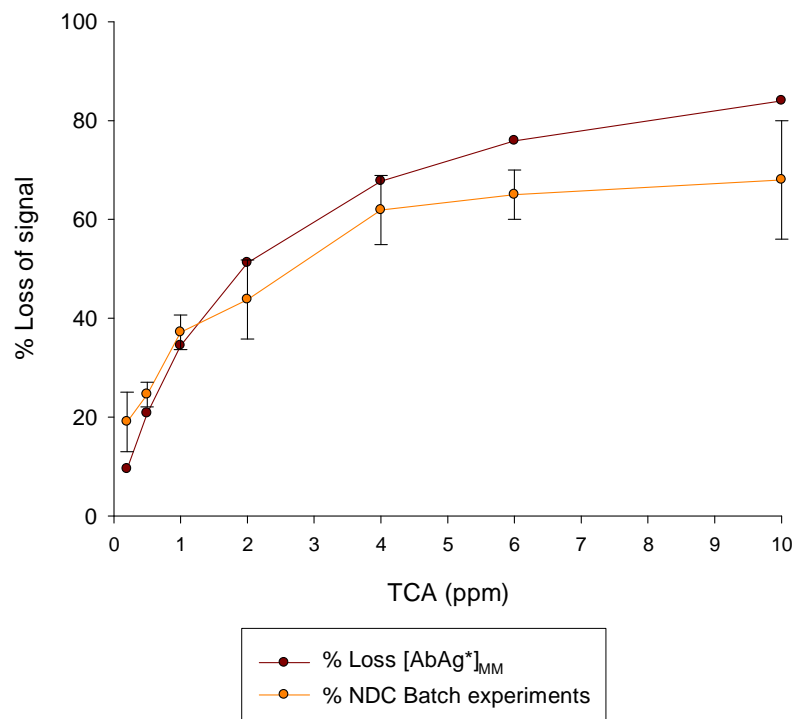


Fig. 4. 14: Experimental and predicted percentage of loss of signal. Analyte concentration $A_g = 0.2$ ppm to $A_g = 10$ ppm of TCA. K/K^* : 0.65; Ab_0 : 0.2 nmoles.dm⁻²; S/V : 0.1 dm⁻¹. Experimental results correspond to $n=5$ replicates for every TCA concentration.

The obtained net displaced current percentages correlated well with the model predictions mainly in the low concentrations of the investigated range. For concentrations higher than 2 ppm the curve seems to reach a plateau earlier than the predicted results.

4.3.3 Loss of current due to buffer effects- “Washing effect”

The objective of these experiments was to further investigate the loss of signal merely because of incubation in buffer solutions. Displacement experiments without analyte ($A_g = 0$) were carried out submerging the electrodes in different buffer volumes without the addition of TCA.

The volume (V) where the electrodes were immersed was changed while the surface of the electrode (S) was kept constant, varying consequently the S/V ratio. The obtained displacement results were contrasted with those predicted by the MM for simulation of loss of signal in absence of analyte. Fig. 4. 15 shows the experimental and predicted loss of signal due to buffer effects ($A_g = 0$). According to experimental results, the buffer displacing effect could vary from 50% ($S/V \text{ dm}^{-1}$: 0.00001) to 14 % ($S/V \text{ dm}^{-1}$: 10) depending on the S/V ratio. On the other hand as described in Chapter 3, the MM predicted total washing of the signal independently of the investigated S/V ratio for K^* of values 10^5 M^{-1} (10^{-4} nM^{-1}).

Finally for the DEI developed in this work, it is experimentally demonstrated that the loss of signal due to buffer effects (washing effects) depend on evaluated S/V ratio. Of experimental importance is the fact that total or high washing effects can be controlled in order to have a discernable displacement signal different from buffer effects.

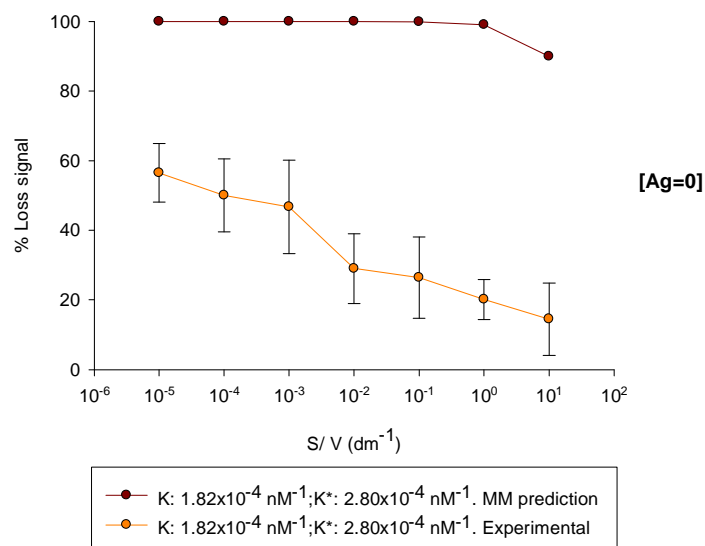


Fig. 4. 15: Buffer displacement effects on varying Surface/Volume (S/V) ratio of experimental and predicted results. $A_{g0}=0$ ppm TCA. A_{b0} : 0.2 nmoles. dm^{-2} . Experimental results correspond to $n=5$ replicates for every S/V ratio.

4.3.4 TCA - TCP Cross-reactivity

The importance of the differentiation of TCA and TCP lies on the fact that TCP is the precursor of TCA and its main competitor in real samples. It is important to have a system of detection that differentiates both compounds.

In this sense, displacement experiments were carried out using TCP or TCA as displacing agent in order to evaluate the loss of signal generated by each compound.

The results obtained (Fig. 4. 16) demonstrated that when same concentration of displacing agent are compared, TCA gave raise to higher displacement effects.

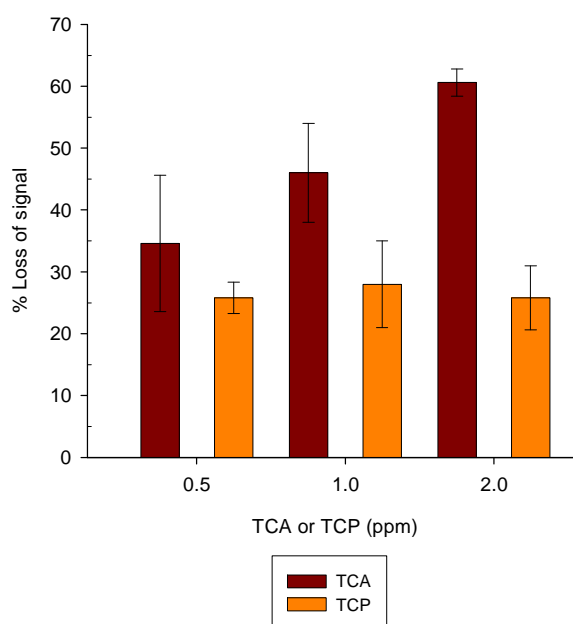


Fig. 4. 16: Loss of signal on Au-s-Cu-mAb-H3HRP immunoelectrodes after incubation with TCP or TCA solutions

These results gave optimistic indications of the behaviour that the DEI developed could have when measuring TCA in solutions different than buffer spiked samples. Further investigations of the DEI response in complex matrix would better illuminate the DEI

performance under such conditions. Nevertheless inhibition of competition assay on immunoelectrodes caused by wine matrix has been reported [66].

4.4 Discussion

4.4.1 Controlling the Non-Specific Adsorption (NSA) phenomenon

As explained in the Introduction of this chapter (section 4.1.2), proteins easily adsorb onto gold surfaces. Non-specific physical adsorption (NSA) of bioactive macromolecules such as antibodies and enzymes generally results in an activity loss [16]. Also, the NSA would negatively affect the displacement principle of the immunosensor since the displaced/lost signal would not totally represent the displacement by means of TCA. Considering these last observations, it was necessary to find a favourable option to control NSA of the proteins.

On the other hand, Au-SAM was chosen to lay the foundations to immobilize the components of the immunosensor because of Au good attributes for SAM formation. SAM-free Au sites should be further modified in order to avoid NSA. As described before, the presence of proteins on the electrode surface would block the electron transfer; hence other alternative to proteins as blocking agent should be found. Cu UPD was selected as non-insulating NSA controller agent since it have been demonstrated that ones the SAM is formed on gold surface, Cu UPD can be carried out without damaging the SAM and also stabilizing the SAM (See section 5.1.2). On the other hand, we take advantage of the fact that Cu UPD could be oxidized. In this sense, the surface of Cu would not be that available for the attachment of proteins on its surface.

In summary, Cu UPD was applied as potential NSA controller because of its suitability to be applied on Au –SAM surfaces playing a stabilizing role and also decreasing the possibilities of NSA of proteins without insulation of the electrochemical signal,

The use of Cu UPD demonstrated great potential to contribute to control the Non-Specific Adsorption (NSA) of H3HRP. The benefits of Cu UPD as NSA barrier was evidenced by the significant different currents observed for **Au-S-Cu-mAb-H3HRP** immunoelectrodes that resulted 58 % higher compared with control electrodes that contrasts with the 22 % difference between **Au-S-mAb-H3HRP** immunoelectrodes and their controls (Fig. 4. 11) .

Also positive contribution of Cu to the displacement phenomenon was observed since the loss of signal of DEI submerged in TCA solution was significantly distinguished (Net Displaced Current, NDC_{TCA}) from electrodes submerged simply in buffer solutions. With the addition of 2 ppm of TCA, **Au-S-Cu-mAb-H3HRP** immunoelectrodes demonstrated 29 % of NDC, while no significant NDC was observed for **Au-S-mAb-H3HRP** immunoelectrodes (Fig. 4. 11).

The different performance of metals (like Au and Cu) with regard to NSA phenomenon agrees with the specificity of proteins to metals studied in the literature. The different electronic configurations of the metals lead to different binding probabilities of sulfur and protonated group of the proteins residues with the surface [11]. Other authors [19, 21, 25, 26] studied the modification of surface using compounds with polar functional groups, hydrogen bond accepting groups, no hydrogen bond donating groups and not net charge to make protein resistant surfaces but, because of Cu metallic nature, the use of Cu as

blocking agent has the additional advantage of preventing insulation of the electrochemical signal caused by the presence of proteins on the electrode surface [10].

4.4.2 Detection of displacement phenomenon

Displacement principles on optimized DEI were demonstrated in on-line experiments where a net displaced current (%NDC_{TCA}) of 28 % was achieved with the addition of 4 ppm of TCA. Nevertheless, on-line experiments undergo noisy response during addition of solutions and some problems of homogenization were detected. Consequently once displacement phenomenon was demonstrated batch experiments were carried out to continue the investigation of the DEI response.

The minimum TCA concentration where discernable displacement phenomenon was observed corresponded to 0.2 ppm TCA according to the limit of detection calculated in Eq. 4. 7, that established that only percentages of net displaced currents equal or higher than 18 % could be considered as statistically discernable from blanks (buffer additions instead of TCA). A closer look of the investigated concentration range (Fig. 4. 14) indicates that the displacement of the signal seem to reach a plateau. Since the NSA of proteins was controlled but not totally eliminated, this plateau could be attributed to a residual signal caused by non-specifically adsorbed molecules. The presence of non-specifically adsorbed molecules that are electrochemically active and do not undergo displacement would be the cause of divergences of experimental with predicted results from the mathematical model. It is noteworthy that protein adsorption to solid-water interfaces is a multistep process, where the later steps are related to structural rearrangement of the protein and dehydration

effects that make the adsorption process irreversible [11] and assures their permanence on the electrode surface.

Displacement electrochemical immunosensor for TCA detection was first time developed here. Despite the available low affinity constant (K : mAb to TCA affinity constant), an operative immunosensor, based on the selection of the labelled sub-optimum and the possibility of controlling NSA with the use of non-insulating Cu UPD was developed. Although limits of detection of ppm were reached, the designed DEI still has big potential to reach lower limits of detection with the use of higher affinity antibodies (Chapter 3, section 3.3.2.6) and further control of NSA.

4.4.3 Fitting of predicted and experimental results

Regarding to the fitting of experimental results with the MM predictions in Chapter 3, the MM predicted sufficiently well the concentration range of work of the DEI in batch experiments. Nevertheless, deviation of the exact fitting of experimental and predicted results is observed.

The presence of still some NSA contribution, the possibility of changes in the antibody affinity due to immobilization [86] and experimental sources of unavoidable error could be mentioned as origin of such deviations.

On the other hand, no agreement with the predictions related to loss of current in absence of analyte was found. The predicted total loss of current only due to buffer effect was not

experimentally observed; opposite to this the experiments demonstrated that the washing effect could be controlled by changing the volume (V) where displacement takes place. Also, the validity of the selection of S/V ratio equal to 0.1 dm^{-1} is demonstrated with the detection of a discernable net displaced signal and the experimental estimation that one of the lowest washing effects is observed for such S/V ratio (Fig. 4. 15).

It should be reminded that most DEI experiments and the ones contrasted with the MM correspond to batch experiments because of practical experimental reasons explained before. Nevertheless, it could be foreseen that the fitting of on-line experiments results with the MM would have been harder since the MM should have been also considered dynamic factors like flow rates or diffusion effects. The assumption of local equilibrium of the MM could have also been a greater source of inconsistency of the MM predictions with on-line experiments.

4.4.4 DEI range of operation

As pointed out in previous section, the range of operation of the DEI reported here is units of ppm with a LOD of 0.2 ppm. Nevertheless, there is still the possibility of obtaining limits of detection matching the human threshold (ppt of TCA) by exploitation of affinity constants (K) values of 10^9 M^{-1} or higher (Chapter 3, section 3.3.2.6).

Despite the fact that the achieved limit of detection may not match human thresholds the main contribution of the developed DEI is the use of displacement procedure. Displacement procedure avoids pre-treatment and labelling of the sample (labelless) and also opens the

doors for reagentless immunosensing if mediator and substrate derivates are introduced in the DEI preparation. Additionally, the displacement procedure reported here could be completed within only 20 minutes once the immunoelectrodes are prepared.

Little about electrochemical immunosensor for TCA detection has been reported [66]. Works report limits of detection of 87 ppt and 29 ppt (with or without ethanol respectively) using immunoelectrodes prepared on carbon screen printed electrodes. Polyclonal antibodies were immobilized through incubation of carbonate solution of the antibody on the electrode and BSA was used as blocking agent. The reported immunoelectrode works under direct competition assay (DCI) with an incubation time of the electrode in competing solutions (TCA and labelled competitor) of 1 hr.

The reported here DEI could have advantages compared to the DCI since DEI still have potential to improve its LOD, it requires shorter experimental time and provides the possibility of reagentless detection.

4.5 Conclusions

The feasibility of developing an electrochemical displacement immunosensor, despite the low affinity constant existent has been shown. The non-specific adsorption phenomenon was partially but successfully controlled by the use of non-insulating Cu UPD monolayer formation, which, together with amperometric displacement detection, can be the basis for the development of reagentless and labelless immunosensors.

Chapter 4

*Strategy for Displacement Electrochemical Immunosensors Development:
the 2,4,6-trichloroanisole (TCA) case*

Main advantages of the developed immunosensor lie on the detection time rather than on the net limit of detection and the use of displacement principles that settles the foundations for real labelless and reagentless systems.

4.6 Bibliography

- [1] Kissinger, P. *Biosens. Bioelectron.*, 2005, **20**, p. 2512-2516.
- [2] Dornelles Mello, L., Tatsuo Kubota, L. *Food Chem.*, 2002, **77**, p. 237-256.
- [3] Sadana, A. *Engineering Biosensors. Kinetics and Design applications*. 2002, San Diego, California. USA, Academic Press.
- [4] Thèvenot, D. R., Toth, K., Durts, R.A., Wilson, G.S. *Inter. Union Pure Appl. Chem.*, 1999, **71**(12), p. 2333-2348.
- [5] Steward, M. W., Lew, A.M. *J. Immunol. Methods*, 1985, **78**, p. 173-190.
- [6] Wang, J. *Biosens. Bioelectron.*, 2006, **21**, p. 1887-1892.
- [7] Ngo, T. *Anal. Letters*, 2005, **38**, p. 1057-1069.
- [8] Okano, K., Takahashi, S., Yasuda, K., Tokinaga, D., Imai, K., Koga, M. *Anal. Biochem.*, 1992, **202**, p. 120-125.
- [9] Nakanishi, K., Sakiyama, T., Imamura, K. *J. Biosci. Bioeng.*, 2001, **91**, p. 233-244.
- [10] Moulton, S. E., Barisci, J.N., Bath, A., Stella, R., Wallace, G.G. *J. Colloid. Interface Sci.*, 2003, **261**, p. 312-319.
- [11] Eckert, R., Jenny, S., Hörber J. K. H. *Cell Biology International*, 1997, **21**(11), p. 707-713.
- [12] Norde, W. *Advances in Colloid and Interface Science*, 1986, **25**, p. 267-340.
- [13] Haynes, C., Norde, W. *Colloids and Surfaces B: Biointerfaces*, 1994, **2**, p. 517-566.
- [14] Lassen, B., Malmsten, M. *J. Colloid. Interface Sci.*, 1996, **182**, p. 339-349.
- [15] Bensebaa, F., Zhou, Y., Deslandes, Y., Kruus, E., Ellis, T. *Surface Science*, 1998, **405**, p. L472-L476.
- [16] Malmsten, M. *Colloids Surf. B: Biointerfaces*, 1995, **3**, p. 297-308.
- [17] Lahiri, J., Isaacs, L., Tien, J., Whitesides, G.M. *Anal. Chem.*, 1999, **71**, p. 777-790.
- [18] Welinder, K. G. *Eur. J. Biochem.*, 1979, **96**, p. 483-502.
- [19] Liu, V. A., Jastromb, W. E., Bhatia, S. N. *J. Biomed. Mater. Res.*, 2002, **60**, p. 126-134.
- [20] Prime, K. L., Whitesides, G.M. *J. Am. Chem. Soc.*, 1993, **115**, p. 10714-10721.
- [21] Harder, P., Grunze, M., Dahint, R., Whitesides, G. M., Laibinis, P. E. *J. Phys. Chem. B*, 1998, **102**, p. 426-436.
- [22] Castner, D., Ratner, B. *Surface Science*, 2002, **500**, p. 28-60.
- [23] Jeon, S. I., Andrade, J.D. *J. Colloid. Interface Sci.*, 1991, **142**, p. 159-166.
- [24] Jeon, S. I., Lee, J.H., Andrade, J.D., De Gennes, P.G. *J. Colloid. Interface Sci.*, 1991, **142**(1), p. 147-158.
- [25] Chapman, R. G., Ostuni, E., Takayama, R., Homlim E., Yan L., Whitesides, G.M. *J. Am. Chem. Soc.*, 2000, **122**, p. 8303-8304.
- [26] Limbut, W., Kanatharana, P., Mattiasson, B., Asawatreratanakul, P., Thavarungkul, P. *Biosens. Bioelectron.*, 2006, **22**, p. 233-240.
- [27] Basch, H., Ratner, M. *J. Chem. Phys.*, 2004, **120**(12), p. 5771-5780.
- [28] Tachibana, M., Yoshizawa, K., Ogawa, A., Fujimoto, H., Hoffmann, R. *J. Phys. Chem. B*, 2002, **106**, p. 12727-12736.
- [29] Vaughan, R. D., O'Sullivan, C.K., Guilbault, G.G. *Fresenius J. Anal. Chem.*, 1999, **364**, p. 54-57.
- [30] Persson, N., Uvdal, K., Almquist, O., Engquist, I., Kariis, H., Liedberg, B. *Langmuir*, 1999, **15**, p. 8161-8169.
- [31] Whelan, C., Kinsella, M., Meng Ho, H., Maex, K. *J. Electrochem. Soc.*, 2004, **151**(2), p. B33-B38.
- [32] Rosario-Castro, B., Fachini, E., Hernandez, J., Perez-Davis, M., Cabrera, C. *Langmuir*, 2006, **22**, p. 6102-6108.
- [33] Azzaroni, O., Vela, M.E., Fonticelli, M., Benitez, G., Carro, P., Blum, B., Salvarezza, R.C. *J. Phys. Chem. B*, 2003, **107**, p. 13446-13454.
- [34] John, S. A., Kitamura, F., Tokuda, K., Ohsaka, T. *Langmuir*, 2000, **16**, p. 876-880.
- [35] Akinaga, Y., Nakajima, T., Hirao, K. *J. Chem. Phys.*, 2001, **114**(19), p. 8555-8564.
- [36] Laibinis, P., Whitesides, G., Allara, D., Tao, Y., Parikh, A., Nuzzo, R. *J. Am. Chem. Soc.*, 1991, **113**, p. 7152-7167.

-
- [37] Oyamatsu, D., Susumu, K., Yoneyama, H. *Electroanal. Chem.*, 1999, **473**, p. 59-67.
- [38] Yamamoto, Y., Nishihara, H., Aramaki, K. *J. Electrochem. Soc.*, 1993, **140**(2), p. 436-443.
- [39] Ron, H., Cohen, S., Matlis, M., Rappaport, M., Rubinstein, I. *J. Phys. Chem. B*, 1998, **102**, p. 9861-9869.
- [40] Bockris, J., Reddy, A., Gamboa-Aldeco, M. *Modern Electrochemistry 2A. Fundamentals of Electrodicts*. Second ed. 2000, New York, Kluwer Academic/Plenum.
- [41] Creager, S. E., Hockett, L.A., Rowe, G.K. *Langmuir*, 1992, **8**, p. 854-861.
- [42] Basch, H., Ratner, M. *J. Chem. Phys.*, 2003, **119**(22), p. 11926-11942.
- [43] Basch, H., Ratner, M. *J. Chem. Phys.*, 2003, **119**(22), p. 11943-11950.
- [44] Hay, P. J., Wadt, W.R. *J. Chem. Phys.*, 1984, **82**(1), p. 299-310.
- [45] Jennings, G., Laibinis, P. *J. Am. Chem. Soc.*, 1997, **119**, p. 5208-5214.
- [46] Shimazu, K., Hashimoto, Y., Kawaguchi, T., Tada, K. *J. Electroanal. Chem.*, 2002, **534**, p. 163-169.
- [47] Nishizawa, M., Sunagawa, T., Yoneyama H. *Langmuir*, 1997, **13**, p. 5215-5217.
- [48] Tarlov, M. *J. Langmuir*, 1992, **8**, p. 80-89.
- [49] Green, T., Charles, P.T., Anderson, G.P. *Anal. Biochem.*, 2002, **310**, p. 36-41.
- [50] Clark, H. R., Barbari, T.A., Rao, G. *Biotechnol. Prog.*, 1999, **15**, p. 259-266.
- [51] Larsson, A., Angbrant, J., Ekeröth, J., Mansson, P., Liedberg, B. *Sens. Actuators B*, 2006, **113**, p. 730-748.
- [52] Van der Voort, D., Pelsers, M.M.A.L., Korf, J., Hermens, W.T., Glatz, J.F.C. *Biosens. Bioelectron.*, 2003, **19**, p. 465-471.
- [53] Valat, C., Limoges, B., Huet, D., Romette, J.L. *Anal. Chim. Acta*, 2000, **404**, p. 187-194.
- [54] Fahnrich, K. A., Pravda, M., Guilbault, G.G. *Biosens. Bioelectron.*, 2003, **18**, p. 73-82.
- [55] Kaptein, W., Zwaagstra, J.J., Venema, K., Ruiters, M. H. J., Korf, J. *Sens. Actuators B*, 1997, **45**, p. 63-69.
- [56] Gerdes, M., Spener, F., Meusel, M. *Quim. Anal.*, 2000, **19**, p. 8-14.
- [57] Taylor, R. F., Schultz, J.S. *Handbook of Chemical and Biological Sensors*. First Ed. ed. 1996, Bristol, U.K., Institute of Physics Publishing Ltd.
- [58] Chaubey, A., Malhotra, B. D. *Biosens. Bioelectron.*, 2002, **17**, p. 441-456.
- [59] Warsinke, A., Benkert, A., Scheller, F.W. *Fresenius J. Anal. Chem.*, 2000, **366**, p. 622-634.
- [60] Sanvicens, N., Varela, B., Marco M.P. *J. Agric. Food Chem.*, 2003, **51**, p. 3932-3939.
- [61] Sanvicens, N., Moore, E., Guilbault, G., Marco, M.P. *J. Agric. Food Chem.*, 2006, **42**, p. 9176-9183.
- [62] Lauster, R., Sanvicens, N., Marco, M.P., Hock, B. *Anal. Letters*, 2003, **36**(4), p. 713-729.
- [63] Alzaga, R., Ortiz, L., Sanchez-Baeza, F., Marco, M.P., Bayona, J.M. *J. Agric. Food Ind.*, 2003, **51**, p. 3509-3514.
- [64] Petrovic, M., Eljarrat, E., Lopez de Alda, M.J., Barcelo, D. *J. Chromatogr. A*, 2002, **974**, p. 23-51.
- [65] Weetall, H. *Biosens. Bioelectron.*, 1999, **14**, p. 237-242.
- [66] Moore, E., Pravda M., Guilbault, G.G. *Anal. Chim. Acta*, 2003, **484**(1), p. 15-24.
- [67] Petri, M., Kolb, D. M., Memmert, U., Meyer, H. *Electrochim. Acta*, 2003, **49**, p. 183-189.
- [68] Nichkova, M., Galve, R., Marco, M.P. *Chem. Res. Toxicol.*, 2002, **15**, p. 1360-1370.
- [69] Hermanson, T. G. *Bioconjugate techniques*, ed. Press, A. 1996, San Diego, California.
- [70] *Enzymatic assay of horseradish peroxidase with ABTS. Sigma quality control test procedure.*
www.sigma-aldrich.com;
- [71] Ron, H., Matlis, S., Rubinstein, I. *Langmuir*, 1998, **14**, p. 1116-1121.
- [72] Ron, H., Rubinstein, I. *Langmuir*, 1994, **10**, p. 4566-4573.
- [73] Vig, J. R. *J. Vac. Sci. Technol. A*, 1985, **3**(3), p. 1027-1034.
- [74] Storri, S., Santoni, T., Minunni, M., Mascini, M. *Biosens. Bioelectron.*, 1998, **13**(3-4), p. 347-357.
- [75] Susmel, S., Guilbault, G.G., O'Sullivan, C.K. *Biosens. Bioelectron.*, 2003, **18**, p. 881-889.
- [76] Smith, A. M., Ducey, M.W., Meyerhoff, M.E. *Biosens. Bioelectron.*, 2000, **15**, p. 183-192.
- [77] Liu, M., Li, Q.X., Rechnitz, G.A. *Anal. Chim. Acta*, 1999, **387**, p. 29-38.
- [78] Wink, T., Zuilen, S.J., Bult, a., Bennekom, W.P. *Analyst*, 1997, **122**, p. 43-50.
- [79] Angerstein-Kozłowska, H., Conway, B.E. *Electrochim. Acta*, 1986, **31**(8), p. 1051-1061.
- [80] Bard, A., Faulkner, L. *Electrochemical Methods. Fundamentals and Applications*. Second ed. 2001, EEUU, John Wiley & Sons, Inc.
- [81] Ding, S., Chang, B., Wu, Ch., Lai, M., Chang, H. *Electrochim. Acta*, 2005, **50**, p. 3660-3666.
- [82] Harrison, D. J. *J. Electroanal. Chem.*, 1990, **278**, p. 193-204.

Chapter 4

Strategy for Displacement Electrochemical Immunosensors Development:
the 2,4,6-trichloroanisole (TCA) case

- [83] Downard, A. J., Roddick-Lanzilotta, A.D. *Electroanalysis*, 1995, **7**, p. 376-378.
- [84] Huang, E., Zhou, F., Deng, L. *Langmuir*, 1999, **16**, p. 3272-3280.
- [85] Miller, J. C., Miller, J.N. *Estadística para Química Analítica*. Second Ed. ed. 1993, Wilmington, Delaware, USA., Addison-Wesley Iberoamericana.
- [86] Rabbany, S., Piervincenzi, R., Judd, L., Kusterbeck, A., Bredehorst, R., Hakansson, K., Ligler, F. *Anal. Chem.*, 1997, **69**, p. 175-182.

Chapter 4

*Strategy for Displacement Electrochemical Immunosensors Development:
the 2,4,6-trichloroanisole (TCA) case*

CHAPTER 5

Overall conclusions

In this thesis, the principles of Displacement Electrochemical Immunosensing were demonstrated through their application to the detection of 2,4,6-trichloroanisole (TCA) as target analyte. Also in this investigation, first indirect competitive ELISA (ICE) for TCA detection with limits of detection in the range of units of ppt and within a relative short experimental time is developed.

To achieve these main goals, the following objectives were accomplished:

1. The rational design of indirect competitive ELISA for TCA detection was demonstrated. The indirect competitive ELISA developed utilizes a monoclonal antibody specifically rose for this work (mAb) and demonstrated to be capable of detecting TCA within a working range of 1ppt to 1 ppm, with a limit of detection of 4.2 ppt.

Accelerated aging studies demonstrated the stability to storage of previously coated and blocked plates, making feasible the ICE detection in less than 80 minutes without the need of amplification of the signal and including the colorimetric detection. Depending on the labeling of the mAb, the developed ICE still offers the potential of an experimental time of 20 minutes, which gives great interest in the application of this assay where short experimental time are decisive in go/no go processes.

2. A mathematical model (MM) of the displacement immunosensor was developed. The mathematical model helped to foresee the concentration work range of the displacement electrochemical immunosensor (DEI) according to ELISA estimated affinity constant of the investigated system. The predictions obtained from the MM guided the selection of investigated TCA concentrations and labeled sub-optimum antigens.
3. The rational design of an electrochemical displacement immunosensor (DEI) was demonstrated. A functional DEI was developed despite the low affinity constant existent and the non specific adsorption (NSA) of proteins. NSA phenomenon was controlled by the use of non isolating Cu UPD monolayer formation which, together with amperometric displacement detection, can be the basis for the development of reagentless and labelless immunosensors.

Development of displacement electrochemical immunosensors: The case of 2, 4, 6-trichloroanisole
MV DUARTE
Tarragona, December 2007
